

Characterisation of Cyclase Associated Protein homologue, CAP2

INAUGURAL-DISSERTATION
zur
Erlangung des Doktorgrades
der Mathematisch-Naturwissenschaftlichen Fakultät
der Universität zu Köln



vorgelegt von
Sunil shekar
aus
Mandya, Indien

Köln, 2004

Referees/Berichterstatter: Prof. Dr. Angelika A. Noegel
Prof. Sigrun Koshing

Date of oral examination: 09.02.2005
Tag der mündlichen Prüfung

The present research work was carried out under the supervision of Prof. Dr. Angelika A. Noegel, in the Institute of Biochemistry I, Medical Faculty, University of Cologne, Cologne, Germany. From October 2001 to February 2005.

Diese Arbeit wurde von October 2001 bis February 2005 am Biochemischen Institut I der Medizinischen Fakultät der Universität zu Köln unter der Leitung von Prof. Dr. Angelika A. Noegel durchgeführt.

To my beloved family

Acknowledgements

First & foremost I'm immensely grateful to Prof. Angelika A. Noegel for giving me an opportunity to work in her group and also for her guidance and encouragement all through my doctoral studies.

I heartily thank Dr. Iakowos Karakesisoglou (Akis), for his kind advice, guidance and good friendship. My Sincere thanks goes to Dr. Fransisco Rivero Crespo, Dr. Ludwig Eichinger and Dr. Andreas Hasse for their guidance and timely advice.

I would like to thank Rosie, Berthold, Rolf, Maria, Martina, Katrin and Alex for their kind help whenever asked.

I would like to express my gratitude to Bettina Lauss (our Former secretary) and Dorte Püsche for making all the official work easy.

I would like to thank Budi Tungal for solving the problems with my computer.

I also thank Prof. Gabriele Pfitzer And Dr. Martina Krüger for providing myofibrils and Troponin I antibody, Dr. R. Schröder, University hospital, Bonn for providing muscle sections, Dr. J. Kappler, Bonn for providing neuronal glia & cerebral culture, Dr. Evren Caglayan for providing rat VSM cells.

My heartiest gratitude goes to my parents somashekara sastry & shakuntala sastry who stood by me all through my studies and for being the sole reason for me being here today.

I would like to convey my special thanks to Deen who was my bench mate & has helped me in many ways all through my research work apart from being a very good friend of mine. I still enjoy making him angry.

I would also like to thank my former and current labmates Dhamu, Sabu, Kumar, Yogi, Sonia, Christoph, Oleg, Marija, Michael, Henning, Soraya, Hafida, Hameeda, Hua, Thorsten, Wenshu, Vasily, Shubhanjan, Patrick, Carola, Jessica, Nandu, Somesh & all the others for creating a friendly and lively environment which made my stay in the lab more pleasant.

I extend my thanks to sharada for timely help rendered. I would also express my heartfelt thanks to Vel, Madhu, Sabri and all my friends in Cologne who made my stay enjoyable and memorable. I would never forget the joyful moments I had with them especially in the parties.

Last but not the least to the one who is my strength, I am immensely grateful to my lovely wife, Bharathi for her constant support, encouragement and helping me in many ways all through my research work including helping me in writing the thesis.

Sunil Shekar

Table of contents

1. Introduction

1.1 The cytoskeleton	1
1.2 The actin cytoskeleton	1
1.3 Actin and actin binding proteins	2
1.4 Domain structure and function of CAP	4
1.5 Interaction of CAP with adenylyl cyclase	4
1.6 CAP and the actin cytoskeleton	6
1.7 The SH3 binding domain of CAP	8
1.8 Multimerisation domain	8
1.9 Structure of CAP	9
1.10 Localisation of CAP proteins and their role in cell growth	10
1.11 Role of CAP in cell elongation and development	10
1.12 Role of CAP in vesicle trafficking and endocytosis	11
1.13 Aim of the work	12

2 Materials and Methods

Abbreviations	13
---------------	----

2.1 Materials

2.1.1 Enzymes, inhibitors and antibodies	15
2.1.2 Reagents	16
2.1.3 Kits	18
2.1.4 Bacterial host strains	18
2.1.5 Media for <i>E. coli</i> culture	18
2.1.6 Eukaryotic cells	19
2.1.7 Media for cell culture	19
2.1.8 Vectors	20
2.1.9 Oligonucleotides	20
2.1.10 Buffers and other solutions	21
2.1.11 Materials	22
2.1.12 Instruments	22
2.1.13 Computer programs	23

2.2 Molecular biological methods

2.2.1 Plasmid-DNA isolation from <i>E. coli</i> by alkaline lysis miniprep	23
2.2.2 Plasmid-DNA isolation with a kit from Macherey-Nagel	24

2.2.3 Genomic DNA Isolation from ES cells and Balb/c Tail	24
2.2.4 DNA agarose gel electrophoresis	24
2.2.5 Southern blotting	25
2.2.6 Isolation of total RNA from mouse tissue with RNeasy Mini/Midi kit	25
2.2.7 RNA isolation from Tissue culture cells.TRI Reagent method.	26
2.2.8 RNA formaldehyde agarose gel electrophoresis	26
2.2.9 Sample preparation for electrophoresis	26
2.2.10 Formaldehyde agarose gel preparation	26
2.2.11 Northern blotting	27
2.2.12 Radiolabelling of DNA	27
2.2.13 Chromatography through Sephadex G-50 spin column	28
2.2.14 Hybridisation of Northern blots with radiolabelled DNA probe	28
2.2.15 Elution of DNA fragments from agarose gels	29
2.2.16 Measurement of DNA and RNA concentrations	29
2.2.17 Restriction digestion of DNA	29
2.2.18 Dephosphorylation of 5'-ends of linearised vectors	29
2.2.19 Creation of blunt ends	30
2.2.20 Ligation of vector- and DNA-fragments	30
2.2.21 Ligation of polylinker and DNA-fragments	30
2.2.22 Polymerase chain reaction (PCR)	30
2.2.23 Transformation of <i>E. coli</i> cells with plasmid DNA	31
2.2.24 Removal of the stop codon in the CAP2 cDNA by PCR technique	31
2.3 Protein biochemical methods	
2.3.1 Extraction of protein homogenate from mouse tissues and cell cultures	31
2.3.2 Cell fractionation	32
2.3.3 Expression of recombinant 6xHis-tag protein	32
2.3.4 Urea Extraction of the N-terminal CAP2	33
2.3.5 Ni-NTA-pull down of tissue lysates	33
2.3.6 Immunoprecipitation with polyclonalCAP2 antibody and monoclonal GFP antibody	34
2.3.7 Affinity purification of polyclonal antibodies by blot method	35
2.3.8 SDS-polyacrylamide gel electrophoresis	35
2.3.9 Gradient gel electrophoresis	36
2.3.10 Coomassie blue staining of SDS-polyacrylamide gels	37

2.3.11	Drying of SDS-polyacrylamide gels	37
2.3.12	Western blotting using the semi-dry method	37
2.3.13	Ponceau S staining of western blots	38
2.3.14	Immunodetection of membrane-bound proteins	38
2.3.15	Enzymatic chemiluminescence (ECL) detection system	39
2.3.16	BCIP/NBT colour development substrate reaction	39
2.4 Cell culture methods		
2.4.1	Preparation of mouse embryonic cardiomyocytes	40
2.4.2	Preparation of myofibrils	40
2.4.3	Staining of myofibrils	41
2.4.4	Immunofluorescence	41
2.4.5	Immunohistochemical staining of formalin-fixed paraffin-embedded sections	41
2.4.6	Microscopy	42
2.5 Disruption of the cytoskeleton using various drugs		
2.5.1	Digitonin experiment	42
2.6 Gene targeting protocols		
2.6.1	Target vector construction	43
2.6.2	Probe generation	43
2.6.3	Embryonic stem cell culture	43
2.6.4	MEF cell culture and Mitomycin treatment	44
2.6.5	ES cell culture	44
2.6.6	ES cell transfection	45
2.6.7	Antibiotic selection and picking of ES cell clones	45
2.6.8	Genomic DNA isolation	46
3.Results		
3.1	Analysis of the CAP2 (Cyclase associated protein 2) cDNA of <i>M. musculus</i>	47
3.2	Multiple alignment of the mouse CAP2 protein with different CAP homologues	47
3.3	Transcription pattern of CAP2	50
3.4	Generation of the polyclonal antibody for CAP2	50
3.5	Characterization of the CAP2 antibody	51
3.6	CAP2 over-expression studies in HEK 293 cells	53
3.7	CAP2 interacts with CAP1	54
3.8	Analysis of distribution of CAP2 in tissues and cell lines by western blotting	55
3.9	Search for binding partners of CAP2	56

3.10 CAP2 localisation in skeletal muscle	57
3.11 CAP2 localisation in mouse skin	59
3.12 Expression of CAP2 in brain	61
3.13 Analysis of expression of CAP2 in different parts of the adult and newborn mouse brain by western blotting	63
3.14 Localization of CAP2 in rat primary cerebellar cultures	64
3.15 Expression of CAP2 in rat primary glia cells	65
3.16 Localization of CAP2 in Heart	66
3.17 Expression of the CAP2 in primary cardiomyocytes	67
3.18 Expression of CAP2 in HL-1, a cardiomyocyte cell line	68
3.19 Expression of CAP2 in Primary rat vascular smooth muscle cells (ratVSM)	69
3.20 Expression of CAP2 in myofibrils	70
3.20.1 CAP2 does not localize to the A-bands in the myofibrils	70
3.20.2 CAP2 does not localize to the Z-bands of the myofibrils	71
3.20.3 CAP2 localizes to the M-bands of the myofibrils	72
3.21 Expression of CAP2 in a 16-day-old mouse embryo	73
3.22 Localization of CAP2 in PAM 212 (mouse keratinocytes)	73
3.23 CAP2 localization in PAM212 cells fixed with paraformaldehyde	75
3.24 Sub cellular fractionation of PAM212 cells	75
3.25 Influence of cytoskeletal drugs on the subcellular distribution of CAP2	76
3.25.1 Nuclear localization of CAP2 is not affected by drug disrupting microfilament cytoskeleton	76
3.25.2 Nuclear localization of CAP2 is affected by drug disrupting microtubule cytoskeleton	77
3.26 CAP2 is also a component of the nuclear membrane	78
3.27 An overview of nuclear staining in PAM212 cells	79
3.28 Expression of CAP2 in Primary mouse keratinocytes	80
3.29 Expression of CAP2 in Primary human keratinocytes	81
3.30 Role of CAP2 in wound healing	82
3.31 CAP2 interacts with Actin cross-linking filament like protein, ACF7	83
3.32 CAP2 partially co-localizes with ACF7 in COS7 cells	84
3.33 Expression of ACF-7 in PAM212 cells	85
3.34 Expression of ACF-7 in primary mouse keratinocytes	86
3.35 Generation of a CAP2 mouse mutant	86

3.35.1. Analysis of the structure of the mouse CAP2 gene	87
3.35.2 Construction of the targeting vector (CAP2 KO)	88
3.35.3 ES cell transfection and screening	89
4.Discussion	
4.1 Comparison of the CAP2 protein sequence with its homologues	91
4.2 CAP2 tissue distributions and its role	92
4.3 CAP2 associates with the cardiac myofibrils	95
4.4 Over expression of CAP2 in mammalian cells	96
4.5 CAP2 interacts with CAP1	97
4.6 CAP2 and its interacting partners	98
4.7 CAP2 in PAM212 and other primary cell culture	99
4.8 Genomic analysis of CAP2 and its Knockout	103
4.9 Future directions	103
Summary	105
Zusammenfassung	107
Bibliography	108
Erklärung	
Curriculum Vitae	
Lebenslauf	

Introduction

1 INTRODUCTION

1.1 The cytoskeleton

The cytoskeleton is composed mainly of three types of filaments, microfilaments, microtubules and intermediate filaments. Microfilaments are fine, thread-like protein fibers, 7-9 nm in diameter. They are composed predominantly of actin, which is the most abundant cellular protein, often amounting 10 to 20 percent of the total cytoplasmic proteins. Actin exists either as a globular monomer (called G-actin) or as a filament (designated F-actin), the latter formed by head-to-tail polymerisation of asymmetric monomers. Microfilaments in association with the protein myosin are responsible for muscle contraction. They can also carry out cellular movements including gliding, contraction, and cytokinesis.

Microtubules are cylindrical tubes, 20-25 nm in diameter. They are composed of alpha and beta tubulin. Microtubules act as a scaffold to determine cell shape and provide a set of "tracks" for cell organelles and vesicles to move on. Microtubules also form the spindle fibers for separating chromosomes during mitosis. When arranged in geometric patterns inside flagella and cilia they are used for locomotion.

The intermediate filaments average 10 nm in diameter and thus are "intermediate" in size between actin filaments (8 nm) and microtubules (25 nm). There are five major types of intermediate filaments each constructed from one or more proteins characteristic of it. Despite their chemical diversity, intermediate filaments play similar roles in the cell, providing a supporting framework within the cell. For example, the nucleus is held within the cell by a basketlike network of intermediate filaments made of proteins called keratins whereas lamins line the nuclear membrane inside the nucleus. Intermediate filaments also anchor the thick and thin filaments of muscle cells in a fixed position and provide mechanical strength to the long axons found in some neurons.

1.2 The actin cytoskeleton

Actin is a moderate sized protein consisting of approximately 375 residues, which is encoded by a large, highly conserved gene family. Some single-celled eukaryotes like yeast have a single actin gene, whereas many multicellular organisms contain many actin genes. For example, humans have six actin genes and some plants have as many as 60. Each actin molecule contains a Mg^{2+} ion complexed with either ATP or ADP. Thus there are four states of actin: ATP-G-actin, ADP-G-actin, ATP-F-actin and ADP-F-actin. Two of these forms, ATP-G-actin and ADP-F-actin predominate in a cell. The addition of ions, Mg^{2+} , K^+ or Na^+ to

a solution of G-actin will induce the polymerisation of G-actin into actin filaments. This process is also reversible: F-actin depolymerises into G-actin when the ionic strength of the solution is lowered. All subunits in a filament point towards the same filament end. Consequently, at one end of the filament, by convention designated minus end or pointed end, the ATP-binding cleft of an actin subunit is exposed to the surrounding solution and at the opposite end, the plus end or barbed end, the cleft contacts the neighbouring actin subunit. The actin cytoskeleton is organized into bundles and networks of filaments, which are the most common arrangements of actin filaments in a cell. Functionally, bundles and networks have identical roles in a cell: both provide a framework that supports the plasma membrane and therefore determines a cell's shape. Structurally, bundles differ from networks mainly in the organization of actin filaments. In bundles the actin filaments are closely packed in parallel arrays, whereas in a network the actin filaments crisscross, often at right angles, and are loosely packed. In all bundles and networks, actin cross-linking proteins hold the filaments together. The length and flexibility of a cross-linking protein determines whether bundles or networks are formed.

1.3 Actin and actin binding proteins

Actin binding proteins are classified according to their actin binding function. Actin filament severing proteins fragment filaments by mechanisms that do not require the hydrolysis of ATP. The purpose of this severing activity is probably to introduce a device whereby existing actin filament structures may be removed or remodelled to form other structures within the cell. So far, two major groups of actin severing proteins have been identified. The gelsolin group is the archetype of the group of actin binding proteins that sever and cap the fast growing barbed end of actin filaments and that initiate the polymerisation of new filaments by forming a nucleus (Yin et al., 1988; Weeds et al., 1993). The second group, the Actin depolymerising factor (ADF)/Cofilin group comprises low molecular weight actin filament severing proteins which in addition possess actin monomer binding activity.

Actin filaments grow by monomer addition exclusively at their ends, particularly barbed ends. Filament capping proteins like radixin (Funayama et al., 1991) and tensin (Davis et al., 1991) bind to the barbed ends of filaments in cells and are therefore essential for the control of actin polymerisation within the cells or within the local regions of individual cells. DNaseI (Podolski et al., 1988) and tropomodulin (Fowler et al., 1993) are actin-binding proteins that bind to the pointed ends.

Regulation of the actin cytoskeleton is essential for many normal cellular processes such as cell motility and platelet activation (Lauffenburger et al., 1996; Shattil et al., 1994; Zigmond et al., 1996). The actin cytoskeleton is also rearranged in some disease states such as oncogenic transformation (Collard et al., 1996). Signals from growth factors and oncogenes regulate the assembly of cytoskeletal structures through small G proteins. Ras and Rac both stimulate lamellipodia, sheets of microfilaments localized to the periphery of the cell. Rho regulates stress fibers, long parallel arrays of microfilaments and Cdc42 regulates both (Hall et al., 1998).

A major mechanism underlying the actin dynamics is the selective polymerisation of G-actin into F-actin (Carrier et al., 1991). In vitro, at low actin concentrations only G-actin is observed. Once the actin concentration is raised above about 0.1 μM , in physiological salt conditions, it spontaneously polymerises into F-actin and continues to polymerise until the G-actin levels again reach 0.1 μM . Similarly, if actin filaments are diluted they will depolymerise until the concentration of G-actin is raised to 0.1 μM . Thus, the concentration of G-actin is maintained at a level known as the critical concentration. In cells, about half of the actin resides as G-actin despite being present in concentrations greater than 100 μM , far in excess of the critical concentration (Carrier et al., 1997). The G-actin is prevented from polymerising by several classes of actin binding proteins. Capping proteins such as gelsolin, Cap Z and tropomodulin bind F-actin ends to prevent the addition of G-actin (Coluccio et al., 1994; Hartwig et al., 1995; Nachmias et al., 1996; Weber et al., 1994). In addition, actin sequestering proteins such as profilin, thymosin β 4 and CAP1 (mammalian cyclase associated protein; ASP-56) bind G-actin and prevent it from polymerising spontaneously (Gieselmann et al., 1992; Safer et al., 1991; Sun et al., 1995).

CAP is an evolutionarily highly conserved protein. It belongs to the class of G-actin binding proteins and may regulate the pool of actin monomers. CAP (also known as Srv2p), was first identified as a *Saccharomyces cerevisiae* protein that was co-purified with adenylyl cyclase (Fedor-Chaiken et al., 1990; Field et al., 1990). To date, the majority of studies addressing the biological function of CAP come from studies in *S. cerevisiae*. The CAP homologues have molecular weights between 56 kDa for the mammalian homologue and 70kDa for the yeast protein. Mammals have at least two different CAP proteins, CAP1 and CAP2, which share 64% amino acid identity (Swiston et al., 1995; Yu et al., 1994).

1.4 Domain structure and function of CAP

CAP of all the organisms has a conserved domain structure. They consist of two functional domains separated by a proline-rich region, which might act as SH3-binding domain. The amino-terminal domain mediates RAS signalling through adenylyl cyclase in yeast, where it was identified as cyclase associated protein, while the carboxy-terminal domain is involved in the regulation of the actin cytoskeleton and affects the regulation of cell growth and morphogenesis in yeast. At the biochemical level two separate functions could be demonstrated: The domains bind directly to actin and are responsible for dimerisation. In the C-terminal domain a WH2 domain (WH2=WASP Homology 2) is located and the very C-terminus is required for dimerisation. WH2 domains bind to G-actin, however the function of the WH2 domain in CAP is not clearly known. (Paunola E et al., 2002).

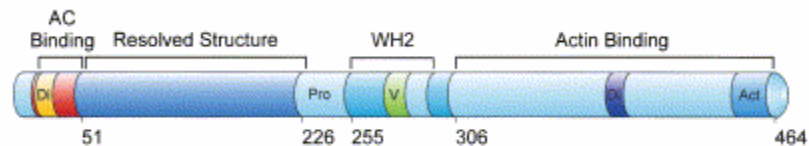


Figure 1: Schematic diagram of the domain structure and organisation of functions of *Dictyostelium discoideum* CAP. CAP has a highly conserved domain structure (Gottwald et al., 1996; Hubberstey and Mottillo 2002; Paunola et al., 2002). An adenylate cyclase binding domain (AC) and a dimerization domain (Di) are located at the amino terminus and are followed by the proline-rich region (Pro) and the WH2 domain, which includes a highly conserved verprolin homology region (V). At the carboxyl terminus is an actin binding domain (Act) and a second dimerization site (Di). (Taken from Ksiazek et al., 2003)

1.5 Interaction of CAP with adenylyl cyclase

Adenylyl cyclase from *S. cerevisiae* contains at least two subunits, a 200 kDa catalytic subunit and a subunit with an apparent molecular mass of 70.000, which has now been called cyclase-associated protein (CAP). A cDNA encoding CAP has been cloned by screening a yeast cDNA expression library in *E. coli* with antisera raised against the purified protein. The cDNA contained an open reading frame encoding a 526 amino acid protein. Adenylyl cyclase activity in membranes from cells that lack CAP is not stimulated by RAS2 protein in vitro. These results suggested that CAP is required for at least some aspects of the RAS-responsive signalling system (Field et al., 1990). The first CAP gene (also called SRV2) was isolated in *Saccharomyces cerevisiae* as a suppressor of the activated RAS2^{Val19} allele (Fedor-Chaiken et al., 1990).

Later on it was shown that the N-terminus of CAP binds adenylyl cyclase to facilitate activation by RAS (Gerst et al., 1991; Mintzer et al., 1994; Shima et al., 1997). In yeast, adenylyl cyclase (CYR1) is a major downstream effector of RAS1 and RAS2, which are

structural, functional, and biochemical homologues of mammalian Ras (Broach et al., 1990; Casey et al., 1994). Further investigations suggested that the N-terminal region of CAP binds to the C-terminal region of CYR1, and this association appeared to be required for the proper in vivo response to Ras. Although the mechanism of regulation of the Ras-CYR1 pathway by CAP was unknown, it has been recently reported that the association with the CAP N-terminal region is essential for the efficient activation of CYR1 by a modified Ras and the effect of CAP was successfully reconstituted in vitro by the purified components only (Shima et al., 1997). These findings suggested that CAP might mediate the stimulatory effect of the modified Ras on CYR1 activation. For the interaction of CAP, RAS2 and adenylyl cyclase a small segment comprising the N-terminal 36 amino acid residues of CAP is sufficient for association with adenylyl cyclase as well as for its function in the Ras-adenylyl cyclase pathway as assayed by the ability to confer RAS2 (Val-19)-dependent heat shock sensitivity to yeast cells. The CAP-binding site of adenylyl cyclase was mapped to a segment of 119 amino acid residues near its C terminus. Both of these regions contained tandem repetitions of a heptad motif $\alpha\text{XX}\alpha\text{XXX}$ (where α represents a hydrophobic amino acid and X represents any amino acid), suggesting a coiled-coil interaction. When mutants of CAP defective in associating with adenylyl cyclase were isolated by screening of a pool of randomly mutagenized CAP, they were found to carry substitution mutations in one of the key hydrophobic residues in the heptad repeats. Furthermore, mutations of the key hydrophobic residues in the heptad repeats of adenylyl cyclase also resulted in loss of association with CAP. These results indicate the coiled-coil mechanism as a basis of the CAP-adenylyl cyclase interaction. (Nishida et al., 1998).

The relevance of these findings for other species is not yet certain. *S. Pombe* CAP can suppress the phenotypes associated with deletion of the C-terminal CAP domain in *S. cerevisiae* but does not suppress the phenotypes associated with deletion of the N-terminal domain (Kawamukai et al., 1992). Furthermore, in *Candida albicans* differences in cAMP responses of the *cap1/cap1* mutant from those of isogenic *CAP1* strains indicate that CAP1 regulates adenylate cyclase activity. cAMP or its membrane-permeable derivative, dbcAMP, partially restored filamentation and enhanced hypha production of the *cap1/cap1* mutant strain, further confirming that CAP1 acts through regulation of cAMP levels (Bahn et al., 2001). In Hydra (*Chlorohydra viridissima*), CAP appears to be involved as a mediator for transducing the signal from the transmembrane HA (head activator) receptor to the cAMP system. Hydra CAP is expressed abundantly in interstitial and epithelial cells. The effect of HA, but not of cAMP, on nerve-cell differentiation was inhibited by pretreatment of Hydra

with a CAP antisense oligonucleotide, suggesting a role for CAP as a mediator in the signal transduction cascade between HA and cAMP (Fenger et al., 1994). In addition to that and most likely independent of RAS signalling, CAP is required to maintain the integrity of the actin cytoskeleton.

1.6 CAP and the actin cytoskeleton

The loss of CAP causes abnormal yeast morphologies and disrupts the actin cytoskeleton. The actin associated phenotypes are partially restored by overexpression of the C-terminus of CAP or the G-actin sequestering protein profilin. Expression of the human CAP in *S. cerevisiae* also suppresses the phenotypes associated with loss of the C-terminal domain of CAP but does not suppress the phenotypes associated with loss of the N-terminal domain. Thus, CAP proteins have been structurally and, to some extent, functionally conserved in evolution between yeasts and mammals (Matviw et al., 1992; Gerst et al., 1991; Vojtek et al., 1991). Apart from that, several homologues have been shown to bind actin directly and, when expressed in yeast, suppress the cytoskeletal phenotypes of *cap* knockout yeast. This suggests that actin sequestering is conserved in all CAP homologues (Gottwald et al., 1996; Hubberstey et al., 1996; Matviw et al., 1992; Vojtek et al., 1993; Yu et al., 1994; Zelicof et al., 1993). Furthermore, the first mammalian homologue of CAP1, ASP-56, was isolated through a search for actin monomer binding proteins (Gieselmann and Mann, 1992). ASP-56 (porcine CAP) could bind actin with a 1:1 stoichiometry and could inhibit actin polymerisation as measured by falling ball viscometry and fluorescently labelled actin polymerisation assays. Similarly, *Dictyostelium discoideum* CAP has been shown to sequester monomeric actin by inhibiting in vitro actin polymerisation in a Ca^{2+} -independent manner with a 1:1 stoichiometry (Gottwald et al., 1996). This sequestering activity of CAP was restricted to the carboxyl-terminal 210 amino acids; the presence of the amino-terminal 215 amino acids had no effect on actin polymerisation (Gottwald et al., 1996). *S. cerevisiae* CAP has been shown to bind G-actin in vitro with a $K_d = 0.4 \mu\text{M}$, equivalent to the binding coefficient of another actin sequestering protein, thymosin β_4 , to platelet actin (Freeman et al., 1995; Weber et al., 1992). Moreover, immunoprecipitates of yeast and mammalian CAPs contain actin, suggesting that CAP is bound to actin in vivo (Vojtek et al., 1993; Amberg et al., 1995).

The carboxyl-terminus of all well-characterized CAPs shows the greatest degree of conservation of any functional domain (Hubberstey et al., 2002). However, the specific residues involved in actin binding have not been characterised, although a comparison of the carboxyl-terminal domains of all reported CAPs reveals four highly conserved regions. A

short deletion of the carboxyl-terminal 27 amino acids eliminated actin binding in *S. cerevisiae* and human CAP (Amberg et al., 1995; Zelicof et al., 1996). Within this region lies a stretch of 7 amino acids comprising the site E(X)₃PEQ. The residues E, P, E, and Q are present in all CAP proteins analysed except the two plant CAPs, which have a substitution of a glutamine for the second glutamate residue. It is not clear so far whether these or other carboxyl-terminal residues are critical for actin binding.

Recent experiments with *Drosophila* CAP have detected a region just downstream from the SH3 binding domain that shows similarity to the verprolin homology domain (LKKAET) found in a variety of actin binding proteins e.g., thymosin, fimbrin, and α -actinin (Vaduva et al., 1997). Verprolin homology domains are also found in members of the WASp family of proteins, known to bind monomeric actin, and interact with and activate the Arp2/3 complex (Rohatgi et al., 1999). It has recently been reported that actin binding protein Abp1p, a protein originally isolated from yeast that interacts with F-actin and activates the Arp2/3 complex, interacts with CAP through its SH3 domain (Drubin et al., 1988; Lila et al., 1997; Goode et al., 2001). Though intriguing, there is no evidence that CAP participates in Arp2/3-mediated nucleation of actin filaments.

It has been shown that phosphatidylinositol 4,5-bisphosphate (PIP₂) can promote the availability of monomeric actin for polymerisation. Addition of PIP₂ at a high molar ratio of CAP to PIP₂ (1:40) inhibited sequestration of actin (Gottwald et al., 1996), suggesting that PIP₂ negatively regulates the CAP-actin interaction, causing the release of G-actin from CAP and consequently F-actin assembly. The carboxyl-terminal domain alone was unaffected by PIP₂ addition, implying that the phospholipid binding site resides within the amino or polyproline domains (Gottwald et al., 1996). The negative effect of PIP₂ on CAP-actin interaction correlates with the positive effect of PIP₂ on activating WASp, which can stimulate actin nucleation by the Arp2/3 complex (Higgs et al., 2000). Therefore, the CAP data support a positive role for PIP₂ in promoting actin polymerisation. However, more studies are needed to determine whether phospholipid regulation of CAP-actin binding is conserved in higher eukaryotes.

Conservation in the carboxyl-terminal domain in all CAPs together with the high degree of conservation in the actin structure and function throughout the evolution suggests that a conserved role in G-actin binding is likely for all CAPs. An important point not yet addressed is whether CAP has a differential affinity for specific actin isoforms within the cell and whether the presence of specific isoforms in specific cell types may affect and potentially control CAP function. No information exists on how the interaction between CAP and actin is

regulated during the activation of signalling cascades. A very recent finding suggests that CAP promotes cofilin-dependent actin turnover in vitro and in vivo (Moriyama and Yahara 2002) and the evidence provided by the findings of Bertling et al. (2004) indicates that CAP promotes rapid actin dynamics in conjunction with ADF/cofilin and is required for several central cellular processes in mammals. It has also been reported that *S. cerevisiae* CAP binds with strong preference to ADP-G-actin (K_d 0.02 μ M) compared with ATP-G-actin (K_d 1.9 μ M) and competes directly with cofilin for binding ADP-G-actin monomers, allows rapid nucleotide exchange to occur on actin, and then because of its 100-fold weaker binding affinity for ATP-actin compared with ADP-actin, allows other cellular factors such as profilin to take the handoff of ATP-actin and facilitate barbed end assembly. These findings suggest that CAP plays an important role in the actin based cellular processes.

1.7 The SH3 binding domain of CAP

A centrally located proline-rich region is conserved in all CAP homologues. In yeast, this domain can be subdivided into two regions, the P1 and the P2 sites. The P1 site, found in almost all homologues, contains a 10 to 12 amino acid stretch composed almost entirely of proline. The P2 region contains a consensus SH3 binding motif (PXXP), binds SH3 domains in vitro, and is required to direct CAP to cortical actin patches (Freeman et al., 1996; Yu et al., 1999). In yeast, Abp1p has been proposed to target CAP to actin cortical patches through its SH3 domain (Lila et al., 1997). In vitro, human CAP1 also binds SH3 domains such as the one of human c-Abl, but binding is observed only at the P1 site and its effects on localisation are not known (Freeman et al., 1996). Since interaction of full-length CAP and c-Abl has not been shown, the significance of this interaction is unclear. However, the important role that c-Abl plays in signalling actin reorganization (Lanier et al., 2000) implies that an interaction between c-Abl and CAP may have important consequences and be biologically relevant. Further support for the role of Abl in CAP function has recently been reported in *Drosophila* (Baum et al., 2001). The mammalian P1 sequence can also bind to profilin in vitro, but the biological significance of the binding is not known (Lambrechts et al., 1997). Moreover, CAP was also shown to act antagonistically with Ena, a member of the Ena/VASP family of proteins that catalyse F-actin formation (Gertler et al., 1995).

1.8 Multimerisation domain

Many reports have shown that CAP can form multimeric complexes with itself (Zelicof et al., 1996; Yu et al., 1999; Hubberstey et al., 1996). Surprisingly, a single dimerisation motif has

not been defined, although it appears that a region in the amino terminus adjacent to the adenylyl cyclase binding site in yeast CAP is important for multimerisation (Yu et al., 1999). The function of this interaction domain is complex, since two-hybrid screens demonstrate that the amino-terminal domain of human CAP (amino acids 1–228) interacts with itself as well as with the carboxyl-terminal domain (amino acids 253–475). Likewise, the carboxyl-terminus interacts with itself and with the amino terminus (Hubberstey et al., 1996). This suggests that at least two binding sites exist within CAP that mediate its interaction. One caveat to these two-hybrid results is the presence of endogenous yeast CAP in cells used in the two-hybrid analysis. Since human and yeast CAP can interact with each other (Zelicof et al., 1996; Hubberstey et al., 1996), yeast CAP could be acting to bridge the interactions between expressed human CAP domains in yeast. The potential interfering properties of endogenous CAP were eliminated by co expressing a GFP-CAP and an untagged CAP in a *cap* yeast strain (Yu et al., 1999). Using this in vivo system, an amino-terminal domain was discovered that inhibited CAP multimer formation. Mutations in this amino-terminal domain also prevented proper localisation of the protein, suggesting that multimer formation and localisation may be linked. Human CAP1 and CAP2, which have an identity of 64% at the amino acid level, can form heteromeric complexes in vivo that may impart specific functional characteristics yet to be revealed (Hubberstey et al., 1996). It is unclear whether CAP proteins form dimers or higher order structures. A prediction of higher order structures comes from the observation that in fractionation profiles from yeast, CAP eluted between 11.3 and 19.5 S (670 kDa), with higher CAP levels present in the latter fractions (Shirley Yang et al., 1999). Recent report suggests that native Srv2 complex (~ 600kDa) isolated from *S. cereveciae* is found to be comprised of only two proteins, actin and Srv2/CAP, present in a 1:1 M ratio (Balcer et al., 2003). This suggests that CAP either forms a multimeric structure larger than a dimer or forms stable complexes with other proteins.

1.9 Structure of CAP

Recent studies on crystal CAP structure revealed that CAP has α helices and β -strands. The NMR characterization of the amino-terminal domain of CAP (CAP (1-226)) from *Dictyostelium discoideum* indicates that the first 50 N-terminal residues are unstructured and that this highly flexible serine-rich fragment is followed by a stable, folded core starting at Ser 51. The NMR structure of the folded core is an alpha-helix bundle composed of six antiparallel helices, in stark contrast to the recently determined CAP C-terminal domain structure, which is solely built by beta-strands (Mavoungou et al., 2004). The crystal structure

of the C-terminal dimerisation and actin monomer binding domain (C-CAP) reveals a highly unusual dimer, composed of monomers possessing six coils of right-handed beta-helix flanked by antiparallel beta-strands. The unusual right-handed beta-helical fold present in C-CAP appears to support a wide range of biological functions (Didatko et al., 2004).

1.10 Localisation of CAP proteins and their role in cell growth

S. Cerevisiae has provided the most detailed analysis of CAP localization. CAP is localized through its poly-proline domain to the cortical actin patches, where active actin turnover takes place (Lila et al., 1997; Freeman et al., 1996; Yu et al., 1999). In higher eukaryotes, CAP is a cytoplasmic protein, but its precise localisation is species specific. *D. discoideum* CAP has been localised near the plasma membranes in resting cells and is remobilised during cell movement (Noegel et al., 1999). Using GFP-tagged CAP deletions, the amino-terminal domain is localised to the plasma membranes whereas carboxyl-terminal domains showed a diffuse cytoplasmic staining, indicating that proper localisation of CAP is domain dependent (Noegel et al., 1999). *Dictyostelium* cells deficient in CAP showed enlarged cell size and defects in cytokinesis and fluid phase endocytosis.

In mammalian cells, CAP is diffusely distributed throughout the cytoplasm and can concentrate at the cell membrane and lamellipodia of migrating fibroblasts (Vojtek et al., 1993; Zelicof et al., 1996; Freeman et al., 2000). Monoclonal antibodies to human CAP1 were recently used to show that human CAP1 colocalised with stress fibers in Swiss 3T3 fibroblasts (Freeman et al., 2000). Microinjection of anti-CAP1 antibodies attenuated stress fiber formation in response to serum stimulation and microinjection of purified CAP1 promoted the formation of actin stress fibers (Freeman et al., 2000). Additional experiments are required to confirm the association of stress fibers with human CAP1. Generally, perturbation of CAP levels in mammalian cells appears to influence the actin dynamics.

1.11 Role of CAP in cell elongation and development

In cotton plants, CAP mRNA has been shown to be highly expressed in young fiber cells vs. other tissues (Kawai et al., 1998). Cotton fibers are outgrowths of single epidermal cells from the integument of ovules in the developing fruit. During production of these fibers, individual cells elongate dramatically to >1000-fold longer than their diameter without undergoing cell division (Meinert et al., 1997). The cytoskeletal proteins actin, tubulin, spectrin, and the intermediate filament protein vimentin are all present during differentiation, and the dynamic regulation of cytoskeletal architecture is essential for fiber elongation to occur.

Analysis of CAP1 and CAP2 mRNA levels in adult rat tissues reveals a marked difference in expression patterns between the two genes (Swiston et al., 1995), which suggests that CAP1 and CAP2 have distinct functional roles and that CAPs are not simply ubiquitous housekeeping genes. The study of CAP transcriptional regulation will undoubtedly shed light on essential functions of CAP in regulating cytoskeletal architecture during development and throughout the adult life.

A recent clue about the role CAP proteins play in development has come from studies of *Drosophila* (Baum et al., 2000; Benlali et al., 2000). These papers have been the subjects of a recent mini review (Stevenson et al., 2000). *Drosophila* CAP (named Act Up-*acu*) was isolated while screening for mutations that disrupt eye development (Benlali et al., 2000). *Drosophila* cells lacking *cap/acu* show increased amounts of actin filaments during eye differentiation as well as defects in the formation of the morphogenetic furrow of the eye imaginal disc, which undergoes a dramatic shape change before neuronal differentiation. *Drosophila cap* mutants were also isolated that were defective in establishing and maintaining oocyte polarity (Baum et al., 2000). CAP (*capulet*) was found to be concentrated in the oocyte, where it functions to inhibit actin accumulation. Mutants in protein kinase A (PKA) in *Drosophila* mirror some of the *cap* mutant phenotypes (i.e. loss of nurse cell cortical actin), and actin defects are enhanced in *cap pka* double germline clones. Therefore, PKA and CAP may be involved in identical pathways that are controlled by cAMP production. It will be interesting to determine whether PKA pathways control CAP activity in vertebrates as well.

The *Drosophila* studies support the role of CAP in eye development and maintaining polarity during early cell differentiation. The *Dictyostelium* studies with the CAP mutant exhibiting poor polarisation behaviour and reduced levels of cGMP and a phototaxis defect (Noegel et al., 2004) suggest that CAP may play a critical role in cell polarity and movement in a diversity of organisms. It is intriguing to speculate that one of the conserved functions of CAP is to control developmental processes that involve cell elongation, migration, movement, and polarity orchestrated by changes in the actin cytoskeleton. On the other hand, CAP plays a role during the adult life, since CAP has been shown to be expressed in a wide variety of adult mammalian tissues (Swiston et al., 1995; Vojtek et al., 1993).

1.12 Role of CAP in vesicle trafficking and endocytosis

The link between the actin cytoskeleton and endocytosis has been well established in lower eukaryotes such as yeast. Recent studies have elucidated the possible role(s) the actin

cytoskeleton plays during endocytosis in mammals. One candidate protein that may link the actin cytoskeleton to endocytosis is mammalian Abp1 (mAbp1) (Kessels et al., 2001).

The first evidence that CAP may be involved in endocytic events was the isolation of a yeast synaptobrevin homologue *SNCI* that could partially suppress *cap* phenotypes (Gerst et al., 1991). More recently, yeast CAP/Srv2p has been shown to be synthetically lethal with *SLA2* in *S. cerevisiae* (Lila et al., 1997). Sla2p is essential in yeast and is involved in the cortical cytoskeleton. CAP may link to a dynamin-mAbp1 complex since yeast CAP can interact with Abp1p in yeast. Yeast CAP (*SRV2*) has been implicated indirectly in endocytic regulation. By screening mutants deficient for endocytosis, a recessive negative form of *SRV2* that was unable to internalise pheromone was discovered (Wesp et al., 1997). Surprisingly, a mutant bearing a complete deletion of *SRV2* was not deficient for endocytosis, suggesting that the mutant form of CAP was causing a disruption of a multiprotein complex (potentially mediated through Abp1p) that inhibited actin regulation and thereby disrupted endocytosis. Rvs167p, a yeast homologue of the mammalian amphiphysin proteins which are key regulators of endocytosis in mammalian cells (Wesp et al., 1997) can interact with Abp1p and recently was shown to interact with a multitude of yeast proteins involved in the actin cytoskeleton and endocytosis in a two-hybrid screen, including Sla2p, CAP, and Act1p (Drees et al., 2001). Therefore, a complex consisting of CAP, Abp1p, Sla2p, and Rvs167p may regulate cytoskeletal turnover during endocytic events.

1.13 Aim of the work

Although CAP proteins have been studied for more than a decade and are present in all organisms, many questions remain unanswered about the mechanisms of CAP function. The role of mammalian CAP2 proteins has not been studied extensively. We are interested in the homologue of mammalian CAP that is CAP2. Our goal is to study CAP2 of Mouse and to assign its exact function. For this purpose we are currently generating a mice knock out strain for this protein in order to learn more about the functions of this protein using a conventional knock out strategy. Furthermore, a detailed study of CAP2 expression in the mouse embryo and in the adult mouse is planned. It has been reported that CAP interacts with itself and its homologue in humans. So we are interested to study the interaction of CAP2 and its homologue in mouse. As CAP is reported to play a role in different cellular processes, we are interested in dissecting the role of CAP2 by identifying its interacting partners and to shed a light on its mechanism of action as well.

Materials and Methods

2 MATERIALS AND METHODS

Abbreviations

AP	alkaline phosphatase
APS	ammonium persulphate
ATP	adenosine 5'-triphosphate
bp	base pair(s)
BCIP	5-bromo-4-chloro-3-indolylphosphate
BSA	bovine serum albumin
cAMP	cyclic adenosine monophosphate
cDNA	complementary DNA
CIAP	calf intestinal alkaline phosphatase
dNTP	deoxyribonucleotide triphosphate
DABCO	diazobicyclooctane
DEPC	diethylpyrocarbonate
DMSO	dimethylsulphoxide
DNA	deoxyribonucleic acid
DNase	deoxyribonuclease
DTT	1,4-dithiothreitol
ECL	enzymatic chemiluminescence
EDTA	ethylenediaminetetraacetic acid
EGTA	ethyleneglycol-bis (2-amino-ethylene) N,N,N,N-tetraacetic acid
ELISA	enzyme linked immunosorbent assay
ES	embryonic stem
G418	geneticin
HRP	horse radish peroxidase
IgG	immunoglobulin G
IPTG	isopropyl- β -D-thiogalactopyranoside
kb	kilo base pairs
β -ME	beta-mercaptoethanol
MEF	mouse embryonic feeder
MOPS	Morpholinopropanesulphonic acid
Mw	molecular weight

NBT	nitrobluetetrazolium
NP-40	nonylphenylpolyethyleneglycol
pNPP	para-nitrophenyl phosphate
OD	optical density
ORF	open reading frame
PAGE	polyacrylamide gel electrophoresis
PCR	polymerase chain reaction
PEG	polyethyleneglycol
PMSF	phenylmethylsulphonylfluoride
RT-PCR	reverse transcript polymerase chain reaction
RNA	ribonucleic acid
RNase	ribonuclease
rpm	rotations per minute
SDS	sodium dodecyl sulphate
TEMED	N,N,N',N'-tetramethyl-ethylendiamine
U	unit
UV	ultra violet
vol.	volume
v/v	volume by volume
w/v	weight by volume
X-gal	5-bromo-4-chloro-3-indolyl- β -D-galactopyranoside

Units of Measure and Prefixes

Unit	Name	Symbol	Prefix (Factor)
Ci	curie	k	kilo (10^3)
$^{\circ}\text{C}$	degree Celsius	c	centi (10^{-2})
kDa	Dalton	m	milli (10^{-3})
g	gram	μ	micro (10^{-6})
hr	hour	n	nano (10^{-9})
L	litre	p	pico (10^{-12})
m	meter		
min	minute		
s	sec		

goat-anti-mouse-IgG, Cy5-conjugated	Sigma
goat-anti-mouse-IgG, alkaline phosphatase conjugated	Sigma
goat-anti-mouse-IgG, Alexa 488 conjugated	Molecular Probes
goat-anti-rabbit-IgG, Alexa 568 conjugated	Molecular Probes
goat-anti-rabbit-IgG, FITC conjugated	Sigma
goat-anti-mouse-IgG, FITC conjugated	Sigma
goat-anti-mouse-IgM, Alexa 488 conjugated	Molecular Probes
biotinylated anti-rabbit IgG	Vector Laboratories
TRITC- Phalloidin	Sigma

Inhibitors

benzamidine	Sigma
DEPC (Diethylpyrocarbonate)	Sigma
PMSF (Phenylmethylsulfonyl fluoride)	Sigma
ribonuclease-inhibitor (RNAsin)	Promega
Complete Inhibitor-Cocktail	Roche

Antibiotics

ampicillin	Grünenthal
kanamycin	Biochrom
penicillin/streptomycin	Biochrom

2.1.2 Reagents

acrylamide	National Diagnostics
agarose (electrophoresis grade)	Life Technologies
acetone	Riedel-de-Haen
Bacto-Agar, Bacto-Pepton, Bacto-Trypton	Difco
BSA (bovine serum albumin)	Roth
chloroform	Riedel-de-Haen
calcium chloride	Sigma
Coomassie-brilliant-blue R 250	Serva
p-cumaric acid	Fluka
DAPI	Sigma

DMEM (Dulbecco's Modified Eagle's Medium)	Biochrom
DMF (dimethylformamide)	Riedel-de Haen
DMSO (dimethyl sulfoxide)	Merck
DTT (1,4-dithiothreitol)	Gerbu
EDTA ([ethylenedinitrilo]tetraacetic acid)	Merck
EGTA (ethylene-bis(oxyethylenitrilo)tetraacetic acid)	Sigma
ethanol	Riedel-de-Haen
ethidium bromide	Sigma
FCS (fetal calf serum)	Biochrom
formamide	Merck
formaldehyde	Sigma
glycine	Degussa
IPTG (isopropyl β -D-thiogalactopyranoside)	Sigma
isopropanol	Merck
β -mercaptoethanol	Sigma
methanol	Riedel-de-Haen
methylbenzoate	Fluka
mineral oil	Pharmacia
MOPS ([morpholino]propanesulfonic acid)	Gerbu
Ni-NTA agarose	Qiagen
Protein A agarose	Sigma
RNase A	Sigma
SDS (sodium dodecylsulfate)	Serva
sodium azide	Merck
TEMED (tetramethylethylenediamine)	Merck
Tris (hydroxymethyl)aminomethane	Sigma
Triton X-100 (t-octylphenoxypolyethoxyethanol)	Merck
X-Gal(5-bromo-4-chloro-3-indolyl- β -D-galactopyranoside)	Roth
yeast extract	Oxoid

Radionucleotides

α -³²P-deoxyadenosine-5'-triphosphate (10 mCi/ml) Amersham

Reagents not listed above were purchased from Clontech, Fluka, Merck, Roth, Serva, Sigma, Promega and Riedel-de-Haen, respectively.

2.1.3 Kits

Nucleobond PC 500	Macherey-Nagel
NucleoSpin Extract 2 in 1	Macherey-Nagel
NucleoSpin Plus	Macherey-Nagel
RNeasy midi kit	Qiagen
pGEMT easy Cloning Kit	Promega

2.1.4 Bacterial host strains

E. coli M15

E. coli DH5 α

E. coli XL1Blue

2.1.5 Media for *E. coli* culture

LB medium, pH 7.4 (Sambrook and Russell, 2001)

10 g bacto-tryptone

5 g yeast extract

10 g NaCl

adjust to pH 7.4 with 1 N NaOH

add H₂O to make 1 liter

For LB agar plates, 0.9% (w/v) agar was added to the LB medium and the medium was then autoclaved. For antibiotic selection of *E. coli* transformants, 50 mg/l ampicillin, kanamycin or chloramphenicol was added to the autoclaved medium after cooling it to approximately 50°C. For blue/white selection of *E. coli* transformants, 10 μ l 0.1 M IPTG and 30 μ l X-gal solution (2% in dimethylformamide) was spread per 90 mm plate and the plate was incubated at 37°C for at least 30 min before using.

SOC medium, pH 7.0 (Sambrook and Russell, 2001)

20 g bacto-tryptone, 5 g yeast extract, 10 mM NaCl, 2.5 mM KCl. Dissolve in 900 ml deionised H₂O, adjust to pH 7.0 with 1 N NaOH. The medium was autoclaved, cooled to approx. 50°C and then the following solutions, which were separately sterilized by filtration (glucose) or autoclaving, were added: 10 mM MgCl₂.6 H₂O, 10 mM MgSO₄.7 H₂O.

20 mM glucose, add H₂O to make 1 liter.

2.1.6 Eukaryotic cells

C3H/10T1/2 mouse fibroblasts

N2A mouse neuroblastoma cell line

COS-7 monkey SV40 transformed kidney cell line

C2F3 mouse myoblasts

C3H10T1/2 Fibroblast

ES cells (IB 10)& R1

PAM212 mouse keratinocytes

Mouse and human primary keratinocytes (kindly provided by Dept of Dermatology, Medical Faculty, University of Cologne)

HEK293 Human embryonic kidney cell line

Primary neuronal cell cultures and glia cell cultures were a kind gift from Dept of Physiological chemistry, University of Bonn

Rat VSM primary cell culture (kindly provided by Dr. Evren Caglayan, Department of Inner Medicine I, University of Cologne)

HL-1 cardiomyocytes cell line a kind gift from Prof William C. Claycomb, LSU, New Orleans, LA, USA.

2.1.7 Media for cell culture

COS7 (monkey kidney fibroblasts)- DMEM high glucose-500 ml, 10% FBS, 2 mM glutamine, penicillin/streptomycin

MB50 (human myoblasts)- DMEM low glucose-250 ml, Nutrient F10 medium –250 ml, 20% FBS, 2 mM glutamine, penicillin/streptomycin, basic fibroblast growth factor (bFGF).

Differentiation medium for MB50

DMEM low glucose-250 ml, Nutrient F10 medium -250 ml, 2% horse serum, 2 mM glutamine, penicillin/streptomycin

Human primary fibroblasts

Minimum Essential Medium (Gibco) 500ml, 10%FBS, penicillin/streptomycin, nonessential amino acids (6 ml), Bicarbonate (Gibco)(7.5%), glutamine.

Neuroblastoma cells (N2A)

DMEM low glucose 500ml, 10% FBS, nonessential amino acids, 2 mM glutamine, penicillin/streptomycin.

10T1/2 mouse fibroblasts

DMEM low glucose-500 ml, 10% FBS, 2 mM glutamine, penicillin/streptomycin

PAM212

DMEM high glucose-500 ml, 10% FBS, 2 mM glutamine, penicillin/streptomycin

HEK293

DMEM high glucose-500 ml, 10% FBS, 2 mM glutamine, penicillin/streptomycin

Rat VSM

DMEM high glucose-500 ml, 10% FBS, 2 mM glutamine, penicillin/streptomycin

HL-1

Claycomb medium-87 ml, 10% FBS, 2 mM glutamine, penicillin/streptomycin,
Norepinephrine 0.1mM.

2.1.8 Vectors

pQE-30	Qiagen
pGEM-T Easy Kit	Promega
pc DNA 3.1 –myc-his	Invitrogen
pBluescript	Stratagene
pGK Neo	(kindly provided by Dr.Neil Smith, Center for Biochemistry, Biochemie 2, University of Cologne)
PEGFP	Clontech

2.1.9 Oligonucleotides

Oligonucleotides for PCR (polymerase chain reaction) were purchased from Sigma, Roth GmbH (Karlsruhe) and metabion (Martinsried).

Oligonucleotides for CAP2 full length cDNA.

BglMCA113 5'GTTAGATCTATCTCTTGGATGTCAGGC

BglMCA115 5' TATAGATCTATGACAGACATGGCGGGA

Oligonucleotides for CAP2 full length cDNA with out STOP codon.

Cap2-1/fw 5'GCGGCCGCCTATGACAGACATGGCGGG

bh1cap113ns 5' AGGATCCGGCCATGATCTCTGCAGG

Oligonucleotides for the probes of the knock out vector

1PBAMf 5' TCCAGAATACTGGGATTACAGCTACC

1PBAMr 5' CGAGGCAACATGGCATGCAATAC

2PbamF 5' ACCAATATGATGGAACCTGTTTTG
 2PbamR 5' ATCCATTATCTGGGCTGCAGG
 1PNCOf 5' GGATGCTAAGTGGCAGAGAAC
 1PNCOr 5' CCAGCCCCTATGTTATGTTGA
 2Pncof 5' CACAAGCACTAATTTCTTTTGAAG
 2Pncor 5' TGTAGGGTGGGCCTTCTAGTG
 Oligonucleotides for the left arm and the right arm of the knockout vector

1SACTF 5' TCCCCGCGGC TGCCCTGCAG AATTCTGCAT
 1SACTR 5' TCCCCGCGGC TTCAGAAGGA CAGCAACTTC ATT

1SALT3R 5' CGCGTCGACT GATGAGGAAG TGCATGGTGA TGC
 1CLATF 5' CCATCGATTC AGGAGGATGA AGATCAGGAA TT

2.1.10 Buffers and other solutions

Buffers and solutions not listed below are described in the methods section.

PBS (pH 7.2):	10x NCP-buffer (pH 8.0):
10 mM KCl	100 mM Tris/HCl
10 mM NaCl	1.5 M NaCl
16 mM Na ₂ HPO ₄	5 ml Tween 20
32 mM KH ₂ PO ₄	2.0 g sodium azide

10x MOPS (pH 7.0/ pH 8.0):

20 mM MOPS
 50 mM sodium acetate
 1 mM EDTA in 1x PBS

20x SSC:	TE-buffer (pH 8.0):
3 M NaCl	10 mM Tris/HCl (pH 8.0)
0.3 M sodium citrate	1mM EDTA (pH 8.0, adjusted with NaOH)
autoclaved	

2.1.11 Materials

cryotubes, 1 ml	Nunc
Eppendorf tubes, 1.5 ml and 2 ml	Sarstedt

hybridization tubes	Hybaid
3mm filters	Whatmann
nitrocellulose, type BA85	Schleicher and Schüll
nylon membrane, Biodyne	PALL
filter, sterile 0.45 µm and 0.2 µm	Gelman Science
plastic cuvettes	Greiner
quartz cuvettes Infrasil	Hellma
Superdex75 PC3.2/30	Pharmacia Biotech
15 ml tubes, type 2095	Falcon
50 ml tubes, type 2070	Falcon
X-ray film X-omat AR-5	Kodak

2.1.12 Instruments

blotting chamber Trans-Blot SD	Bio-Rad
centrifuges: Beckman Avanti J25	Beckman
Sorvall RC 5C plus	Sorvall
Biotech fresco	Heraeus Instruments
crosslinker UVC 500	Hoefer
pH-meter 766	Knick
heating blocks: type DIGI-Block JR	neoLab
type thermomixer	Eppendorf
hybridization oven	Hybaid
incubator Lab-Therm	Kühner
microscope: light microscope, Type DMI	Leica
Multiphor II/Immobiline focussing system	Pharmacia Biotech
PCR-thermocycler	MWG-Biotech
pump system Biologic Workstation	Bio-Rad
rotors: type JA-10	Beckman
typeJA-25.50	Beckman
SLA-1500	Sorvall
SLA-3000	Sorvall
SS-34	Sorvall
TLA 45	Beckmann
shaker 3015	GFL

lab-shaker	Kühner
SMART-system	Pharmacia Biotech
spectral photometer type Ultraspec 2000	Pharmacia Biotech
Ultra-Turrax	IKA Labortechnik
ultracentrifuge Optima TLX	Beckmann
UV-Monitor TFS-35 M	Faust
UV-transilluminator	MWG-Biotech
Vortex REAX top	Heidolph
water bath	GFL

2.1.13 Computer programs

For alignment analysis of cDNA sequences the GCG software package (University of Cologne) and the BLAST (NCBI) program were used. Protein sequences were aligned using the programs ClustalW and TreeView. For prediction of motif and pattern searches the ExPaSY (SIB) software package was used. Annealing temperatures of primers were calculated with the program “Primer Calculator” available in the Internet (<http://www.williamstone.com>).

2.2 Molecular biological methods

2.2.1 Plasmid-DNA isolation from *E. coli* by alkaline lysis miniprep

With this DNA isolation method plasmid DNA was prepared from small amounts of bacterial cultures. Bacteria were lysed by treatment with a solution containing sodium dodecylsulfate (1% SDS) and 0.5M NaOH (SDS denatures bacterial proteins and NaOH denatures chromosomal and plasmid DNA). The mixture was neutralised with potassium acetate, causing the plasmid DNA to reanneal rapidly. Most of the chromosomal DNA and bacterial proteins precipitate, as does SDS forming a complex with the potassium, and are removed by centrifugation. The reannealed plasmid DNA from the supernatant was concentrated by ethanol precipitation.

2.2.2 Plasmid-DNA isolation with a kit from Macherey-Nagel

NucleoSpin Plasmid is designed for the rapid, small-scale preparation of highly pure plasmid DNA (minipreps) and allows a purification of up to 40 µg per preparation of plasmid DNA. The principle of this plasmid-DNA purification kit is based on the alkaline lysis miniprep. Plasmid DNA was eluted under low ionic strength conditions with a slightly alkali

buffer. For higher amounts of plasmid DNA, the Nucleobond AX kit from Machery-Nagel was used. The plasmid DNA was used for sequencing and transfection of eukaryotic cells. The protocols were followed as described in the manufacturer's manual.

2.2.3 Genomic DNA Isolation from ES cells and Balb/c Tail. (Kühn et al, 1997)

Isolation of ES cell DNA.

ES cells at 60% confluency were trypsinised and washed with 1x TSE. The pellet was resuspended well in 250µl TSE (TSE = 10mM Tris, 150mM NaCl, 10mM EDTA). 250µl of TSE were added containing 0.4% SDS and 0.6-0.8 mg/ml proteinase K (final concentration 0.2% SDS and 0.3-0.4mg/ml proteinase K) resuspend first in TSE alone and then add 2x SDS/proteinaseK. Incubated 55°C overnight (at least 5-6 hours) or until no cellular debris is visible. Phenol/chloroform extracted and chloroform/isoamyl alcohol (24:1) extracted and ethanol precipitated. Spin down in a microfuge for 10 minutes, wash once with 70% EtOH, and resuspend in minimal volume of TE. Alternatively, the visible precipitate can be drawn out by a Pasteur pipet with flame (and sela) and use to spin out DNA precipitate. Immerse once in 70% EtOH and transfer to a new tube. After removal of EtOH traces resuspend immediately in TE and digestions can be carried out right away.

Isolation of genomic DNA from mouse tails.

Tail samples ~ 1cm long were transferred into 1.5ml eppendorf tube and lysed with 700µl lysis buffer (100mM Tris-Cl pH 8.5, 5mM EDTA, 100mM NaCl, 0.2% SDS, 200mM NaCl, 100-400µg proteinase K/ml). Incubated several hours to overnight at 55°C with occasional agitation until tissue dissolved. Samples were centrifuged at maximum speed for 10 minutes to pellet hair and debris. Clear supernatants were precipitated by adding equal volume of isopropanol. Pellets were washed once with 70% EtOH and the DNA was resuspended in ~ 150-200µl TE.

2.2.4 DNA agarose gel electrophoresis

10x DNA-loading buffer:	50X Tris acetate buffer (1000 ml) (pH:8.5)
40% sucrose, 0.5% SDS	242.2 g Tris 0.25% bromophenol blue, in TE (pH 8.0)
57.5 ml acetic acid	100 ml of 0.5 M EDTA (pH 8.0)

Agarose gel electrophoresis was performed to analyse the length of DNA fragments after restriction enzyme digests and polymerase chain reactions (PCR), as well as for the purification of PCR products and DNA fragments. DNA fragments of different molecular weight show different electrophoretic mobility in an agarose gel matrix. Optimal separation results were obtained using 0.5-2% gels in TAE buffer at 10 V/cm. Horizontal gel electrophoresis apparatus of different sizes were used. Before loading the gel, the DNA sample was mixed with 1/10 volume of the 10x DNA-loading buffer. For visualization of the DNA fragments under UV-light, agarose gels were stained with 0.1 µg/ml ethidium bromide. In order to define the size of the DNA fragments, DNA molecular standard markers were also loaded onto the gel.

2.2.5 Southern blotting (Southern et al., 1975)

Southern blotting is the transfer of DNA fragments from an electrophoresis gel to a membrane. After immobilization, the DNA was subjected to hybridization analysis to identify the bands containing DNA complementary to the radioactively labelled probe. In this work the alkaline transfer on a nylon membrane was performed. First the gel was washed in 0.25 M HCl, incubated in 0.4 M NaOH for 20 minutes and placed on top of two layers of Whatmann 3mm paper having contact to a reservoir of 0.4 M NaOH. After overlaying the gel with a nylon membrane, that had been wetted with water, three wet Whatmann 3mm paper and a thick stack of paper towels, the transfer was performed for about 18 hours. After washing the membrane it was air-dried and the DNA immobilized by the UV-crosslinking.

2.2.6 Isolation of total RNA from mouse tissue with RNeasy Mini/Midi kit

Working with RNA always requires special precautions in order to prevent degradation by ubiquitous RNases, e.g. wearing gloves and using RNase-free water and material. The RNeasy technology combines the selective binding properties of a silica-gel-based membrane with centrifugation. A specialized high-salt buffer system allows up to 100 µg (mini) or 1 mg (midi) of RNA longer than 200 bases to absorb to the RNeasy silica-gel membrane. An appropriate amount of different mouse tissues was transferred into a lysis buffer containing guanidine isothiocyanate and β-mercaptoethanol followed by disruption and homogenisation using a rotor homogeniser. After centrifugation the supernatant was transferred to a new tube and mixed with one volume of 70% ethanol. This mixture was loaded on the RNeasy spin column placed in a collection tube. After another centrifugation and discarding the flowthrough, the RNeasy column was treated with DNase I and washed

with a washing buffer. To elute the RNA from the column an appropriate volume of RNase-free water was pipetted directly onto the spin-column membrane. The obtained RNA was used for cDNA synthesis by RT-PCR and for northern blot analysis. Exact compositions of the buffers used for RNA isolation are listed in the Qiagen RNeasy Handbook.

2.2.7 RNA isolation from Tissue culture cells. TRI Reagent method. (Chomczynski et al, 1987)

It is a single step method for RNA isolation using a monophasic solution of phenol and guanidine isothiocyanate (TRI reagent). This facilitates effective inhibition of RNase.

Cells in small dish $\sim 5 \times 10^6$ cells were lysed in 1ml of TRI reagent. Centrifuged at 13,000 rpm at 4°C for 10 minutes, the supernatant was transferred into fresh eppendorf and allowed to stand at room temperature for 5 minutes. 200µl chloroform (Tris or water saturated to separate aqueous and organic phase) was added and allowed to stand at room temperature for 5 minutes. The solution was centrifuged at 13,000 rpm at 4°C for 15 minutes (RNA remain in the aqueous phase, DNA in the interphase, proteins in the organic phase)

Precipitate the RNA by adding equal volume of isopropanol (precipitated RNA) and allowed to stand at room temperature for 5 min or -80°C overnight. The precipitate was centrifuged at 13,000 rpm at 4°C for 30 minutes. Pellet washed with 70% ethanol and air dried and reconstituted in 20µl of DEPC treated water.

2.2.8 RNA formaldehyde agarose gel electrophoresis

The formaldehyde-agarose denaturing electrophoresis (Lehrach H et al., 1977) is used for separation and resolution of single stranded RNA.

2.2.9 Sample preparation for electrophoresis

In general, 30 µg of purified total RNA was mixed with an equal volume of RNA-sample buffer and denatured by heating at 65°C for 10 min. After denaturation, the sample was immediately transferred on ice and 1 µl of RNA-loading buffer was added. Thereafter, the RNA samples were loaded onto a denaturing formaldehyde-agarose gel.

2.2.10 Formaldehyde agarose gel preparation

For a total gel volume of 150 ml, 1.8 g agarose (final concentration 1.2%) was initially boiled with 111 ml DEPC-H₂O and 15 ml of RNA-gel-casting buffer, pH 8.0, in an Erlenmeyer

flask, cooled to 60°C and 24 ml of 36% formaldehyde solution were added. The agarose solution was mixed by swirling and poured into a sealed gel-casting chamber of the desired size (12 x 20 cm). After the gel was completely set, the denatured RNA samples were loaded and the gel was run in 1x RNA-gel-running buffer, pH 7.0, at 100 V until the bromophenol blue dye had migrated the appropriate distance through the gel. A test gel was sometimes run with 5 µg of total RNA to check the quality of the RNA samples. In such a case, 10 µg/ml ethidium bromide was added to the RNA-sample buffer during sample preparation and after electrophoresis, the gel was examined under UV light at 302 nm and was photographed using the gel-documentation system.

10x RNA-gel-casting buffer (pH 8.0):

200 mM MOPS

50 mM sodium acetate

10 mM EDTA

adjust pH 8.0 with NaOH

RNA-sample buffer:

50% formamide

6% formaldehyde

in 1x RNA-gel-casting buffer, pH 8.0

Internal RNA-size standard:

26S rRNA (4.1 kb), 18S rRNA (1.9 kb)

10x RNA-gel-running buffer (pH 7.0):

200 mM MOPS

50 mM sodium acetate

10 mM EDTA

adjust pH 7.0 with NaOH and autoclave

RNA loading dye

50% sucrose, RNase free

0.25% bromophenol blue

in DEPC-H₂O

2.2.11 Northern blotting

After electrophoresis, the RNA formaldehyde agarose gel was rinsed in sufficient amount of deionised H₂O for 5 min and then equilibrated in 10x SSC for 5 min. The resolved RNA was then transferred (Sambrook *et al.*, 1989) from the gel to the nylon membrane (Biodyne B membrane, Pall) After overnight transfer with 20x SSC, the transferred RNA was immobilised by baking the membrane in an oven at 80°C for 1 h.

2.2.12 Radiolabelling of DNA

The Prime-it kit (Stratagene) was used for radio labelling of DNA fragments following the method suggested by the manufacturer. Briefly, 0.1-0.3 µg DNA sample was suspended in 24-µl ddH₂O (final volume). Then 10 µl of random-oligonucleotide-primer (supplied along with the kit) was added and the DNA template was denatured at 95°C for 5 min. After denaturation, 10 µl of 5x dNTP mix without dATP (supplied along with the kit), 5µl of α ³²P

and 1 μ l Klenow enzyme (5 U/ μ l, supplied along with the kit) was added and the reaction-mixture was incubated at 37°C for 10 min. After 10 min the reaction was immediately stopped by adding 2- μ l stop-mix (supplied along with the kit). Now the reaction-mixture was diluted with 100 μ l TE, pH 8.0 to increase the reaction volume and the reaction-mixture was overlaid on a 0.9 ml Sephadex G-50 spin column. The free nucleotides present in the reaction-mixture were separated by centrifugation at 3,000 rpm (Sorvall RT7 centrifuge) for 2 min through the Sephadex G-50 spin column and the radiolabelled DNA probe was collected in a 1.5 ml eppendorf tube. The purified radiolabelled DNA probe was denatured by heating at 100°C for 5 min, cooled on ice and used for hybridization of northern-blots.

2.2.13 Chromatography through Sephadex G-50 spin column

This technique (Sambrook et al., 1989), which employs gel filtration to separate high-molecular weight DNA from smaller molecules, was used to separate radiolabelled DNA from unincorporated α ³²P ATP. 30 g of Sephadex G-50 (Pharmacia) was slowly added to 250 ml of TE, pH 8.0, in a 500-ml bottle and the beads were allowed to swell overnight at room temperature. Next day, the supernatant was decanted and was replaced with an equal volume of TE, pH 8.0. The beads were autoclaved and stored in a screw-capped bottle at 4°C. For preparation of Sephadex G-50 spin column, the swollen Sephadex G-50 beads were packed in a disposable 1-ml syringe plugged with sterile glass wool and the column was spun at 3,000 rpm (Sorvall RT7 centrifuge) for 2 min. Sephadex G-50 was added until the packed column volume was 0.9 ml. The column was then used for separation of the radiolabelled DNA probe.

2.2.14 Hybridization of Northern blots with radiolabelled DNA probe

Northern blots were rinsed briefly with 2x SSC and incubated in a heat sealable hybridization bag (Life technologies) in 15-20 ml of pre-hybridization buffer for 1h at 37°C on a shaking platform. After pre-hybridization, the denatured radiolabelled DNA probe was added directly to the pre-hybridization-buffer in the hybridization bag and the hybridization was performed by incubating the blot overnight at 37°C. After hybridization, the blot was washed twice with 2x SSC/0.1% SDS for 5 to 10 min each at room temperature with gentle shaking followed by two washings with wash buffer for 30 min each at 37°C with gentle shaking. The blot was then wrapped in a plastic wrap and exposing the blot to X-ray film at -70°C for desired time was performed by autoradiography.

Church buffer:0.5 M Na₃PO₄ (pH 7.15)

7% SDS

1 mM EDTA

1% BSA

50 µg/ml salmon sperm

Wash buffers:

1) 2x SSC, 1% SDS

2) 0.4x SSC, 1% SDS

3) 0.2x SSC, 1% SDS

After 1 hour of prehybridizing the blots at 65°C in Church buffer, radioactively labelled probes were added to a portion of fresh Church buffer and hybridization took place for 18 hours at the same temperature. Several washing steps were performed at 65°C, as needed. Afterwards blots were exposed to an X-ray film at -70 °C.

2.2.15 Elution of DNA fragments from agarose gels

Elution of DNA fragments from agarose gels was performed using the NucleoSpin Extract 2 in 1 kit from Macherey-Nagel. Bands of interest were cut out of the gel and the agarose was melted at 50°C in a binding buffer. After several centrifugation steps with wash buffer, the DNA bound selectively to a silica membrane column and was eluted with a low salt solution.

2.2.16 Measurement of DNA and RNA concentrations

Concentrations of DNA and RNA were estimated by determining the absorbance at a wavelength of 260 nm. A ratio of OD₂₆₀/OD₂₈₀ >2 indicate negligible protein contaminations. Protein contaminations were estimated from absorbance at 280 nm.

2.2.17 Restriction digestion of DNA

Restriction enzyme digestions, DNA ligations and other recombinant DNA preparations were performed using standard protocols (Sambrook, 1989). All DNA constructs were verified by DNA sequencing. Digestion of DNA with restriction endonucleases was performed in buffer systems provided by the manufacturers at the recommended temperatures.

2.2.18 Dephosphorylation of 5'-ends of linearised vectors10x CIAP-Puffer (pH 9.0):

0.5 M Tris/HCl

10 mM MgCl₂1 mM ZnCl₂

10 mM spermidin

In order to prevent linearized vectors from religation, the 5' end phosphate groups were hydrolysed with calf intestinal alkaline phosphatase (CIAP) for 30 minutes at 37°C followed by heat inactivation at 70°C for 10 min.

2.2.19 Creation of blunt ends

Due to the 3' exonuclease activity of Klenow enzyme it is possible to transform overhanging 3' ends of DNA (sticky ends) into blunt ends. After the reaction for 30 minutes at 37°C, heat inactivation for 10 minutes at 70°C was necessary.

2.2.20 Ligation of vector- and DNA-fragments

T4-DNA-ligase catalyzes the ligation of DNA fragments and vector DNA. 1 U T4-ligase was incubated with about 25 ng of DNA fragment overnight at 10°C.

2.2.21 Ligation of polylinker and DNA-fragments

DNA fragment and the polylinker were ligated using Manufactures Protocol of New England BioLabs.

2.2.22 Polymerase chain reaction (PCR)

PCR can be used for *in vitro* amplification of DNA fragments (Saiki *et al.*, 1985). A double stranded DNA (dsDNA) serving as a template, two oligonucleotides (primers) complementary to the template DNA, deoxyribonucleotides and heat resistant *Taq*-DNA-polymerase are required for this reaction. Primers may be designed having non-complementary ends with sites for restriction enzymes. The first step in PCR reactions is the denaturing of dsDNA at 94°C. Second, the reaction mixture was incubated at different annealing temperatures, depending on the G/C content of the primers. Different programs provide an accurate calculation of the annealing temperature based on the nearest neighbours method and are freely available on the Internet. The third step with a temperature of 72°C allows the elongation of the new strand of DNA by the *Taq*-DNA-polymerase. A PCR machine (thermocycler) can be programmed to regulate these different cycles automatically. A “standard program” is presented below:

I. Initial denaturing: 94°C, 5 min

II. Cycles (25-35):

Denaturing (94°C, 15 sec.)

Annealing (60-68°C, 30 min)

Elongation (72°C, 1-10min)

III. Final elongation: 72°C, 10 min

IV. Cooling to 4°C

2.2.23 Transformation of *E. coli* cells with plasmid DNA

LB-Medium:

10 g Bacto-Trypton

5 g yeast extract

5 g NaCl

SOC-Medium:

20 g Bacto-Trypton

5 g yeast extract

0.5 g NaCl

20 mM Glucose

For transformation of *E. coli* cells the heat shock method was used. DNA and competent cells were incubated for 15 minutes on ice and then for 40 seconds at 42°C. After cooling on ice for 2 minutes, the bacteria were incubated for 1 hour at 37°C in SOC-medium without any antibiotics. Finally, the bacteria were plated on agar plates containing selective antibiotics, and incubated overnight at 37°C. For further analysis single colonies were picked, inoculated and incubated for 12 hours in LB-medium on a shaker. From clones of interest glycerol stocks were made. For this, samples of *E. coli* cultures were mixed with an equal volume of 50% glycerol and frozen at -80°C.

2.2.24 Removal of the stop codon in the CAP2 cDNA by PCR technique

Using CAP2 cDNA as template, which is in pGEM, PCR was performed with two primers (one forward and one reverse). After 25 rounds of PCR, the PCR product was checked on the gel.

2.3 Protein biochemical methods

2.3.1 Extraction of protein homogenate from mouse tissues and cell cultures

For characterization of polyclonal antibodies and identification of endogenous CAP2, homogenates from mouse tissues and cell cultures were extracted. For this mice were sacrificed by cervical dislocation. Dissected organs were briefly rinsed in ice cold PBS buffer and frozen in liquid nitrogen. Afterwards ice-cold equilibrating buffer containing protease inhibitors was added. After homogenisation, the cell lysate was mixed with SDS-loading buffer boiled at 95°C for 5 minutes and centrifuged for 5 minutes at 12000rpm. In the case of

cell lines, cells from a big dish were harvested by trypsinising the cells at 37°C for 5 minutes and then medium was added to stop the reaction of trypsinising. The cells were pelleted at 4°C for 5 minutes at 1500 rpm. Then cells were resuspended in equilibrating buffer containing 0.25M sucrose and sonicated by giving 5 pulses of 10 sec each with a 15 sec rest between each pulse. After the sonication the cell lysate was spun at 1500 rpm at 4°C for 10 minutes. The supernatant was then centrifuged at 12,000rpm for 15 minutes at 4°C referred to as 12k sup and 12k pellet. The supernatant was then subjected to ultra centrifugation. The samples were centrifuged at 100,000 g for 150 minutes at 4°C. Then the supernatant was treated as cytosol and the pellet as the membrane (micro membranes). Afterwards samples were treated as described for the tissues.

The equilibrating buffer contains 50 mM Tris, pH 8.0, 5 mM EDTA, 5 mM EGTA, 10 mM MgCl₂, 100 μM PMSF, 150μM beta mercaptoethanol and a protease inhibitor cocktail tablet.

2.3.2 Cell fractionation

For nuclei preparation, PAM212 cells were trypsinised, counted and washed once in PBS. They were resuspended in equilibrating buffer (0.32M sucrose, 50 mM Tris, pH 8.0, 5 mM EDTA, 5 mM EGTA, 10 mM MgCl₂, 1mM DTT, 0.5% NP40, 100 μM PMSF, 150μM beta mercaptoethanol and a protease inhibitor cocktail tablet.; 1x10⁷ cells/ 400μl buffer) and sonicated on ice (sonifier UP200S, dr.hielscher, 40 s, amplitude 50%, cycle 0.5). This step was repeated until no more intact cells were observed by light microscopy. The resulting homogenate was centrifuged at 500 g for 5 minutes, washed twice in 1ml buffer without NP40 and centrifuged again. The resulting pellet contains purified nuclei. Then the nuclei were resuspended in a SDS-loading buffer boiled at 95°C for 5 minutes and centrifuged for 5 minutes at 12,000rpm. Further the supernatant was centrifuged at 12,000rpm for 15 minutes at 4°C referred to as 12k sup and 12k pellet. These samples were treated same as the nuclei pellet.

2.3.3 Expression of recombinant 6xHis-tag protein

For expression of recombinant 6xHis-N-Terminal CAP2 (23kDa), the QIA express system by Qiagen was used. The host strain E. coli M15 was transformed with the pQE-30 vector encoding the His-tag fusion protein and expression was induced by the addition of IPTG, which leads to the inactivation of the lac repressor protein. Single colonies (5-10) of recombinant cells were picked and grown overnight in 10 ml of LB medium containing

ampicillin and Kanamycin (100 µg/ml) at 37°C and 250 rpm. 5 ml of the overnight grown culture were inoculated into 45 ml of fresh LB medium containing ampicillin and kanamycin (100 µg/ml). The culture was then allowed to grow at 37°C till an OD of 0.5-0.6 measured at 600 nm was obtained. Now the induction of expression was initiated by adding IPTG. In order to standardize the conditions of maximum expression of the fusion protein, induction was performed with varying concentrations of IPTG (0.1 mM, 0.5 mM and 1.0 mM final concentration) at two different temperature conditions (30°C and 37°C). Samples of 1 ml were withdrawn at different hours of induction (0 hr, 1 hr, 2 hr, 3 hr, 4 hr and 5 hr), the cells were pelleted and resuspended in 100 µl of 1x SDS sample buffer. The samples were denatured by heating at 95°C for 5 min and 10 µl of each sample were resolved on a 12% SDS-polyacrylamide gel.

2.3.4 Urea Extraction of the N-terminal CAP2

. The protein expression was induced with 1mM IPTG for 4 hrs at 37°C and the bacteria were collected by centrifugation at 5000 x g for 10 minutes. After the induction, the culture was transferred to a 500 ml centrifuge bottle (Beckman) and the cells were collected by centrifugation at 4,000 rpm (Beckman Avanti J25, rotor JA-10) for 10 min at 4°C. The pellet was resuspended in 10 ml of ice-cold lysis buffer containing lysozyme (1 mg/ml) and Triton X-100 (0.5%) and supplemented with fresh protease inhibitors, collected in a 50 ml tube and incubated on ice for 20 min. Incubation in lysis buffer was followed by a brief sonication (3 pulses of 10 s each with a 15 s rest between each pulse), keeping the tube immersed in ice. Sonication was followed by homogenisation using a Dounce homogeniser for 2-3 min in order to ensure complete and efficient cell lysis. The lysate was then subjected to gradual increases in the molarity of urea. For every 1 M urea the lysate was pelleted at 15,000 rpm (Beckman Avanti J25, rotor JA-25.50) for 15 min at 4°C followed by next concentration of urea and continued till 8 M urea. The supernatant samples (10 µl) collected from each round of solubilisation were dissolved in 1x SDS sample buffer and run on SDS-polyacrylamide gel to be analysed by Coomassie staining.

Lysis buffer:

50mM NaH₂pO₄

300mM NaCl

10mM imidazole

2.3.5 Ni-NTA-pull down of tissue lysates

After inducing the protein expression of N-terminal CAP2 protein the bacteria were

collected by centrifugation at 5000 x g for 10mts. The pellet was resuspended in lysis buffer containing protease inhibitors (complete inhibitor Cocktail). After adding lysozyme (1 mg/ml), the lysate was incubated for 30minutes on ice followed by sonication. The lysate was centrifuged at 10,000 g for 30 minutes at 4°C and the supernatant was used for the subsequent steps after confirming the expressed protein present in some amounts in the supernatant. The lysate was incubated with Ni-NTA beads (50ul) shaking 4 hours at 4°C. Then the lysate was centrifuged at 2000 rpm for 3 minutes. The Ni-NTA beads were washed thrice with the equilibrating buffer, containing 50 mM Tris, pH 8.0, 5 mM EDTA, 5 mM EGTA, 10 mM MgCl₂, 100 μM PMSF, 10mM Na₂ H₂ P₂O₇, 1mM ATP, 20mM NaF, 1mM Na₃VO₄, 150μM beta mercaptoethanol and a protease inhibitor cocktail tablet. Then the beads were incubated with tissue lysate, which was precleared with the Ni-NTA beads and was prepared as in the section 2.3.1 (except that, 10mM Na₂ H₂ P₂O₇, 1mM ATP, 20mM NaF, 1mM Na₃VO₄ was added here) overnight at 4°C. Then the beads were centrifuged at 2000 rpm for 3 minutes. Then the beads were washed four times with the equilibrating buffer containing 0.5% TritonX- 100. Then the beads were resuspended in 50 μl of 1x SDS sample buffer. The samples were denatured by heating at 95°C for 5 min and 20 μl of each sample were resolved on a 3-15% gradient SDS-polyacrylamide gel. As a control the His tagged ABD-enaptin in pQE 31 vector was treated same as the N-terminal CAP2 pQE 31 vector in all the steps of the experiments.

2.3.6 Immunoprecipitation with polyclonal CAP2 antibody and monoclonal GFP antibody (mAb K3-184-2)

For immunoprecipitations, HEK293 cells were cotransfected with GFPCAP1 and Myc CAP2 and HEK293 cells cotransfected with GFP C-ACF7 and Myc CAP2 grown in 10cm diameter dishes were washed with PBS and lysed in 500ul of ice cold lysis buffer (50 mM Tris, pH 8.0, 5 mM EDTA, 5 mM EGTA, 10 mM MgCl₂, 100 μM PMSF, 10mM Na₂ H₂ P₂O₇, 1mM ATP, 20mM NaF, 1mM Na₃VO₄, 1% PEG 8000, 1% Triton X-100, 150μM beta mercaptoethanol and a protease inhibitor cocktail tablet) for 20 minutes on ice. Cleared lysates were incubated with anti-GFP (mAb K3-184-2) and anti-CAP2 (purified) antibodies for 2 hours followed by incubation with protein A-sepharose beads (Amersham Biosciences) for 1 hour at 4°C on a rotary wheel. Before incubating with the antibodies the lysates were precleared with the protein A-sepharose beads (Amersham Biosciences) for 1 hour at 4°C on a rotary wheel. Beads were then washed thrice with lysis buffer without NaF, Na₃VO₄, ATP and Triton X-100. Precipitates were resolved by SDS-PAGE and analysed by immunoblotting using the respective antibodies.

2.3.7 Affinity purification of polyclonal antibodies by blot method

TBS	:	8 g NaCl, 0.2 g KCl and 3 g Tris/HCl in 1 liter, pH 7.2
Buffer I	:	1% BSA, 0.05% Tween 20 in PBS
Buffer II	:	0.1 M glycine, 0.5 M NaCl, 0.5% Tween 20, pH 2.6

The recombinant protein, which was used to produce the polyclonal antibody, was analysed by SDS-PAGE and the gel was afterwards transferred to a PVDF membrane. The membrane was stained with Ponceau S to confirm the transfer efficiency and the blot corresponding to the recombinant protein was cut out. The blot was then destained with TBS. The portion of the blot where the recombinant protein was immobilized was blocked by incubating the blot for 2 hours in buffer I. 1 volume of serum was diluted with 4 volumes of TBS and incubated with the stripes at 4°C for 2 hours. The unbound antibody was washed with TBS 4x 5 minutes at 4°C. After washing, the antibodies bound to the recombinant protein on the membrane stripes were eluted with buffer II, 1 ml, 2x, 1.5 minutes at 4°C. The eluted antibody was neutralised with 100 µl of 1 M Tris (pH 8.0) immediately after elution. The antibody can be stabilised with 0.5% BSA.

2.3.8 SDS-polyacrylamide gel electrophoresis

SDS-polyacrylamide gel electrophoresis was performed using the discontinuous buffer system. (Laemmli UK et al., 1970). Discontinuous polyacrylamide gels (10-15% resolving gel, 5% stacking gel) were prepared using glass-plates of 10 cm x 7.5 cm dimensions and spacers of 0.5 cm thickness. A 12-well comb was generally used for formation of the wells in the stacking gel. The protein samples were resuspended in 1x SDS sample buffer. The samples were denatured by heating at 95°C for 5 min and loaded into the wells in the stacking gel. A molecular weight marker, which was run simultaneously on the same gel in an adjacent well, was used as a standard to establish the apparent molecular mass of proteins resolved on SDS-polyacrylamide gels. The molecular weight markers were prepared according to the manufacturer's specifications. After loading the samples onto the gel, electrophoresis was performed in 1x gel-running buffer at a constant voltage of 100-150 V until the bromophenol blue dye front had reached the bottom edge of the gel or had just run out of the gel. After the electrophoresis, the resolved proteins in the gel were either observed by Coomassie blue staining or transferred onto a nitrocellulose membrane.

SDS-sample buffer 1x

50 mM Tris/HCl, pH 6.8
 2 % (v/v) SDS
 10 % (v/v) glycerine
 0.1 % (v/v) bromophenol blue
 2 % (v/v) β -mercaptoethanol

10x Gel-running buffer:

1.9 M glycine
 0.25 M Tris/HCl, pH 8.8
 1% SDS

2.3.9 Gradient gel electrophoresis

Gradient gels were used for visualising both high molecular weight proteins and low molecular weight proteins. Gradient gels were made with a gradient mixer and typically a gel with a gradient of 3%-15% acrylamide was made. The top of the gel had 3% of acrylamide whereas the bottom part had 15% of acrylamide. The middle part of the gel had a gradient from 3% till 15%. The gradient mixer was connected to a peristaltic pump, which delivered the solution into the gel-casting tray. 15% acrylamide was being added into the near well of the outlet from the mixer.

Stock solutions for preparing Gradient gels

100 ml stock solution	3%	6%	10%	12%	15%	4% Stacking Gel
1.5M Tris/HCl, pH 8.8	25 ml	25 ml	25 ml	25 ml	25 ml	-
0.5% tris/HCl, pH 6.8	-	-	-	-	-	20 ml
PAA (30%)	10 ml	20 ml	33.3 ml	40 ml	50 ml	13.3 ml
SDS (10%)	1 ml	1 ml	1 ml	1 ml	1 ml	1 ml
H ₂ O	64 ml	54 ml	40.6 ml	34 ml	24 ml	65.6 ml

Solutions required for individual gradient gel

	Gradient gel solution per mixing well		1 gel	Stacking gel
Stock solution /Gel	4.5 ml	4.5 ml	9.0 ml	3.0 ml
APS 10%	15 μ l	15 μ l	22 μ l	30 μ l
TEMED	8 μ l	8 μ l	10 μ l	16 μ l

2.3.10 Coomassie blue staining of SDS-polyacrylamide gels

After electrophoresis, the resolved proteins were visualised by staining the gel with Coomassie blue staining solution. The gel to be stained was placed in the Coomassie blue staining solution immediately after electrophoresis and the gel was allowed to stain at room temperature with gentle agitation for at least 30 min. After staining, the staining solution was poured off and destaining solution was added. The gel was then destained at room temperature with gentle agitation. For best results, the destaining solution was changed with fresh destaining solution several times until protein bands were clearly visible.

Coomassie blue staining solution:

0.1% Coomassie-brilliant- blue R250,
50% ethanol
10% acetic acid
Filter the solution before use

Destaining solution:

7% acetic acid
20% ethanol

2.3.11 Drying of SDS-polyacrylamide gels

After destaining, the gel was immersed in gel-dry buffer for 10-15 min at room temperature. Two sheets of cellophane (Novex), slightly bigger than the size of the gel, were also immersed in gel-dry buffer. The gel was then carefully placed between two moistened sheets of cellophane avoiding trapping of air-bubbles, clamped between the gel-drying frames (Novex) and dried overnight at room temperature.

Gel-drying buffer:

25% ethanol 5% glycerine

2.3.12 Western blotting using the semi-dry method

The proteins resolved by SDS-polyacrylamide gel electrophoresis (SDS-PAGE) were electrophoretically transferred from the gel to a nitrocellulose membrane by using the method described by (Towbin *et al.*, 1979) with little modifications. The transfer was performed using Towbin's buffer in a semi-dry blot apparatus (Bio-Rad) at a constant voltage of 10 V for 35-45 min. The instructions provided along with the semi-dry apparatus were followed in order to set up the transfer.

Towbin's buffer (transfer buffer):

39 mM glycine
48 mM Tris/HCl, pH 8.3
0.0375% SDS
20% methanol or ethanol

2.3.13 Ponceau S staining of western blots

To check for the transfer of proteins onto the nitrocellulose membrane, the membrane was stained in 10-15 ml of Ponceau S solution for 2-5 min at room temperature. After staining, the membrane was removed from the Ponceau S solution and rinsed with deionised water to destain until bands of proteins were visible and the background was clear. The position of the constituent proteins of the molecular weight marker and/or the protein of interest was marked and the membrane was washed with several changes of NCP to completely remove the stain. Now the membrane carrying the transferred proteins was used for immunodetection of specific protein.

Ponceau S solution: Ponceau S concentrate (Sigma):

1 ml Ponceau S concentrate (Sigma) 2% w/v Ponceau S in 30% w/v TCA

19 ml distilled H₂O and 30% w/v sulfosalicylic acid

2.3.14 Immunodetection of membrane-bound proteins

The western blot was immersed in blocking buffer (1x NCP) and the blocking was performed with gentle agitation either for overnight at 4°C or for 2-3 h at room temperature with several changes of 1x NCP. After blocking, the blot was incubated at room temperature with gentle agitation with either commercially available primary antibodies at a proper dilution (in 1x NCP) for 1-2 h, or hybridoma-supernatant for overnight. After incubation with primary antibody, the blot was washed 5-6 times with 1x NCP at room temperature for 5 min each with repeated agitation. Following washings, the blot was incubated for 1 h at room temperature with a proper dilution (in 1x NCP) of the enzyme conjugated secondary antibody directed against the primary antibody. The secondary antibody was conjugated with either Horseradish peroxidase (HRP) or alkaline phosphatase (AP). After incubation with a secondary antibody, the blot was washed as described above. After several washings, the substrate reaction was carried out depending upon the enzyme coupled to the secondary antibody. Enzymatic chemi-luminescence (ECL) detection system was used for blots incubated with HRP-conjugated secondary antibody, whereas the BCIP/NBT colour development substrate reaction was used for blots incubated with AP-conjugated secondary antibody.

10x NCP-Buffer (pH 8.0)

12.1 g Tris/HCl

87.0 g NaCl

5.0 ml Tween 20

2.0 g sodium azide

2.3.15 Enzymatic chemiluminescence (ECL) detection system

The blot was incubated in ECL-detection-solution for 1-2 min and then wrapped in a saran wrap after removing the excess ECL-detection-solution. Now an X-ray film was exposed to the wrapped membrane for 1 to 30 min and the film was developed to observe the immunolabelled protein.

ECL-detection-solution:

2 ml 1 M Tris/HCl, pH 8.0

200 μ l 250 mM 3-aminonaphthylhydrazide in DMSO

89 μ l 90 mM p-Coumaric acid in DMSO

18 ml deionised H₂O

6.1 μ l 30% H₂O₂ (added just before using)

2.3.16 BCIP/NBT colour development substrate reaction

The blot was developed using 5-bromo-4-chloro-3-indolyl-phosphate (BCIP) as a substrate and nitro blue tetrazolium (NBT) as a colour indicator. The blot was incubated in 10 ml of BCIP/NBT substrate solution at room temperature with gentle agitation for 5 min or until sufficient colour development has occurred. The reaction was stopped by washing the membrane several times with deionised water and the membrane was allowed to dry on a piece of blotting paper.

BCIP/NBT substrate solution:

66 μ l 50mg/ml NBT (Promega)

33 μ l 50mg/ml BCIP (Promega)

10 ml 0.1M Na₂CO₃, pH 10.0

Molecular weight standard marker:

LMW-Marker (Pharmacia) (kDa): 94; 67; 43; 30; 24; 20.1; 14.4

2.4 Cell culture methods

Various adherent cell lines were used for immunofluorescence and western blotting analysis. Trypsin was used to detach cells from the plates when passaging subconfluent cultures and to harvest the cells.

2.4.1 Preparation of mouse embryonic cardiomyocytes

A pregnant mice was sacrificed by cervical dislocation, abdomen was dissected & the embryos were taken out into a petridish with sterile filtered ADS buffer . Heart was taken out from each embryo & only the ventricles were retained discarding the atrium. These ventricles were again rinsed in ADS buffer to get rid of the blood & was taken into an eppendorf tube ,minced into small bits & was digested with 1ml enzyme solution containing 1mg/ml Worthington collagenase and 1mg/ml sigma porcine pancreatin in ADS buffer for 15 minutes at 37 degrees. Then the mixture was triturated with a pipette tip, the supernatant was taken into a 15ml falcon tube with 5 ml DMEM medium containing 10% FBS & 1% Penicillin/streptomycin . Again the above step was repeated for the residue & the supernatant was collected into 5ml medium. The third time only the enzyme solution was added to the residue & was triturated several times ,the whole mixture was taken into another falcon tube containing 5 ml medium. All the 3 falcon tubes were centrifuged for 5 mins at 700 RPM at room temperature. The supernatant was discarded & the pellet in each tube was resuspended in 1 ml medium & transferred into 3 wells in a well plate with coverslips coated with 0.1% gelatin. This was incubated for 1 hour in an incubator at 37°C with 5% CO₂ . Then the cell suspension from each well was transferred into several wells depending on the number of cells & was kept in the incubator for 24hrs which facilitates the settling of cardiomyocytes. After 24 hrs the cells were fixed using 2.5% paraformaldehyde & was used for immunostaining.

ADS buffer contains Glucose 5.5mM, MgSO₄ 0.8mM, KCl 5mM, NaH₂PO₄ 1mM, HEPES 20mM and NaCl 116mM

2.4.2 Preparation of myofibrils

Myofibrils were prepared from adult mice strain Him. All experiments were approved by the Institutional Animal Care and Use Committee.

The mice were sacrificed by cervical dislocation and the heart was removed. Papillary muscles were dissected from the left ventricle, skinned with 1 % v/v Triton-X-100 in skinning solution (5 mmol/L K-phosphate pH 6.8, 5 mmol/L Na-azide, 3 mmol/L Mg-acetate, 5 mmol/L K₂EGTA, 3 mmol/L Na₂ATP, 3 mmol/L MgCl₂, 6 mmol/L KOH and a protease inhibitor cocktail) for 2 h and stored at 4 °C in the same solution without Triton-X-100. Myofibrillar suspensions were prepared immediately before experiments by homogenising skinned papillary muscles with a blender (Ultra Turrax) for 10 s at 4 °C.

2.4.3 Staining of myofibrils

The myofibril suspension were centrifuged at 380x g for 4 minutes and the pellet was resuspended with the blocking buffer containing PBG with 10% FCS and incubated for 30 minutes at 4°C, again centrifuged at 380x g for 4 minutes and resuspended with primary antibody and incubated for an hour at 4°C and then followed by washing with PBG thrice and secondary antibody was incubated for 45 minutes at 4°C followed by washing with PBG thrice and then spread over a cover slip and allowed to settle down on the cover slip and then cover slip was fixed on to the slide using Gelvatol.

2.4.4 Immunofluorescence

Cells were grown on coverslips kept on six well plates. Nicely spread cells are used for fixing. Two ways of fixing was used. In the first way, the cells are incubated with 3% paraformaldehyde for 10 minutes at room temperature, washed 3 times with PBS and permeabilised with 0.5% Triton X-100 for 5 minutes. In the second method, the cells are fixed and permeabilised by incubating with cold methanol (-20°C) for 10 minutes. The fixed cells were then washed three times with PBS for 5 minutes followed by three times washing with PBG. After washing, the cells were incubated with the primary antibody for one hour. After one hour, the cells were washed 6 times with PBG for 5 minutes. After the washing step the cells were incubated with the secondary antibody, which has a fluorescent tag for one hour. The cells were then washed again with 3 times PBG and 3 times with PBS and embedded in slides using Gelvatol. For the control, the first antibody was replaced by incubation with PBG followed by incubation with the secondary antibody.

2.4.5 Immunohistochemical staining of formalin-fixed paraffin-embedded sections

Solutions

Xylene

Ethanol

0.01 M Phosphate buffer saline (pH 7.4)

Solution of 1% gelatine in PBS (PBG)

10 mM Citric buffer, pH 6.0

The paraffin in the sections was removed by incubating the sections 3 times in xylene for 5 minutes. The sections were rehydrated in a series of incubation with 96% ethanol (2 times, 5 minutes), 80% ethanol, 70% ethanol, 50% ethanol and 30% ethanol one minute each, and finally rinsed with water. The slides are washed with freshly prepared citrate buffer pH

6.0 and boiled in a microwave at 300 Watts in the same buffer for 15 to 20 minutes. The sections were kept again at room temperature in citrate buffer for about 20 minutes, rinsed in distilled water and then with PBS (3 times, 5 minutes). The sections were blocked for one hour using a PBG solution containing 5% horse serum. The sections were incubated with the primary antibody for 24 hours at 4°C. Slides were washed 3 times for 4 minutes. Afterwards the sections were incubated with a secondary antibody conjugated to a fluorescent tag for one hour at room temperature. The sections were washed again as before and mounted in Gelvatol/DABCO (Sigma).

The staining of sections with the VECTOR MOM kit (VECTOR laboratories) was done according to the manufacturer's instructions.

2.4.6 Microscopy

Confocal images of immunolabelled specimens were obtained using the confocal laser scanning microscope TCS-SP (Leica) equipped with a 63x PL Fluotar 1.32 oil immersion objective. A 488-nm argon-ion laser for excitation of GFP fluorescence and a 568-nm krypton-ion laser for excitation of Cy3 or TRITC fluorescence were used. For simultaneous acquisition of GFP and Cy3 fluorescence, the green and red contributions to the emission signal were acquired separately using the appropriate wavelength settings for each photomultiplier. The images from green and red channels were independently attributed with colour codes and then superimposed using the accompanying software.

2.5 Disruption of the cytoskeleton using various drugs

Disruption of the actin cytoskeleton was done using Latrunculin B at a final concentration of 2.5 µM. The cells were treated with latrunculin B for different time limits, washed and fixed in 3% PFA.

To disrupt the microtubule cytoskeleton, colchicin was dissolved in methanol and used at a concentration of 12.5 µM. Cells were treated with colchicin for 90 min and coverslips were fixed at different time points using methanol.

2.5.1 Digitonin experiment

For the permeabilization experiments with digitonin, fixed cells (3% paraformaldehyde) were washed in ice-cold PBS and afterwards treated with 40 µg/ml digitonin (Sigma) in PBS for 5 minutes on ice.

2.6 Gene targeting protocols

2.6.1 Target vector construction

The pGK-NEO vector was used as the backbone for the target vector construction. The 1SACTF fw and 1SACTR rv primers were used to amplify the 5' arm (4.5 kb, left arm) of the vector from IB-10 ES cell genomic DNA using the Pfu DNA polymerase (Invitrogen). The amplified fragment was cloned into pGK-NEO vector at SACII site. The 3' arm (2.35 kb) of the knockout plasmid was amplified with the 1CLATF fw and 1SAL3TR rv primers using the Pfu DNA polymerase and the ES cell genomic DNA as a template. The fragment was first ligated into the pGMT-easy vector. The 3' arm was cut out from pGMT-easy vector with SmaI and SALI and ligated into the pGK-NEO vector using the same enzyme sites. All the constructs were sequenced and cloning directions and sequences were verified. The size of the complete target vector was 11.7 kb.

2.6.2 Probe generation

5' arm (left arm) probes

The 500 bp two probes were generated for each arm. Two probes of around 500 bases each were designed for the 9.2 kb BamHI fragment. One is upstream (5' end) of the left arm (4.5 kb) and the other one is (3' end) downstream of the left arm. The probes were PCR amplified using the specific primers (1PBAMf, 1PBAMr for the upstream probe 2PbamF, 2PbamR for the downstream probe) and genomic DNA of ES cells as the template with the Advantage Taq polymerase (Clontech). The PCR-fragment was cloned into pGEM.T Easy. The 5' probes could be cut out with the EcoRI enzyme respectively.

3' (right arm) probes

Again two probes of length 470 bp probe was amplified from ES cell genomic DNA using the 1PNCOF, 1PNCOr and 2PncOF, 2PncOR for upstream and downstream probes of the right arm, respectively. The PCR fragment was cloned into the pGEM.T Easy. The probe could be cut out from the plasmid using the EcoRI.

2.6.3 Embryonic stem cell culture

Media and materials

MEF media	DMEM (4500 mg/l glucose) (Sigma):	500 ml
	FCS	: 50 ml
	L-glutamine	: 6 ml
	Non-essential amino acids	: 6 ml
	Pen/Strep	: 6 ml

	Pyruvate	:	6 ml
ES cells media	DMEM knockout (GIBCO)	:	500 ml
	Knockout SR (GIBCO)	:	90 ml
	L-glutamine	:	6 ml
	Non-essential amino-acids	:	6 ml
	Pen/Strep	:	10 ml
	Pyruvate	:	6 ml
	ESGRO (Murine LIF, 10^7 U/ml, Chemicon)	:	50 μ l
	β -mercaptoethanol (Sigma)	:	6 μ l
Selection media		:	ES cell media and 400 μ g/ml of G418
Freezing media		:	ES cell media, 30% FCS and 20% DMSO
Gelatin (2%) (Sigma)		:	Final concentration 0.1% (w/v) in sterile PBS
Mitomycin C (Sigma)		:	Mitomycin dissolved in sterile PBS (400 μ g/ml)
10X Trypsin (0.5%)(GIBCO)		:	Used at 2x dilution
Trypsin Inhibitor (Sigma)		:	Dissolved in sterile PBS at a concentration of 5mg/ml and used with 1:10 dilution with 2x trypsin

2.6.4 MEF cell culture and Mitomycin treatment

ES cells were grown on feeder cells called mouse embryonic fibroblasts (MEF), which are inactivated by the treatment with mitomycin C. MEFs are primary cells isolated from transgenic neomycin mouse which are resistant to G418 selection. MEFs were grown in normal cell culture plates for normal proliferation, but grown on 0.1% gelatin treated cell culture plates (NUNC) when we required to plate the ES cells on them. Once the MEFs were confluent, they were inactivated by the addition of 150 μ l of mitomycin C (400 μ g/ml) for 2 hours. Mitomycin will arrest the cell division, so there will not be any further growth of the cells. After 2hrs, cells were washed thoroughly with PBS to get rid of all the mitomycin C, trypsinised and plated onto gelatin coated cell culture plates.

2.6.5 ES cell culture

ES cells are cultured normally on mitotically inactive embryonic feeder cells (MEF). MEF cells should be mitomycin C treated and plated on gelatinised plates, one day in advance

of any ES cell manipulation. Confluent MEFs should be washed with PBS and supplied with ES cell media for at least two hours before the plating of ES cells. Frozen ES cells were thawed quickly by placing a vial in a water bath at 37⁰C and the content of the vial was added to 10 ml ES media in a 15 ml falkon tube. The cells were centrifuged at 500 rpm for 5 min and the pellet was resuspended in ES cell medium and plated on feeder cells. ES cell medium should be changed every 24 hrs.

2.6.6 ES cell transfection

For the transfection experiment 100 µg of the targeting vector was linearised by digestion with the Sall enzyme. The linearisation of the plasmid was confirmed on an agarose gel. The DNA was then extracted with phenol:chloroform (1:1) and then with chloroform alone. The DNA was precipitated with 96% ethanol, pelleted at 12,000 rpm for 10 min. The pellet was washed with 96% ethanol and with 76% ethanol. The air dried DNA was dissolved in millipore water at a concentration of 1 µg/µl.

ES cells were cultured on a 10 cm plate and on the day of transfection, the ES cell media was changed 2 hr prior to the transfection. After 2 hrs, the cells were washed with PBS and then 0.1% trypsin was added for 4 min till the cells detached from the plate. Cell clumps were disintegrated by slowly pipetting up and down several times and then centrifuged down at 500 x rpm in a Beckman CS 6R centrifuge. The cells were washed with PBS and resuspended in 350 µl of ES cell media and then transferred into a 4 mm transfection cuvette (BioRad). 50 µl of the target vector DNA was added mixed properly and kept on ice for 10 minutes. The transfection was done at 250V and 500 µF and typically a time constant between 8-12 was obtained. Cells were again kept on ice for 5 min and then plated into 4 mitomycin treated MEF 10 cm plates.

2.6.7 Antibiotic selection and picking of ES cell clones

Selection of ES cells resistant to neomycin was started after 48 hrs of transfection. For IB10 ES cells, 350 µg/ml (total) of G418 was used for selection and for R1 cells we used 400 µg/ml of G418. Usually on the third day, the untransfected cells will start to die. The selection is continued for another 7 days when small EScell colonies will start to appear. When the colonies grew large enough with firm boundaries, the colonies were picked using a 20 µl pipette under a light microscope with a 2.5X objective. On the day of picking, several 24 well plates plated with MEF were kept ready. Individual colonies were picked into a 96 well round

bottom plate along with 7 μ l medium and 50 μ l of 2X trypsin was added and kept for 10 min at 37⁰C. The trypsin was later neutralised with 20 μ l of trypsin inhibitor and mixed with 50 μ l of ES cell media. The cells were pipetted up and down several times slowly to break the cell clumps. The individual colonies were then plated onto the 24 well plate kept ready with feeder cells thermacoal box. The cells kept for genomic DNA isolation were further grown and harvested when the plates became confluent.

2.6.8 Genomic DNA isolation

TNES 50 mM Tris (pH: 7.4)
 100 mM EDTA (pH: 8.0)
 400 mM NaCl
 0.5% SDS

6 M NaCl

Proteinase K : 20 mg/ml

Trypsinised ES cells were mixed with 500 μ l of TNES buffer and 10 μ l of 20 mg/ml proteinase K solution and incubated at 55⁰C overnight in a shaking incubator. 150 μ l of a saturated (5 M) NaCl solution was added the next day to salt out the proteins. The sample was centrifuged at high speed for 5 minutes in order to pellet the precipitated proteins. The genomic DNA in the supernatant was precipitated by 96% ethanol and the pellet was washed with 70% ethanol. The pellet was dried and the genomic DNA was resuspended in 50 μ l of 10 mM Tris/HCl, pH 7.4.

Results

3 RESULTS

3.1 Analysis of the CAP2 (Cyclase associated protein 2) cDNA of *M. musculus*

A CAP2 cDNA has been isolated in our group by M. Leichter (2002). The CAP 2 cDNA has 1432 nucleotides (Figure 3.1). There are two possible ATG start codons present of which the second one appears to be the true start codon since it is embedded in the translation initiation consensus sequence as defined by Kozak (1987). The CAP2 cDNA encodes 476 amino acids. We compared the sequence with the one of different mammalian CAP homologues using the FastA program to study the homology at the nucleotide level. CAP2 has 86% homology to the human CAP2 cDNA and 89% homology to the one of rat.

```

1      ATGACAGACA TGGCGGGACT GATGGAGAGG CTGGAACGTG CAGTCATCCG GCTGGAGCAG CTGTCTGCAG
71     GGTTAGACGG ACCTCCCAGA GGCTGCGGGG AAGTGAATGG TGTCAATGGA GGTGTGGCAC CGTCCGTGGA
141    AGCTTTTGAC AAACTGATAA ACAGTATGGT GGCCGAGTTC TTAAAGAACA GCCGAGTCCT TGCTGGTGAC
211    GTAGAGACTC ACGCAGAAAT GGTGCACGGT GCTTTCCAAG CCCAGCGTGC TTTTCTTCTC ATGGTCTCGC
281    AGTACCAACA ACCCCAGGAG AATGAAGTTG CTGTCCTTCT GAAGCCATA TCGGAGAAGA TTCAAGAAAT
351    ACAGACTTTC CGAGAGAGAA ACCGGGGAAG CAACATGTTT AACCACTCTT CGGCAGTCAG TGAAAGCATC
421    GCCGCCTGG GCTGGATAGC CGTGTCCCCC AAACCTGGTC CTTATGTCAA GGAGATGAAC GACGCTGCCA
491    CCTTTTACAC AAACAGGGTC CTGAAAGACT ACAAGCACAG CGATCTGCGC CACGTGGATT GGGTGGAGTC
561    CTACCTCAAC ATCTGGAGCG AGCTGCAAGC CTACATCAGG GAACACCACA CCACAGGCCT CACTTGGAGC
631    AAAACAGGTC CTGTGGCATC CACAGCGTCA GCGTTTTCCA TCCTCTCCTC TGGGCCTGGT CTCCC GCCAC
701    CACCTCCACC ACCACCTCCT CCTGGGCCAC CTCACCCCTT TGAGAATGAG GATAAAAAGG AGGAGCCCTC
771    CCCTTCTCGC TCAGCTTTAT TTGCCAGCT CAATCAAGGA GAAGCCATCA CTAAAGGGCT CCGGCATGTC
841    ACAGATGACA AGAAGACATA CAAGAATCCC AGCCTGAGGG CTCAAGGACA GATTCGCTCT CCAACCAAAA
911    CTCACACGCC GAGCCCCACA TCTCCAAAAT CGAATTCTCC TCAGAAACAT ACTCCAGTGT TGGAGCTGGA
981    AGGGAAGAAG TGGAGAGTGG AATACCAAGA GGACAGGAAT GACCTTGTCA TCTCCGAGAC CGAGCTGAAA
1051   CAAGTGGCTT ACATTTTCAA ATGTGACAAA TCCACTCTTC AGATAAAGGG AAAAGTGAAC TCCATCACTG
1121   TCGATAACTG CAAGAAGTTT GGCCTGGTGT TTGATCATGT GGTGGGCATT GTGGAAGTGA TCAACTCCAA
1191   GGACATTCAG ATCCAGGTAA TGGGGAGAGT ACCAACAATC TCCATTAATA AGACAGAAGG ATGCCACCTG
1261   TACCTCAGTG AAGATGCACT AGACTGTGAG ATCGTGAGCG CGAAGTCGTC CGAGATGAAT GTCCTGGTCC
1331   CTCAGGATGA CGATTATAGA GAATTCCCCA TTCCCGAGCA GTTCAAGACA ATATGGGATG GCTCCAAGCT
1401   GGTCAACGAA CCTGCAGAGA TCATGGCCTG A

```

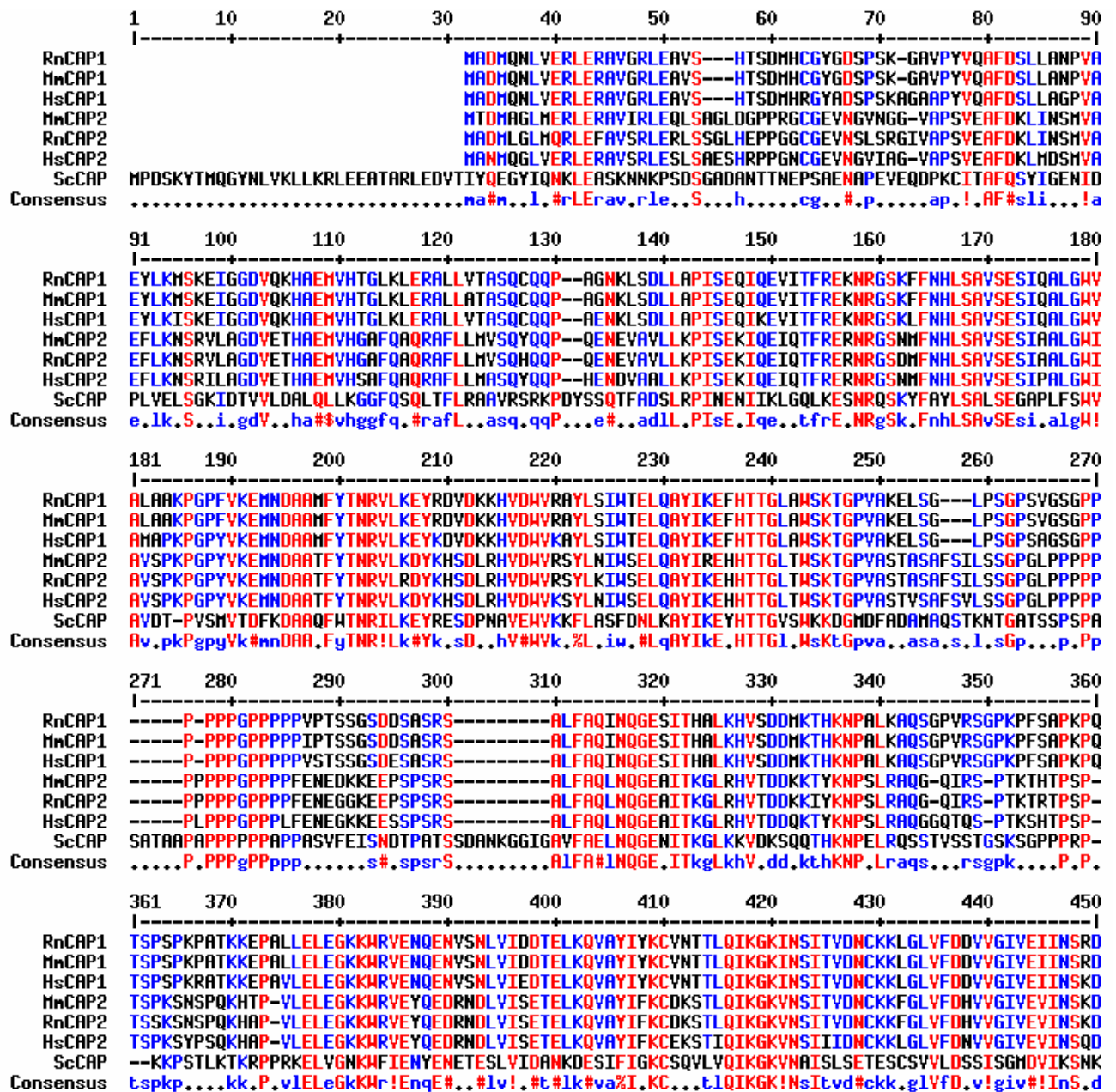
Figure 3.1: Sequence of the mouse CAP2 cDNA (taken from M. Leichter, 2002): The highlighted region (in yellow) is the Kozak consensus sequence including the start methionine codon (in bold). Red colour indicates the stop codon.

3.2 Multiple alignment of the mouse CAP2 protein with different CAP homologues

The comparison of the protein sequence of mouse CAP2 with CAP of *S. cerevisiae* revealed that it has similar features as the yeast protein. The domain structure shows that CAP2 of mouse has an amino terminus with a sequence which is predicted to bind to adenylyl cyclase,

a carboxy terminal domain which binds to actin and in between these two domains there is a proline rich region. Comparison of the protein sequences of mouse CAP1 and CAP2 revealed that CAP2 has 64% identity and 76% similarity with CAP1 (Figure 3.2 A, B). The proteins have 33% identity and 53% similarity to the *S. cerevesiae* CAP. CAP2 has 86% identity and has 94% similarity with its mammalian homologues like the rat and the human protein.

A



```

451   460   470   480   490   500   510   520   530
|-----|-----|-----|-----|-----|-----|-----|-----|
RnCAP1 YKVQVMGKVPTISINKTDGCHAYLSKNSLDCEIVSAKSSEMNVLIPT-EGGDFNEFPVPEQFKTLWNGQKLVTTVTEIAG
MmCAP1 YKVQVMGKVPTISINKTDGCHAYLSKNSLDCEIVSAKSSEMNVLIPT-EGGDFNEFPVPEQFKTLWNGQKLVTTVTEIAG
HsCAP1 YKVQVMGKVPTISINKTDGCHAYLSKNSLDCEIVSAKSSEMNVLIPT-EGGDFNEFPVPEQFKTLWNGQKLVTTVTEIAG
MmCAP2 IQIQVMGRVPTISINKTEGCHLYSEDALDCEIVSAKSSEMNVLVP--QDDYREFPIPEQFKTIWDGSKLVTEPAEIMA
RnCAP2 IQIQVMGRVPTISINKTEGCHLYSEDALDCEIVSAKSSEMNVLVP--QDDYREFPIPEQFKTIWDGSKLVTEPAEIMA
HsCAP2 IQIQVMGRVPTISINKTEGCHLYSEDALDCEIVSAKSSEMNILIP--QDDYREFPIPEQFKTIWDGSKLVTEPAEIMA
ScCAP  FGIQVNHSLPQISIDKSDGGNIYLSKESLNTEITSCSTAINVNLPIGEDDDYVEFPIPEQHKHSFADGKFSAVFEHAG
Consensus ..!QVng.vPtISI#kt#Gch.YLSk#sL#cEIvsakSsemN!l.P..#ddD%.EFP!PEQfKt.u.g.Kl.t.v.Eiag

```

B

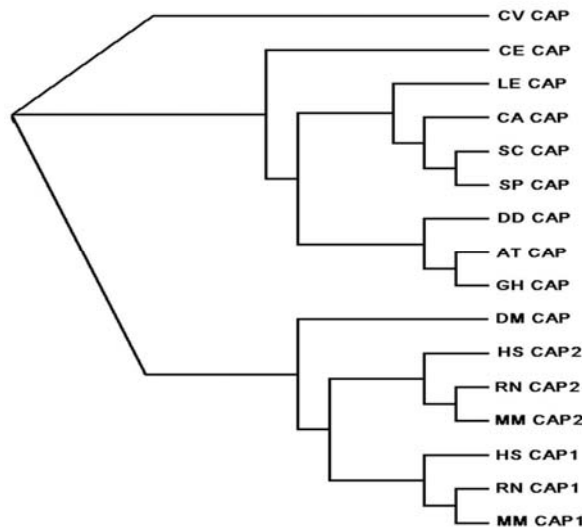


Figure 3.2: Sequence comparison of CAP of different species. A, Sequence comparison of CAP from mammals with CAP from *S. cerevisiae* using the multalin computer program. The darkly red supported amino acids represent the ranges with highest homologies. B, Sequence comparison of CAP from different organisms by Clustal W shown as Dendrogramme. The abbreviations are used as follows below. The accession numbers of the EMBL data base are also given: CV, *Chlorohydra viridissima* S47091, *Caenorhabditis elegans* AAK68198, LE *Lentinula edodes* BAA26003, *Candida albicans* AAD42978, *Saccharomyces cerevisiae* CAA86887, FR *Schizosaccharomyces pombe* CAB 41657, dd *Dictyostelium discoideum*, RK, *Arabidopsis thaliana* CAB80166, GH *Gossypim hirsutum* BAA36585, DM *Drosophila melanogaster* AAD27865, HS CAP1 *Homo sapiens* Q01518, HS *Homo sapiens* CAP2 P40123, MM1 CAP1 *Mus musculus* mm, CAP2 *Mus musculus*, RN CAP1 *Rattus norvegicus* A46584, RN CAP2 *Rattus norvegicus* JC4386.

These results are confirmed by analysing the phylogenetic tree of the CAP family proteins (Figure 3.2 B, taken from M. Leichter, 2002). From the multiple alignment data analysis of the different protein sequences, we conclude that CAP1 and CAP2 of mouse have similarities to the CAP protein from different species to a very large extent. The CAP proteins of mouse have around 48% identity to the *Dictyostelium* CAP whereas the CAP protein of *Arabidopsis thaliana* has around 75% identity to the mouse homologues. The degree of homology between the Mouse CAP1 and CAP2 varies within the regions of both the sequences. Comparison studies reveal that homology between the mouse CAP1 and CAP2 is slightly higher in the C-terminal region (~74%) than in the middle region (~ 65%). The N-terminal region has less

homology (~55%), which makes CAP2 more variable in the N-terminal region as compared to that of mouse CAP1.

3.3 Transcription of the CAP2 gene

RNA from different tissues of 8 weeks old mice (Balb/c) and from different mouse cell lines was isolated and northern blot analysis was performed using a ^{32}P labelled CAP2 specific probe of 634 bp derived from the N-terminus of the CAP2 cDNA. Transcripts of 3 kb and 3.5 kb in length were detected in a limited number of tissues agreeing with the data obtained for rat (Swiston et al., 1995). The tissues expressing CAP2 were muscle, testis and heart whereas the CAP2 transcript was not detected in brain, spleen, liver, kidney and lungs (Figure 3.3) Northern blots were also performed with RNA isolated from the following mouse cell lines: Neuroblastoma (N2A), fibroblast (C3H10T1/2) and myoblast (C2F3). No transcripts were detected. PCR analysis using CAP2 specific primers on RT-PCR products also resulted in no amplification of a PCR product. The data were generated in collaboration with M. Leichter (2002). Taken together, we were not able to detect signals in the majority of the tissues and in the cell lines unlike the results obtained for CAP1, which was found in most of the tissues and in most of the cell lines.

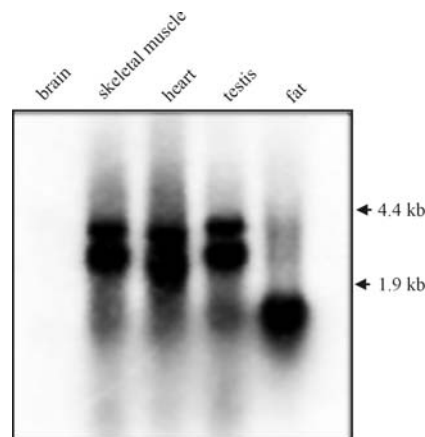


Figure 3.3: Northern blot analysis of CAP2 in different tissues. 20 μg of RNA of different tissues were separated on a 1% formaldehyde-agarose gel, under denaturing conditions transferred on to a nitrocellulose membrane, followed by hybridisation with a CAP2 specific N-terminal probe (1-634). The arrowheads indicates the position of the 28s and 16s ribosomal RNA.

3.4 Generation of polyclonal antibodies specific for CAP2

For investigation of CAP2 at the protein level and to study its biochemical function we generated polyclonal antibodies against the N-terminal region of mouse CAP2. This region was chosen because of lesser homology with CAP1. A 23 kDa polypeptide (amino acids 1-207) was expressed in the expression vector pQE-3 resulting in a His-tagged fusion protein,

the his-tag being located at the amino terminus. The recombinant protein was extracted using 8M urea, separated by SDS-PAGE (15 % polyacrylamide) electroeluted from the gel and used for the immunization of rabbits (Figure 3.4). Serum was collected at 60, 90, 120, 150, 180 and 210 days, respectively, and analysed by western blotting against total homogenate of *E. coli* strain DH5 α expressing the recombinant protein (Figure 3.3).

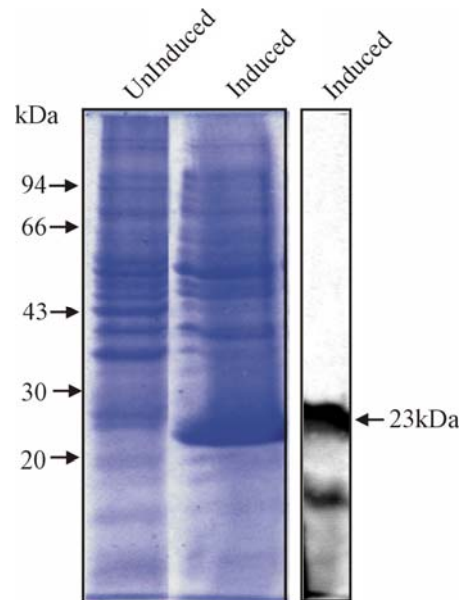


Figure 3.4: Expression of N-terminal CAP2 protein in *E. coli* and western blot analysis using polyclonal antibodies raised against the N-terminal CAP2 polypeptide. **A:** The pQE30 plasmid containing N-terminal CAP2 sequences was transformed into *E. coli* DH5 α cells. Protein expression was induced by addition of 1 mM IPTG. Aliquots from uninduced cells and induced cells for 4 hours at 37°C were resolved in 10 % SDS polyacrylamide gels and the proteins stained with Coomassie blue. The arrow indicates the position of the recombinant protein. **B:** The induced recombinant protein was resolved on 10% SDS polyacrylamide gel and transferred onto a nitrocellulose membrane by semidry blotting, the blot was incubated with polyclonal antibodies 1:5000 followed by incubation with horseradish peroxidase coupled secondary anti rabbit antibody. Detection was done with the ECL detection system. A 23 kDa protein was recognised (arrow) corresponding to the recombinant protein and a band of lower molecular weight, which might be a breakdown product.

The signal was detected at the expected size of the recombinant protein indicating that the CAP2 antibodies recognize the His tagged N-terminal CAP2 protein.

3.5 Characterization of the CAP2 antibodies

As CAP2 and CAP1 show a high homology we next tested the specificity of the antibodies for CAP2. Towards that we generated full length CAP2 fused with a Myc tag at its C-terminus and a full length CAP2 GFP fusion protein where GFP was located at the N-terminus of CAP2. To test for a cross-reaction with CAP1 we made use of a GFP-CAP1 construct generated by M Leichter (2002). The corresponding plasmids were transfected into HEK 293 cells, a human embryonic kidney cell line. A day after the transfection the cell homogenates were prepared and used for western blot analysis. The CAP2 antibodies recognised the full-length CAP2 Myc and GFP fusion proteins, however, they did not react with GFP-CAP1

(Figure 3.4 A lane 5). The antibodies were specific for the mouse CAP2 protein and also seem to recognise human CAP2 as taken from Figure 3.5 A lane 2, where a faint signal was detected in the whole cell homogenate of HEK 293. The blot was stripped and re-probed with GFP specific monoclonal antibody K3-184-2 to confirm the expression of fusion protein GFP-CAP2 and GFP-CAP1, respectively.

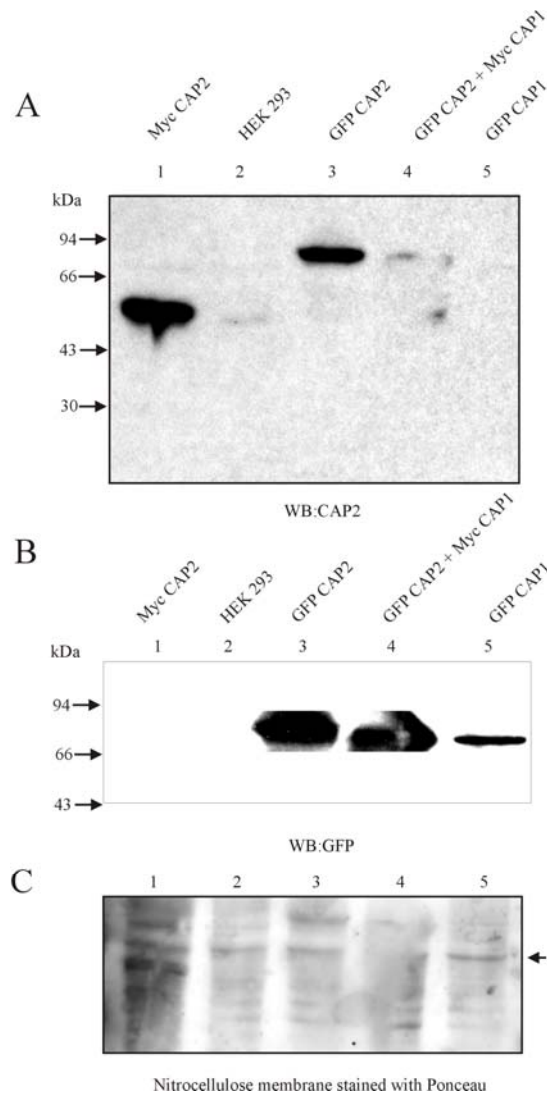


Figure 3.5: Western blot analysis showing the specificity of the CAP2 antibodies. **A:** Homogenates of HEK 293 cells expressing Myc-tagged CAP2, GFP-CAP2, GFP-CAP1, GFP-CAP2 and Myc-CAP1 (co transfected) and HEK 293 homogenate alone were separated in a 12 % SDS polyacrylamide gel and transferred onto a nitrocellulose membrane by semidry blotting. The blot was incubated with the polyclonal CAP2 antiserum (1:5000) detection was done using the ECL system and a secondary anti rabbit antibody conjugated with peroxidase. The CAP2 antiserum recognised full length CAP2 fusions with Myc- and GFP-tags as seen in lanes 1 and 3, respectively. The CAP2 antibodies were found to be specific for CAP2, as they did not recognise GFP-CAP1 in lane 5. **B:** The blot was stripped and re-probed with GFP-specific mAb K3-184-2 recognising the GFP fusion proteins of CAP2 and CAP1, respectively. As both GFP CAP2 in lane3 and GFP CAP1 in lane 5 were recognised by the GFP antibody indicating that both the fusion proteins were expressed. **C:** Nitrocellulose membrane stained with Ponceau. The band indicated by the arrow acts as a loading control.

The expression of GFP-CAP2 and GFP CAP1 was confirmed, as we were able to see the signals at the expected sizes of these proteins (Figure 3.5 B). The bands indicated by the

arrowhead in figure 3.5 C act as a measure for equal loading in the PonceauS stained blot. As we confirmed the specificity of our antibodies for CAP2 recognising only CAP2 but not CAP1 and also slightly cross-reacting with human CAP2, we searched for cell lines from human and rat origins. For these studies we used affinity purified antibodies. This purification step was carried out using the recombinant His-tagged CAP2, which we immobilised onto a PVDF membrane. The eluted antibodies were used for all subsequent studies including western blotting, immunoprecipitation, immunofluorescence and immunohistochemistry.

3.6 CAP2 over-expression studies in HEK 293 cells

CAP2 is expressed only in a limited amount of tissues and cells. For an initial study of its subcellular localisation we expressed N- and C-terminally modified CAP2 carrying a Myc- or GFP-tag in HEK 293 cells. One day after the transfection the cells were fixed with 3 % paraformaldehyde or a methanol-acetone mixture and labelled with specific antibodies.

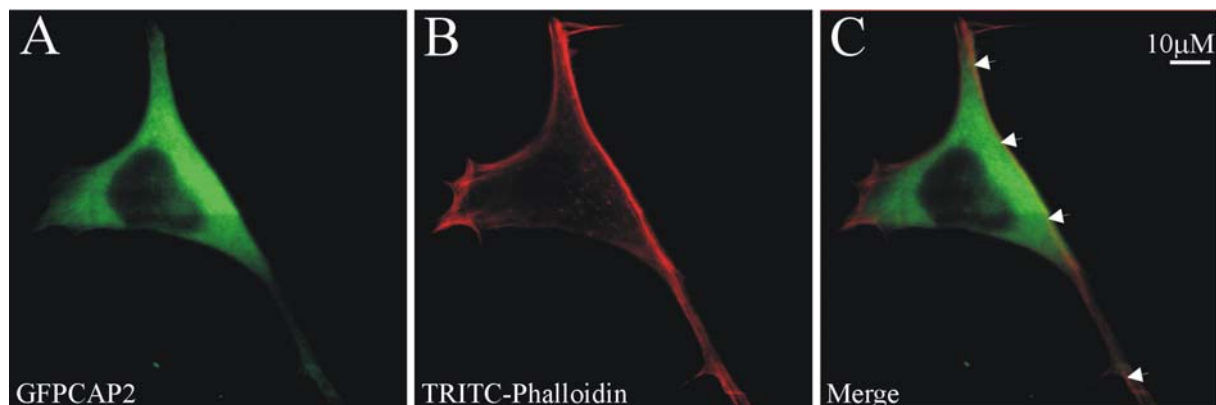


Figure 3.6: Subcellular localisation of GFP-CAP2 in HEK 293 cells. GFP-CAP2 expressing HEK 293 cells (A) were fixed with paraformaldehyde, permeabilised with 0.5% Triton X-100 and labelled with TRITC-phalloidin for the detection of F-actin (B). The GFP-CAP2 expression is shown in (A), the overlay in C. The picture was taken using a confocal microscope.

GFP-CAP2 is diffusely present in the cytosol and does not colocalise with F-actin (Figure 3.6). This contrasts with findings obtained in other organisms. In budding yeast and *Dictyostelium* Srv2/CAP localises to the cortical actin cytoskeleton (Freeman et al., 1996, Noegel et al., 1999) and studies with polyclonal antibodies and tagged versions of CAP1 showed that it is present in the F-actin rich cortical regions in C3H-2K fibroblasts (Moriyama and Yahara 2002; Korte 2004). For CAP2, we observed a diffuse cytosolic staining also for Myc-tagged CAP2 in indirect immunofluorescence analysis with affinity purified CAP2 antibodies, which were detected with an anti-rabbit IgG, secondary antibody conjugated with Alexa 568. These results were similar to the findings reported by M. Leichter (2002).

3.7 CAP2 interacts with CAP1

Earlier studies on CAP suggested that CAP interacts with actin (Amberg et al., 1995; Freeman et al., 1995) and that human CAP2 interacts with human CAP1 (Hubberstey et al., 1996). We therefore explored the possible interaction of mouse CAP2 with other molecules or with itself making again use of GFP-CAP1 and Myc-CAP2 and transiently expressed these proteins in HEK 293 cells by cotransfecting the corresponding plasmids.

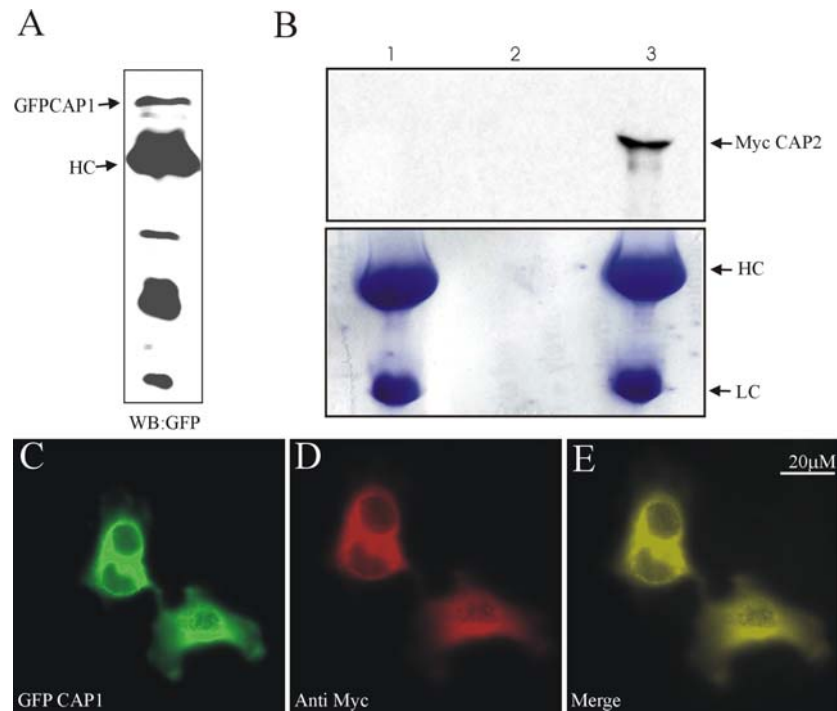


Figure 3.7: Coimmunoprecipitation and co localisation of GFP-CAP1 and Myc-CAP2: *A*: Western blot analysis of the immunoprecipitate beads (same as lane 3 in panel B) with mAb K3-184-2. *B*: Western blot analysis. A cell homogenate from HEK 293 cells transiently expressing GFP-CAP1 and Myc-CAP2 was incubated with mAb K3-184-2 specific for GFP, followed by incubation with protein A agarose beads. The immunoprecipitate was separated on a 12% SDS polyacrylamide gel, blotted to a nitrocellulose membrane and incubated with the CAP2 specific polyclonal antibodies. Detection was with enhanced chemiluminescence using a horseradish coupled secondary antibody. Upper panel, lane 1, protein A agarose beads + mAb K3-184-2. Lane 2, protein A agarose beads incubated with a lysate derived from cells expressing GFP-CAP1 and Myc-CAP2 without antibodies added. Lane 3, protein A agarose beads + mAb K3-184-2 incubated with lysates from HEK293 cells co expressing GFP-CAP1 and Myc-CAP2. The resulting blot was probed with CAP2-specific polyclonal antibodies. The signal detected in lane 3 indicates that Myc-CAP2 coprecipitates with GFP-CAP1. The lower panel shows the corresponding Coomassie stained SDS-polyacrylamide gel. The arrows point to the immunoglobulin heavy chain (HC) and lower chain (LC). *B-D*: Immunofluorescence studies showing the GFP-CAP1 (*B*) and Myc-CAP2 (*C*) distribution. Cells were fixed with 3% paraformaldehyde and permeabilised with 0.5 % Triton X-100. Myc-CAP2 was detected with the polyclonal CAP2-specific antibody. Detection was with anti- rabbit antibody conjugated to Alexa 568. (*D*) The overlay of the GFP-CAP1 and the Myc-CAP2 shows complete colocalisation in the cytosol. CAP1 in addition is also present in cell extensions.

In immunoprecipitation experiments with the GFP-specific mAb K3-184-2 Myc-CAP2 could be precipitated (Figure 3.6 B). We could see that GFP-CAP1 also precipitated (Figure 3.7 A). Control experiments showed that the pull down of Myc-CAP2 depended on the addition of the GFP antibody. This result determines that interactions are conserved in mammals as it has

been already shown that human CAP2 binds to human CAP1 (Hubberstey et al., 1996). Moreover we have done immunofluorescence studies with the same cells to support the findings at this level as well. In coimmunofluorescence studies GFP-CAP1 and the Myc-CAP2 show an overlap in the cytosol, whereas cortical staining was only observed for CAP1.

3.8 Analysis of CAP2 distribution in tissues and cell lines by western blotting

In Northern blot analysis we had detected a CAP2 signal only in some tissues (Section 3.3). Here we screened various tissues and a number of commonly used mouse, rat and human cell lines for the expression of CAP2 by western blots. We found the expression of CAP2 in only four organs, namely heart, brain, skeletal muscle and skin (Figure 3.8 A). Heart, brain and skeletal muscle showed a strong signal, whereas the amounts of CAP2 in skin were lower. The band obtained in Figure 3.7 results from loading 5 times higher amounts of protein for skin. The expression of CAP2 in heart and skeletal muscle is in line with the results from the northern blot analysis, whereas there was no signal obtained in case of brain and skin.

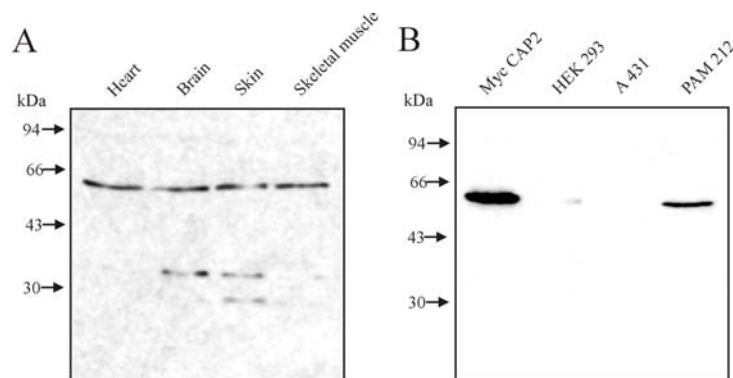


Figure 3.8: Presence of CAP2 in tissues and in Pam212 cells. **A:** homogenates of heart, brain, skin and skeletal muscle tissue were loaded onto 12% SDS poly acrylamide gels and transferred onto nitrocellulose by semidry blotting. The blot was incubated with polyclonal CAP2 antibodies, and, using the ECL detection system, probed with a secondary anti rabbit antibody conjugated to peroxidase. The CAP2 antibodies recognise a 55 kDa size protein, which corresponds in size to CAP2. Here for the skin lysate 5 times more was loaded than for the other tissue lysates. **B:** Cell homogenates from HEK 293 cells expressing Myc-CAP2 as a positive control, HEK 293, A431 (Human keratinocytes) and PAM212 (mouse keratinocytes) were separated on a 12 % SDS polyacrylamide gel and transferred onto a nitrocellulose membrane and probed with CAP2 antibodies, using the ECL detection system for detection with a secondary anti rabbit antibody conjugated with peroxidase. A 55 kDa band could be seen in Myc-CAP2 expressing HEK293 cells, which acted as a positive control, and in the mouse keratinocytes PAM212 cell line. A faint band was seen in the HEK 293 cell line, which confirms that the mCAP2 antibodies recognise the human protein.

Similarly, Bertling et al. (2004) have shown a strong expression of CAP2 in heart, brain and skeletal muscle and very weak expression in lung, liver and testis. On the contrary we were not able to detect any signal in liver and testis but a very weak signal was seen in lungs. The

—

expression of CAP2 was comparatively higher than the expression of CAP1 in heart, brain, skeletal muscle and skin tissues (Korte 2004). In case of the cell lines, we were able to detect a (strong) expression of CAP2 only in PAM212 cells, a mouse keratinocyte cell line. We were not able to detect a signal for CAP2 in any other mouse cell lines. As we already reported a very weak signal in HEK 293 cells, which is a clear indication that the CAP2 antibody also recognises the Human CAP2, we checked the CAP2 expression in A431 cells, which are derived from human keratinocytes. Surprisingly, we did not observe any signal for CAP2 in A431 cells. We also tested the rat VSM cell line which is derived from rat vascular smooth muscle where a very faint signal was detected (data not shown), which indicates that the CAP2 antibodies cross react with rat CAP2 as well. Myc CAP2 expressed in HEK 293 cells was used as a positive control. From these results we can clearly say that the expression pattern of CAP2 and CAP1 are very different in case of both tissues and cell lines since CAP1 is expressed in almost all the cell lines and tissues unlike CAP2, which is expressed only in the PAM212 cell line and a limited number of tissues.

3.9 Search for binding partners of CAP2

Using the recombinant His-tagged N-terminus of CAP2 and the polyclonal antibodies we initiated a search for binding partners. The his-tagged fusion protein was isolated from a bacterial lysate by incubation of the 12 K supernatant, which contained reduced but sufficient amounts of the recombinant protein significant, with Ni-NTA agarose beads. The beads were then incubated with lysates of skin, heart and brain tissues. For control we used the N-terminal actin binding domain of Enaptin. Both samples were treated similarly as described in Materials and methods and the proteins bound to the beads loaded onto a 3% to 15% gradient SDS poly acrylamide gel and the proteins stained with Coomassie blue (Figure 3.9). The band indicated by an arrow (Figure 3.9) was excised and analysed by MALDI-TOF and identified as alkali myosin light chain (MLC3 nm), non-muscle isoform. The myosin molecule consists of 2 heavy chains and 4 associated light chains. Two of the light chains are regulatory light chains (RLC) encoded by the MYL2 gene and 2 are alkali light chains, or essential light chains (ELC), encoded by the MYL3 gene. The light chains stabilise the long alpha-helical neck of the myosin head. Distinct isoforms of the myosin alkali light chains are present in different tissues. Their function in striated muscle and in other tissues is only partially understood (Poetter et al., 1996)

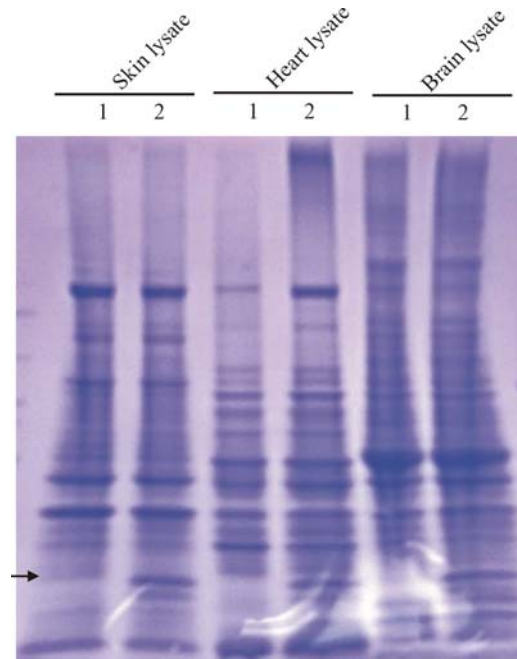


Figure 3.9: N-CAP2 binds to alkali myosin light chain (MLC3 nm) in skin. The Ni-NTa-agarose beads loaded with the N-terminal polypeptide of CAP (1) or Enaptin (2) were incubated with lysates of skin, heart and brain, respectively, and separated on a 3% to 15% gradient SDS polyacrylamide gel and stained with Coomassie blue. The lane 1 from all the lysates represents the pull down with His tagged N-CAP2 bound to Ni-NTa agarose beads and the lane 2 represents the control (His tagged N-ABD of Enaptin bound to Ni-NTa agarose beads). The band in skin indicated by the arrow was absent from the control. It was excised and analysed by MALDI-TOF. The protein was identified as alkali myosin light chain.

3.10 CAP2 localisation in skeletal muscle

Western and northern blot analysis indicates an expression of CAP2 in skeletal muscle. We tried to support these findings also by immunofluorescence microscopy and stained sections of human and rat skeletal muscle.

Skeletal muscle, as its name implies, is the muscle attached to the skeleton. It is also called striated muscle. Seen from the side under the microscope, skeletal muscle fibers show a pattern of cross banding, which gives rise to the other name: striated muscle. The striated appearance of the muscle fiber is created by a pattern of alternating dark A bands and light I bands. The A bands are bisected by the H zone. The I bands are bisected by the Z line (Figure 3.10).

Frozen human and rat muscle sections were obtained from Dr. R. Schröder, University Hospital, Bonn, and stained with the CAP2 antibodies. These sections were also costained with desmin, a marker protein for skeletal muscle, which is the main intermediate filament protein found in skeletal and heart muscle and gives a characteristic staining pattern because it is usually confined to the Z-disc. Surprisingly we observed a striated pattern for CAP2 distribution (Figure 3.11 A, D, G and J) similar to the striated pattern obtained for desmin (Figure 3.11 B, E, H and K) in both human and rat specimens, respectively. The overlay

images (Figure 3.11 C, F, I and L) for both proteins indicate however that CAP2 does not colocalise with the desmin and therefore should not be present in the Z-disc. The striated staining of CAP2 is rather in-between the Z-disc indicating CAP2 might be present in the neighbouring A-band, I-band or M-band in the skeletal muscle sections of both human and rat.

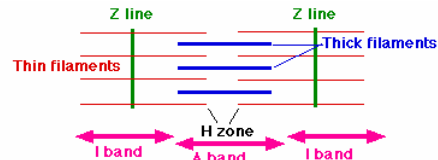


Figure 3.10: Schematic diagram representing the sarcomere and depicting the position of Z-line, I-band and A-band (taken from users.rcn.com/.../BiologyPages/M/Muscles.html).

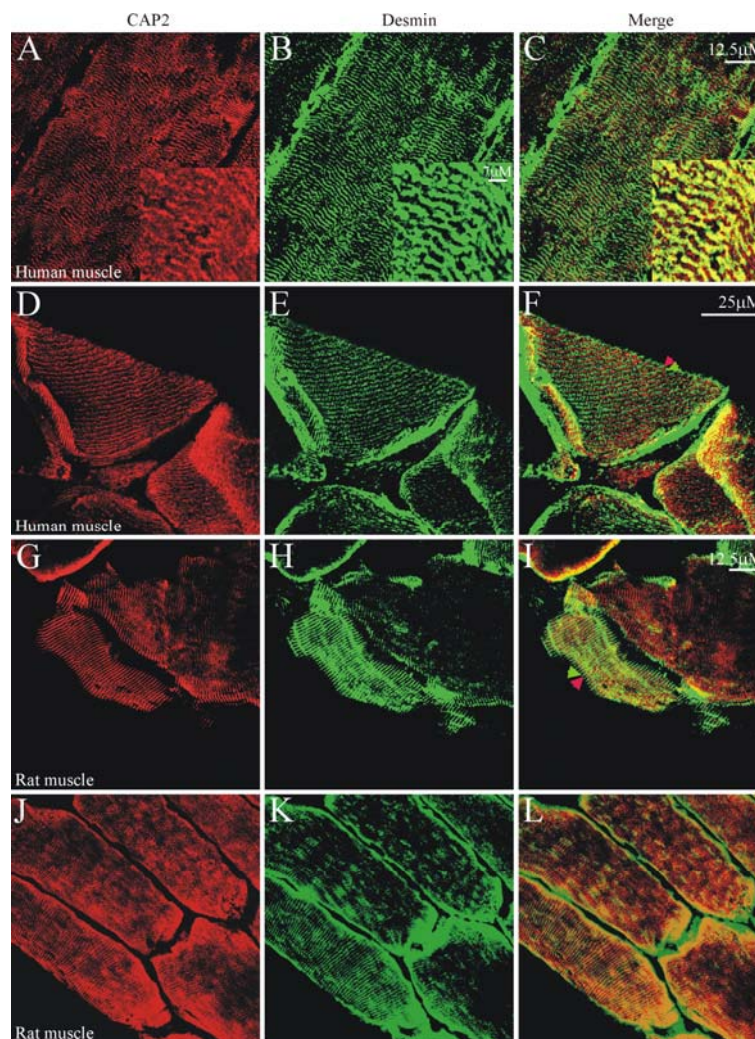


Figure 3.11: Localization of CAP2 in skeletal muscle. Cryosections of human and rat muscle were fixed with 3% paraformaldehyde and permeabilised with 0.5% Triton X-100. Adult human and rat muscle sections were stained with CAP2 specific antibodies and costained with desmin specific monoclonal antibodies, respectively. A-F (human muscle) and G-L (rat muscle) represents a comparison of CAP2 and desmin distribution in human and rat skeletal muscle. A and D for human, G and J for rat shows CAP2 staining; B and E (human), H and K (rat) shows desmin staining; C and F (human), I and L (rat) shows the overlay respectively. CAP2 was detected with anti-rabbit IgG secondary antibody conjugated with Alexa 568 and desmin by anti-mouse IgG secondary antibody tagged with Alexa 488. CAP2 does not colocalise with desmin, indicating that CAP2 is not present in the Z-disc region. Confocal microscopy was used to take these images.

3.11 CAP2 localisation in mouse skin

The skin is considered the largest and the heaviest organ of the body occupying 16% of the total body weight and having many different functions. It functions in thermoregulation, protection, metabolic functions and sensation. The skin is divided into two main regions, the epidermis and the dermis (Figure 3.12), each providing a distinct role to the overall function of the skin. The dermis is attached to an underlying hypodermis. The epidermis is a multilayered structure (stratified epithelium), which renews itself continuously by cell division in its deepest layer, the basal layer. The principal cell type, the epidermal cell, is most commonly referred to as a keratinocyte. The cells produced by cell division in the basal layer constitute the prickly cell layer and as they ascend towards the surface they undergo a process known as keratinisation, which involves the synthesis of the fibrous protein keratin. The basal layer is composed of columnar cells, which are anchored to a basement membrane lying between the epidermis and dermis. The basement membrane is a multilayered structure from which anchoring fibrils extend into the superficial dermis. Interspersed amongst the basal cells are melanocytes, large dendritic cells responsible for melanin pigment production. Basal cells are mitotically active, but they lose this potential when they detach from the basement membrane and enter the outward path towards the skin surface. The layer of cells directly contacting the basement membrane, termed the basal layer, contains proliferating cells. During differentiation the epithelial cells undergo apoptosis and lose their nuclei and become the dead layer of the epidermis, the stratum corneum (Alonso and Fuchs, 2003).

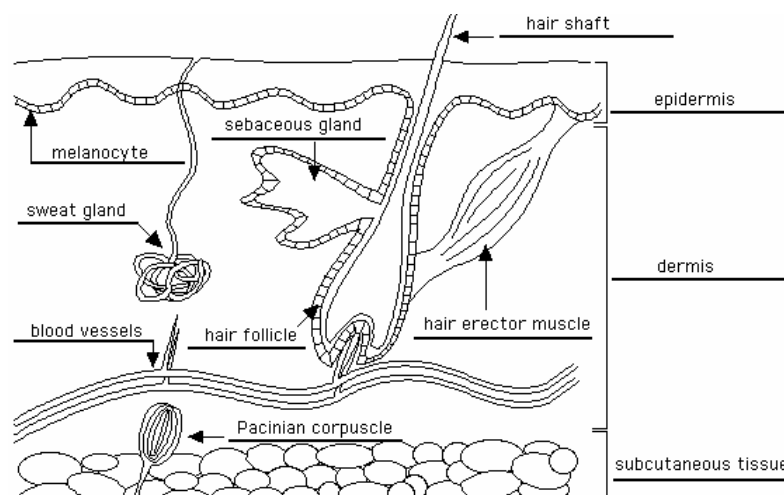


Figure 3.12: A diagram showing a cross section of skin, illustrating its overall histology (taken from <http://www.enchantedlearning.com/subjects/anatomy/skin/>).

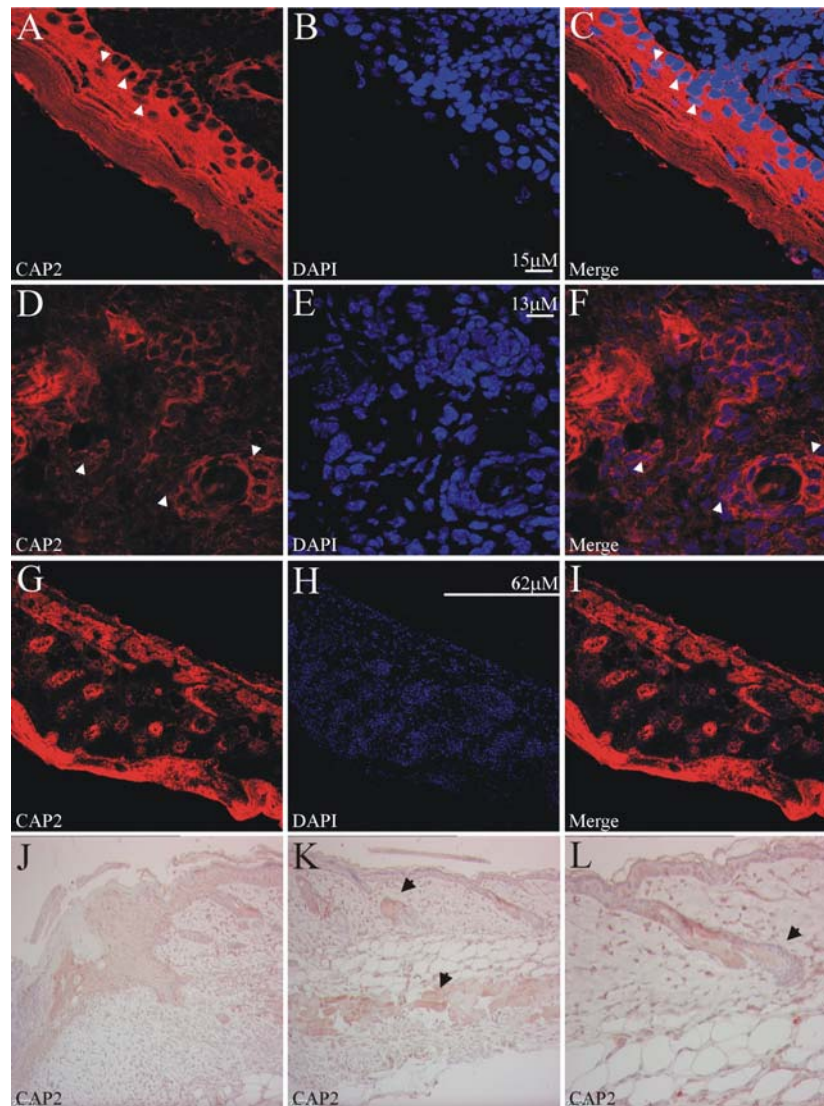


Figure 3.13: Immunofluorescence and histological studies of CAP2 in skin. A paraffin section of a mouse skin was deparaffinised using xylol and ethanol of varying percentage. The Section was incubated with CAP2 specific antibodies and DAPI for nuclei staining .The CAP2 antibodies were detected by anti-rabbit IgG secondary antibody conjugated to Alexa 568 (panel A-I images were taken by confocal microscopy). For the histological staining (J-L) CAP2 antibodies were detected by biotin labelled anti-rabbit secondary antibody after quenching the peroxidase activity and blocking. Peroxidase is conjugated with an avidin-biotin system and DAB is used as the substrate for peroxidase.

The confocal images of skin staining revealed that CAP2 is present in the epidermal layer of the skin (Figure 3.13 A, B and C), panel B was stained for nuclei with DAPI, C shows the overlay of CAP2 and DAPI. These images also indicate that CAP2 is localised in the basal layer of the epidermis, where keratinocytes are present. The keratinocytes differentiate and move to the outer layers to form a dead layer, which is devoid of nuclei as can be clearly seen in panel B. The arrowheads in panel C point to cells in which CAP2 staining was also seen in the nucleus. CAP2 staining was furthermore observed strongly in the hair follicle regions, (Figure 3.13 D, E and F). D, CAP2 staining, E, DAPI and F, overlay. The higher magnification of a hair follicle shows that at certain places CAP2 is partially colocalising with

DAPI, which is indicated by the arrowheads (panel F). Panels G, H and I are the overview images of CAP2 staining in skin wherein the CAP2 antibodies stain the basal layer of the epidermis and the hair follicle regions in the lower magnification. The histochemical staining shown in panels J, K and L confirms the staining observed with the confocal images. CAP2 is clearly localised in keratinocytes and in the hair follicle (panel L) and CAP2 was stained positively for the sebaceous glands (shown by arrows in panel K) and in the migration tongue of the skin. It showed mostly a cytosolic distribution of CAP2.

3.12 Expression of CAP2 in brain

Our western blot studies showed a strong expression of CAP2 in brain. We therefore planned a more detailed examination of CAP2 in the brain. Towards this we used paraffin embedded sagittal sections from 20 days old mice. We stained these sections with the CAP2 antibodies and detected the binding by a secondary anti-rabbit IgG antibody conjugated to Alexa 568.

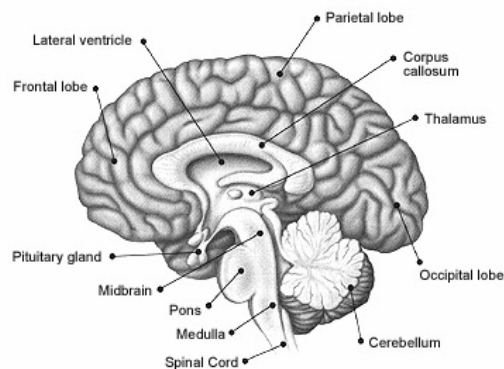


Figure 3.14: Schematic diagram representing the different parts of the brain (taken from www.biologycorner.com/bio3/notes-nervous.html).

In the brain, the neuronal cell bodies comprising the grey matter become clustered into groups called nuclei (singular - nucleus). Nuclei in the central nervous system are analogous to ganglia in the peripheral nervous system. A nucleus is composed of clusters of neuronal cell bodies and should not be confused with the nucleus contained within each cell. In some parts of the brain, neurons and neuroglia differentiating from the mantle layer of the original neural tube migrate outwards through the white matter (myelinated axons) of the marginal layer where they form a peripheral, multi-layered covering of grey matter. This outer covering of grey matter on the cerebral hemispheres is called the cerebral cortex. The cerebellum also has a cerebellar cortex, which develops in a similar way (Figure 3.14).

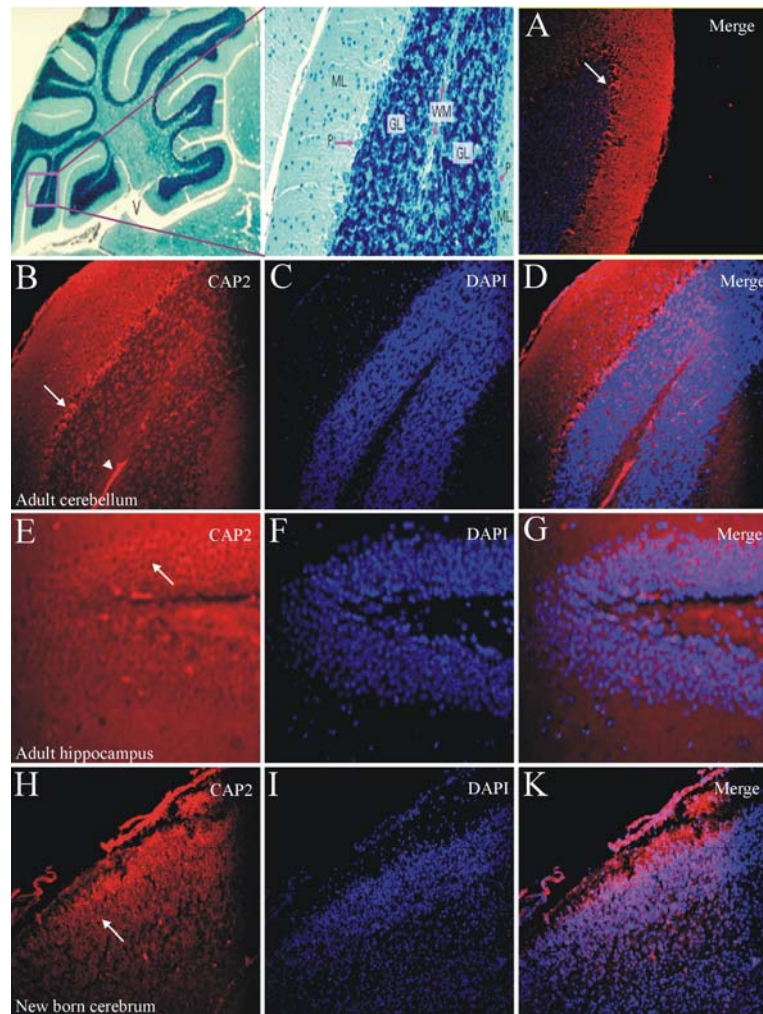


Figure 3.15: CAP2 distribution in cerebrum, cerebellum and hippocampus. Saggital sections of paraffin embedded 20 days old and new born mouse brain were deparafinised and hydrated using xylol and varying percentage of ethanol. The sections were incubated with the CAP2 specific antibodies and afterwards with FITC conjugated anti-rabbit secondary antibodies along with DAPI. A-D shows the cerebellum staining. E-G shows the staining of hippocampus and H-K shows the staining of CAP2 in newborn cerebrum. The first two panels give an overview and were taken from <http://www.uoguelph.ca/zoology/devobio/miller/>.

In Figure 3.15 the first two panels show a sagittal section through a mouse cerebellum. In the first panel the outer portion is composed of grey matter in two layers: the molecular layer (outer, lighter) and the granular layer (inner, dark). The white matter is seen in the middle of the cerebellum. The second panel is a high power image of the cortical area seen in the magenta box on the image to the left. From left to right we see the outer molecular layer (ML), the single row of Purkinje cells (P), the inner granular layer (GL) and a thin strip of the white matter (WM) occupying the central portion of the cerebellum. Purkinje cells are large neuronal cells with numerous dendrites, which are characteristic of the cerebellar cortex. The panels A and B show the staining of CAP2 in the adult cerebellum wherein CAP2 is localized to the molecular layer, CAP2 is also present in the Purkinje cells, which is indicated by the arrows whereas CAP1 is absent from the Purkinje cells (Korte, 2004). The arrowhead shows

the staining of CAP2 in the thin strip of the white matter. The panel C shows the DAPI staining and panel D shows the overlay. The panels E-G represent the staining of the adult hippocampus, where strong expression of CAP2 was observed in the hippocampal neurons in and around the nucleus, which is indicated by the arrow in panel E. A moderate expression of CAP2 was observed in the newborn cerebrum shown in the panels H-K. The CAP2 expression is migrating outwards from the grey matter towards the cerebrum cortex. The arrow in the panel H indicated the direction of migration. This result reveals that CAP2 might play a role in the differentiation of neuronal glia cells.

3.13 Analysis of expression of CAP2 in different parts of the adult and newborn mouse brain by western blotting

As our immunofluorescence studies suggested that CAP2 is present all over the brain, we tried to confirm these results by conventional western blots. Homogenates of different parts of the adult (30 days old) and newborn brain were obtained from Dr. Andreas Hasse. These homogenates were separated on 12% SDS polyacrylamide gels and transferred onto nitrocellulose membrane by semidry blotting. The CAP2 antibodies recognised a 55 kDa band, which corresponds to CAP2.

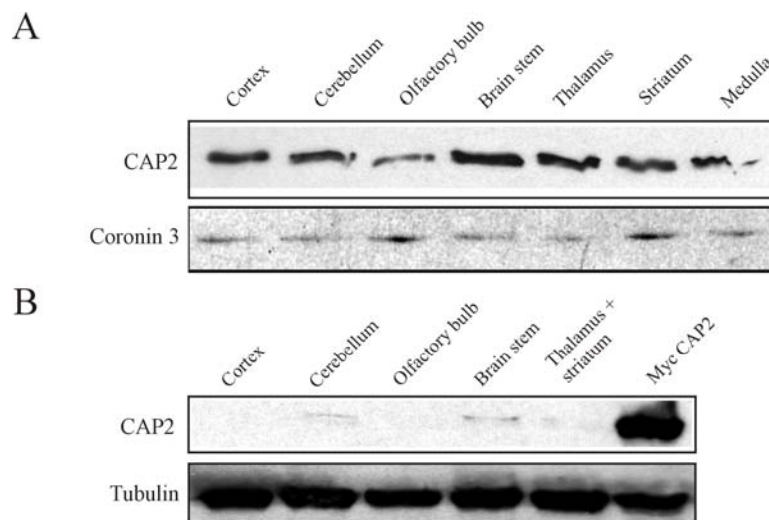


Figure 3.16: CAP2 expression in different parts of adult and newborn mouse brain. A: The homogenates of different parts of adult brain were loaded onto 12 % SDS polyacrylamide gels, the proteins separated and transferred onto nitrocellulose by semidry blotting. The blot was incubated with polyclonal CAP2 specific antibodies and a monoclonal anti Coronin 3 antibody for control. The ECL detection system was used to reveal binding of the antibodies. The CAP2 antibodies recognise the 55 kDa CAP2. B: The homogenates of different parts of newborn brain were loaded onto a 12 % SDS polyacrylamide gel and the proteins transferred onto nitrocellulose membrane by semidry blotting. The blot was incubated with polyclonal CAP2 specific antibody and a monoclonal anti Tubulin antibody for loading control. As positive control for CAP2 a lysate from HEK 293 cells expressing Myc-CAP2 was also loaded. The ECL detection system was used to detect binding of the antibodies.

As expected we observed the expression of CAP2 throughout the brain. (Figure 3.16 A). The expression levels were comparable in all parts of the adult brain except for a slightly reduced

expression in the olfactory bulb. The blot was probed for coronin 3 for which the expression pattern has been established (Hasse et al., in preparation). The result is also comparable to the one obtained for which is also expressed uniformly in all parts of the brain (Korte, 2004). In contrast, Bertling et al. (2004) observed a strong expression of CAP2 in striatum, thalamus and in cortex. In the newborn mice the expression pattern of CAP2 was different (Figure 3.16 B). We were able to detect the protein only in the cerebellum and in the brain stem, agreeing with the western blot data.

3.14 Localisation of CAP2 in rat primary cerebellar cultures

In the immunofluorescence images of the brain we observed strong staining of CAP2 in the white matter, where myelinated axons are present, in cerebellum and in Purkinje cells. These results led us to investigate the expression of CAP2 in primary cerebellar cultures isolated from rat brain. The cerebellar cultures and the staining were carried out in collaboration with Dr. J. Kappler, Institute of Physiological Chemistry, University of Bonn).

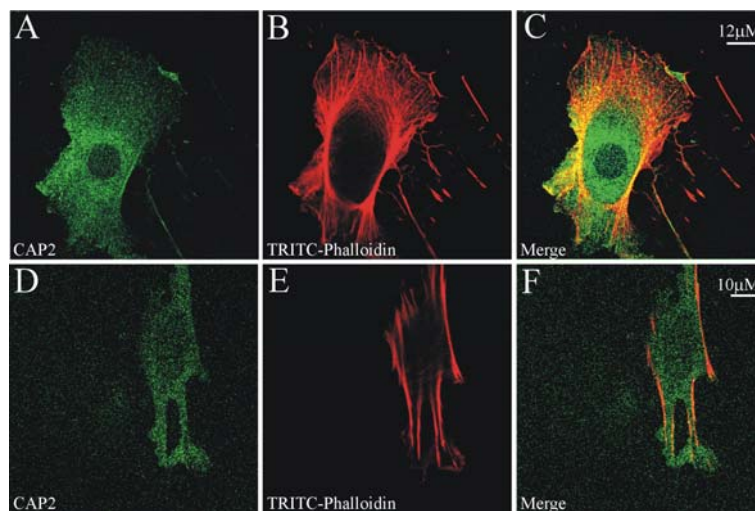


Figure 3.17: Localisation of CAP2 in primary cerebellar culture. Primary cerebellar cells were fixed with paraformaldehyde, permeabilised with 0.5% Triton X-100 and stained with CAP2 specific antibodies and then probed with secondary anti rabbit IgG antibody conjugated to Cy2. The cells were also stained with TRITC-phalloidin for the detection of F-actin. Panels A and D show CAP2 staining, B and E show F-actin, C and F represent the overlay. These images were taken by confocal microscope.

The immunofluorescence images (Figure 3.17) show the presence of CAP2 in the primary cerebellar cells. A diffuse dotted staining of CAP2 was seen in the cytosol with an accumulation around the nucleus in some of the cells (Figure 3.17 A). Occasionally CAP2 was found in the nucleus as well. The comparison with the F-actin distribution (Figure 3.17 C and F) showed that CAP2 partially colocalised with actin fibers at certain regions of the cortex.

3.15 Expression of CAP2 in rat primary glia cells

As we observed CAP2 staining in the myelinated axons of the white matter in brain, we were tempted to check the localisation in glia cells because of its presence in the white matter. Glia cells are specialised cells of the nervous system whose main function is to "glue" neurons together. Specialised glia cells called Schwann cells secrete myelin sheaths around particularly long axons. Glia of the various types greatly outnumbers the actual neurons. Glia cells are also known as neuroglia. There are three main types of glia cells in the central nervous system: microglia, astrocytes, and oligodendrocytes, each of which perform different functions. Glia cells are specialised to support and nourish the neurons and have many regulatory functions.

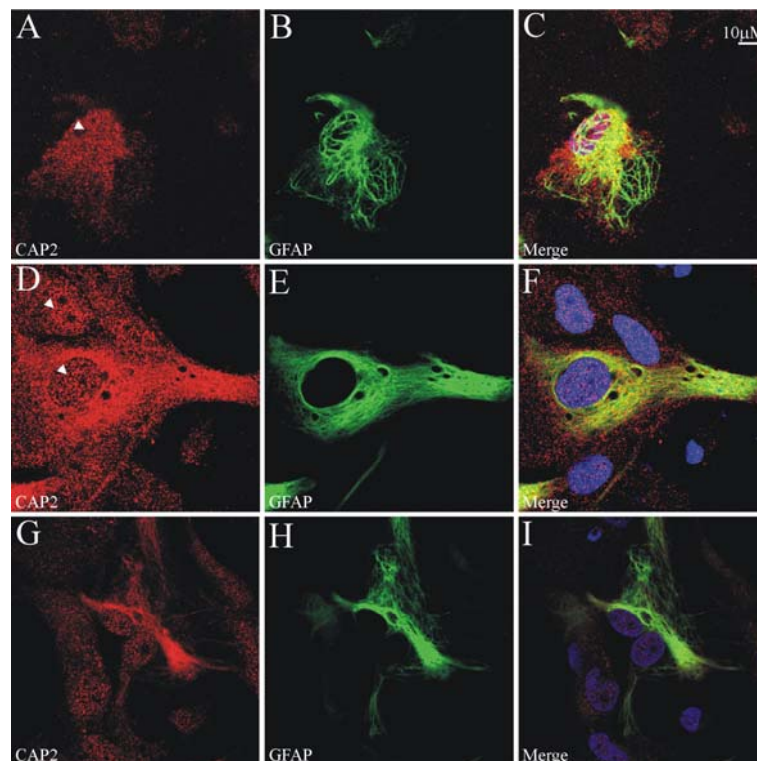


Figure 3.18: Localisation of CAP2 in primary glia cells. Primary glia cells were fixed with paraformaldehyde and permeabilised with 0.5% Triton X-100, costained with CAP2 specific antibodies and anti GFAP antibody, then probed with secondary anti rabbit IgG antibody conjugated to Cy3 and secondary anti mouse IgG antibody conjugated to Alexa 488, respectively. The panels A, D and G show CAP2 staining, panels B, E and H show GFAP staining and the panel C, F and I show the overlay of CAP2 and GAFP. Confocal images are shown.

The primary glia cells were isolated from the rat brain. Staining was with CAP2 specific antibodies and secondary anti rabbit IgG antibody conjugated to CY2, the cells were also costained with anti GFAP antibody detected by secondary anti mouse IgG antibody conjugated to Alexa 488. Glial fibrillary acidic protein (GFAP) is an intermediate-filament (IF) protein that is highly specific for cells of astroglial lineage. The GFAP antibody detects

astrocytes, Schwann cells, satellite cells, enteric glial cells and some groups of ependymal cells. We observed a filament like staining (Figure 3.18) for GFAP, which confirmed the identity with glia cells. In these glia cells we observed a strong expression of CAP2 in the cytoplasm as well as in the nucleus (Figure 3.18 A, D and G) indicated by the arrowheads. The panels B, E and H show the GFAP staining. The overlay images C, F and I show that CAP2 staining partially overlaps with GFAP. The nuclear staining of CAP2 was not present in all glia cells (Figure 3.18 G; H and I).

3.16 Localization of CAP2 in the heart

There are three layers of the heart similar to those found in the vasculature. However, these layers have different names, the luminal side of the atrium, which is defined as the endocardium and includes the collagenous connective tissue lying just beneath the endothelial cells (sub-endothelial tissue). The muscular layer is defined as the myocardium and contains the cardiac muscle cells. The outer layer is called the epicardium and contains collagenous connective tissue, blood vessels, and nerve and has a mesothelial cover. The epicardium of the atrium does not contain an abundant supply of vessels and nerve as found in the ventricle. The collagenous connective tissue presents as thicker bundles of collagen fibers in the epicardium than in the endocardium.

In heart, one of the organs showing CAP2 expression, CAP2 was observed in sarcomeres (Figure 3. 20 B) and in the endothelial cells as indicated by arrows (Figure 3. 20 A).

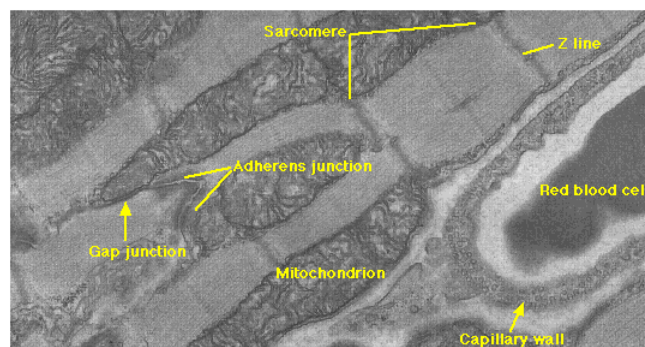


Figure 3.19: Section of the cardiac muscle (taken from <http://users.rcn.com/~jkimball.ma.ultranet/biologypages/M/muscles.html>)

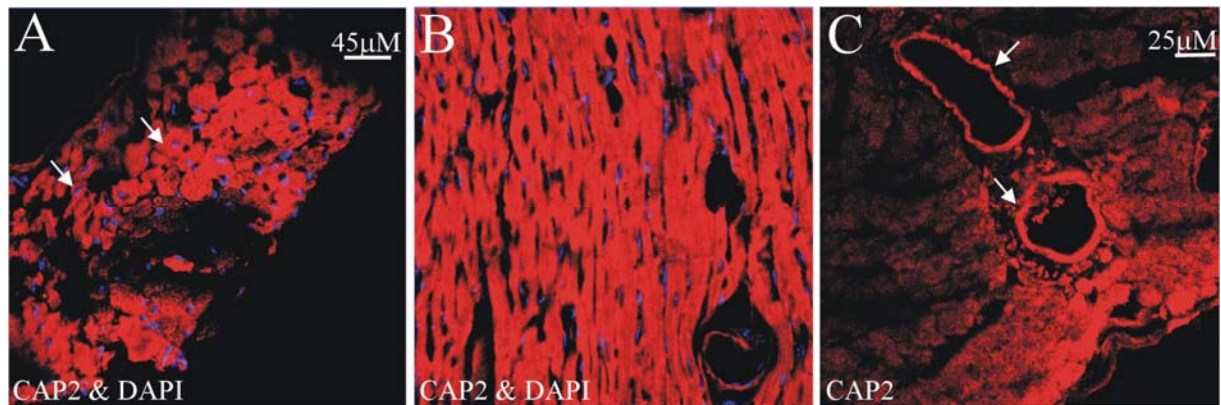


Figure 3.20: Expression of CAP2 in the heart: Heart sections were deparafinised and hydrated using xylol and varying percentage of ethanol. The sections were incubated with the CAP2 specific antibodies and afterwards with Alexa 568 conjugated anti-rabbit secondary antibodies along with DAPI. Panels A and B stained for CAP2 and DAPI, panel C stained for CAP2 only.

CAP2 expression was also observed in the capillary wall as indicated by arrows (Figure 3. 20 C).

3.17 Expression of the CAP2 in primary cardiomyocytes

To investigate CAP2 expression in the heart in more detail and at a higher level, we isolated cardiomyocytes from embryonic mice. We used the embryos of 17 and 19 days. This part of the work was carried out in collaboration with Prof. Gabriele Pfitzer, Institute of Vegetative Physiology, University of Cologne. The cardiomyocytes were costained with CAP2 specific antibodies and cardiac specific Troponin I antibodies. Troponin I was used as a specific marker for the cardiomyocytes. We observed a strong expression of CAP2 in the nucleus as well as in the cytosol. The staining was of punctate nature in the cytosol and at the cortex (Figure 3.21). The Troponin I staining was confined to the cytosol and around the nucleus. In the overlay images we see a partial colocalisation of CAP2 with Troponin I. The colocalisation was slightly stronger in 19 days old embryonic cardiomyocytes as the expression of Troponin I increases with the age. In addition, CAP2 is present in the nucleus (Figure 3.21 A-D).

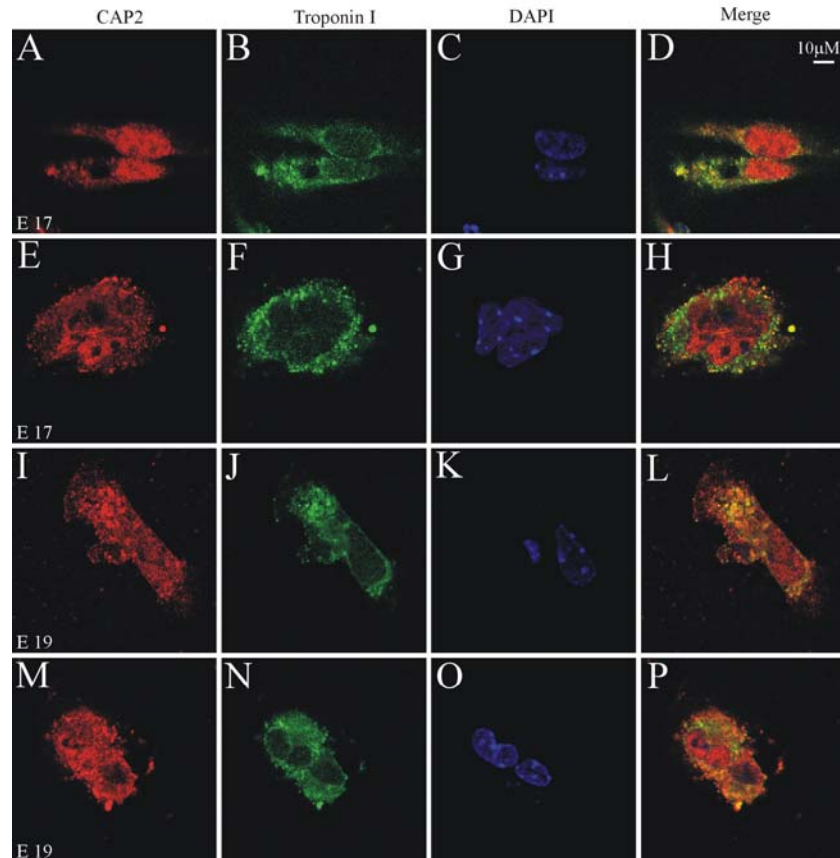


Figure 3.21: Expression of CAP2 in primary embryonic cardiomyocytes. Primary embryonic cardiomyocytes were fixed with paraformaldehyde and permeabilised with 0.5% Triton X-100, they were costained with CAP2 specific antibodies and a cardiac specific Troponin I antibody, then probed with a secondary anti rabbit IgG antibody conjugated to Alexa 568 and a secondary anti goat IgG antibody conjugated to FITC respectively along with DAPI. The panels A-H shows the staining of 17 days old embryonic cardiomyocytes and the panels I-P represents the staining of 19 days old embryonic cardiomyocytes. These pictures were taken by confocal microscopy.

3.18 Expression of CAP2 in HL-1, a cardiomyocyte cell line

The HL-1 cell line is derived from mouse cardiomyocytes. This cell line was a gift from Prof William C Claycomb, Dept of biochemistry and molecular biology, LSU, New Orleans, LA. Furthermore, we were screening for cell lines, which express CAP2 apart from the PAM212 mouse keratinocytes (Figure 3.8). When HL-1 cells were stained with CAP2 antibodies and cardiac specific Troponin I antibody as a marker for cardiomyocytes.

We observed CAP2 in the nucleus and in the cytosol as observed with primary cardiomyocytes (Figure 3.22). In most of the cells CAP2 was enriched in the nucleus (Figure 3.22 A and E, D and H). Troponin I exhibited a diffused pattern confined to the cytosol and the cortex. In some of the cells the CAP2 staining was very faint in the nucleus but strong around the nucleus. In these cases the staining of Troponin I was also strong around the nucleus (Figure 3.22 I, J, K and L).

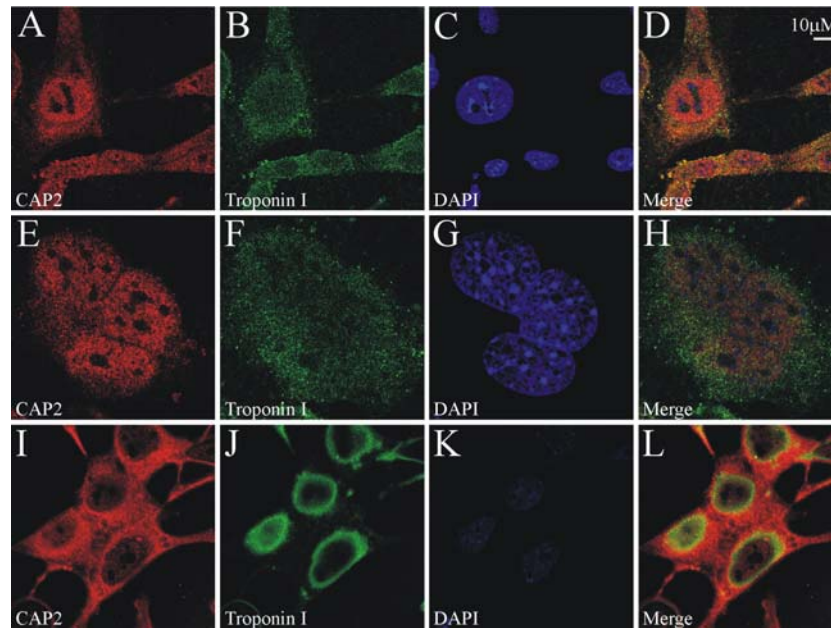


Figure 3.22: Localization of CAP2 in HL-1 cells. The HL-1 cells were fixed with paraformaldehyde and permeabilised with 0.5% Triton X-100, costained with CAP2 specific antibodies and cardiac specific Troponin I antibody, then probed with a secondary anti rabbit IgG antibody conjugated to Alexa 568 and secondary anti goat IgG antibody conjugated to FITC, respectively, along with DAPI. The panels A, E and I show the staining with the CAP2 antibodies, panels B, F and J shows the staining with the Troponin I antibody, Panel C, G and K, DAPI staining and panels D, H and L, overlay images, respectively. These pictures were taken by confocal microscopy.

3.19 Expression of CAP2 in primary rat vascular smooth muscle cells (ratVSM)

The finding of CAP2 expression in the capillary walls of the heart initiated an investigation of

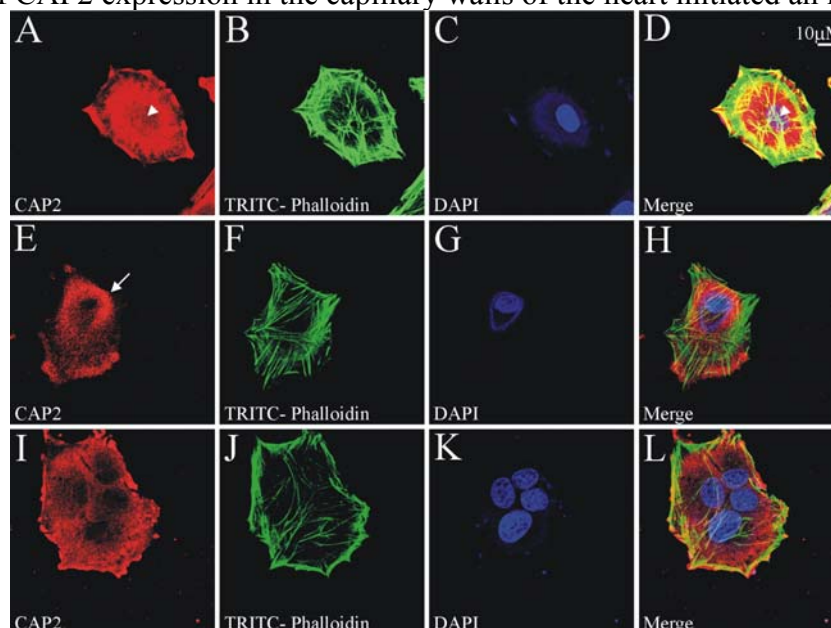


Figure 3.23: Localization of CAP2 in primary rat VSM cells. The rat VSM cells were fixed with paraformaldehyde and permeabilised with 0.5% Triton X-100, were stained with CAP2 specific antibodies, then probed with secondary anti rabbit IgG antibody conjugated to Alexa 568 along with TRITC-Phalloidin for observation of F-actin and DAPI. The panels A, E and I show the CAP2 staining, panels B, F and J the TRITC-Phalloidin staining, panels C, G and K, DAPI staining, panels D,H and L are the overlay images, respectively. Confocal images are shown.

CAP2 expression in primary rat vascular smooth muscle cells (VSM), which we obtained from Dr. Evren Caglayan, Department of Inner Medicine I, University of Cologne.

In the confocal images (Figure 3.23) we observed a strong enrichment of CAP2 in and around the nucleus and also at the cortex of the cell (Figure 3.23 A, E and I). The arrowhead indicates the nuclear localization and the arrows show the expression around the nucleus. The overlay images (figure 3.23 D, H and L) show the partial colocalisation of CAP2 with F-actin in some parts of the cell cortex.

3.20 Expression of CAP2 in myofibrils

As CAP2 was found in sarcomere regions of the heart and the skeletal muscle, we investigated the localisation of CAP2 in myofibrils in more detail. Myofibrils are cylindrical organelles, found within muscle cells. They represent bundles of filaments that run from one end of the cell to the other and are attached to the cell surface membrane at each end. The filaments of myofibrils, the myofilaments, consist of 2 types, thick and thin filaments. Thin filaments consist primarily of actin; thick filaments primarily of myosin. In striated muscle such as skeletal and cardiac muscle the actin and myosin filaments each have a specific and constant length on the order of a few micrometers, far less than the length of the elongated muscle cell (a few millimetres in the case of human skeletal muscle cells). The filaments are organised into repeated subunits along the length of the myofibril. These subunits are called sarcomeres. When the myofibrils were stained with CAP2 specific antibodies we observed a striated staining pattern confirming the expression of CAP2 in myofibrils. We were however not able to determine the exact localisation i.e. A, Z or M bands at this level.

3.20 1 CAP2 does not localize to the A-bands in the myofibrils

In this experiment we costained the myofibrils with CAP2 and Troponin I antibodies. Troponin I was chosen as an A-band specific protein. In contracted myofibrils we observed an overlap of both proteins. However, a clear differentiation is not possible in this case (Figure 3.24 A-C). We therefore performed a staining of relaxed myofibrils. The images obtained show clearly that CAP2 and Troponin I do not colocalise (Figure 3.24 F).

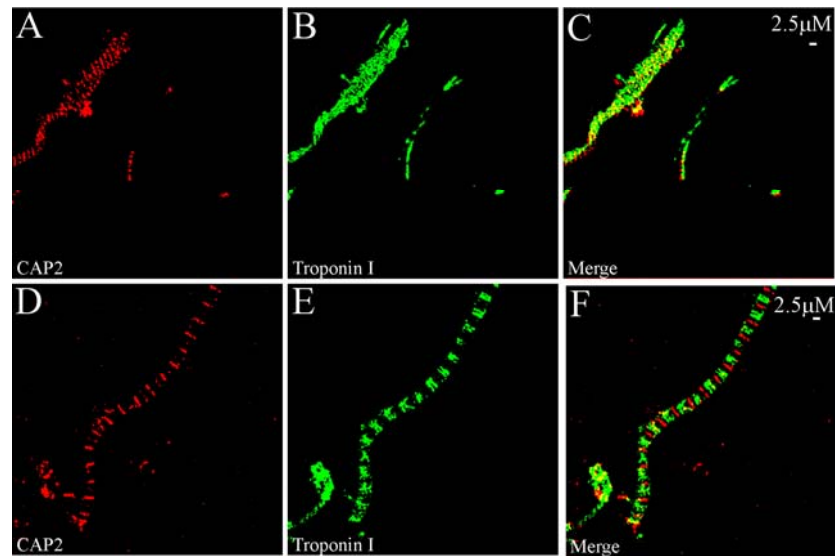


Figure 3.24: CAP2 does not localise to A-bands in myofibrils. Myofibrils were stained with CAP2 and cardiac specific Troponin I antibodies, then probed with a secondary anti rabbit IgG antibody conjugated to Alexa 568 and secondary anti goat IgG antibody conjugated to FITC, respectively. The panels A-C show the staining of contracted myofibrils, panels D-F the staining of relaxed myofibrils. The images were taken by a confocal microscope.

Thus it is clear that CAP2 is not present in the A-bands of the myofibrils.

3.20 2 CAP2 does not localise to the Z-bands of the myofibrils

To identify a possible association with the Z-band we carried out a colocalisation study using antibodies specific for alpha-actinin, which is highly specific for the Z-bands. Also in this case no colocalisation was observed (Figure 3.25 F).

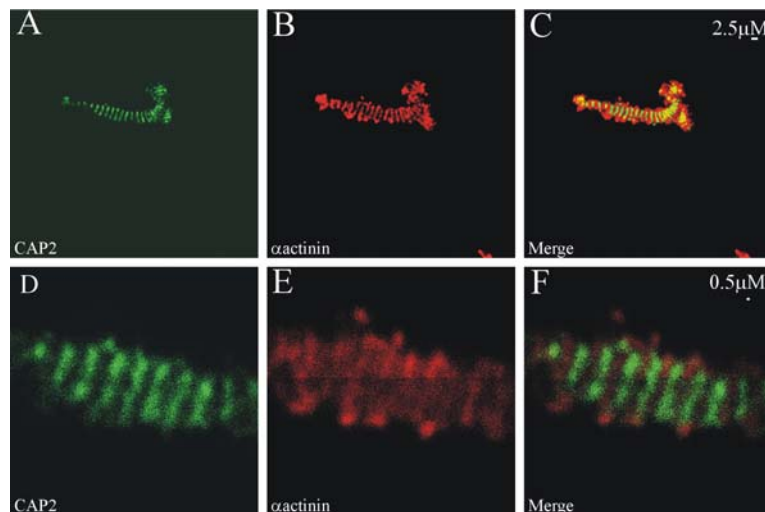


Figure 3.25: CAP2 does not localise to the Z-bands in myofibrils. Myofibrils were costained with CAP2 and alpha-actinin antibodies, then probed with secondary anti rabbit IgG antibody conjugated to FITC and secondary anti mouse IgM antibody conjugated to Alexa 568, respectively. The panels A-C, localisation of CAP2 and alpha-actinin in myofibrils, lower magnification; panels D-F, higher magnified images of A-C, respectively. Confocal microscope images are shown.

3.20 3 CAP2 localises to the M-bands of the myofibrils

In order to probe for M-band localisation, we performed a costaining with a myomesin antibody. Myomesin is specifically present in the M-bands and is referred as a M-band protein. CAP2 was prominently present in the M bands and clearly colocalised with myomesin (Figure 3.26 A-C). In addition we observed a faint expression of CAP2 in between two M- bands, which might be the neighbouring I-bands. This part of the work was carried out in collaboration with Prof Gabriele Pfitzer, Institute of Vegetative Physiology, University of Cologne.

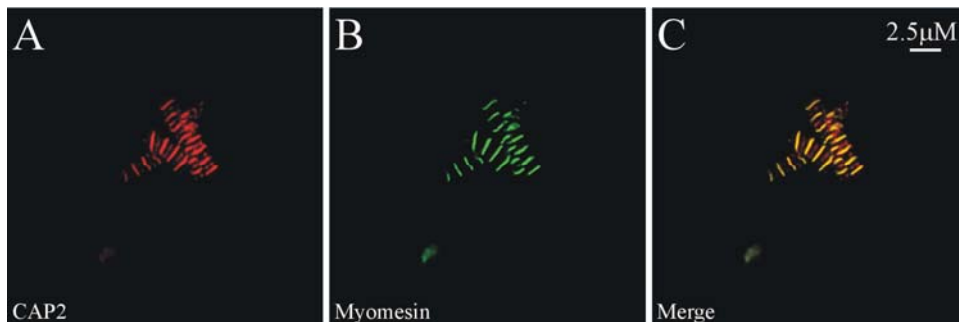


Figure 3.26: CAP2 localises to the M-bands in the myofibrils. Myofibrils were costained with CAP2 specific antibodies and a myomesin antibody, then probed with secondary anti rabbit IgG antibody conjugated to Alexa 568 and a secondary anti mouse IgG antibody conjugated to Alexa 488, respectively. Panel A shows the localisation of CAP2, B of myomesin and C represent the overlay. Confocal images are shown.

3.21 Expression of CAP2 in a 16-day-old mouse embryo

To investigate the pattern of expression of CAP2 during mouse embryogenesis, we have used a sagittal paraffin section of a 16-day mouse embryo. Images were taken with a fluorescent microscope. CAP2 is present in the pituitary cerebellar primordium of the brain, caudal lobe of right lung, and auricular part of the right atrium of the heart and primordium follicle of vibrissa, which later develop into the sensory taste buds in the tongue (Figure 3.27). In our western blot and the northern blot analysis CAP2 expression was not detected in lungs of the adult mouse, but we did observe the expression of CAP2 in heart and brain. The results obtained with the embryo staining were comparable with the results obtained by Bertling et al. (2004) where a very weak expression of CAP2 in lung and a strong expression in heart and brain of the mouse embryo at 17 day were reported.

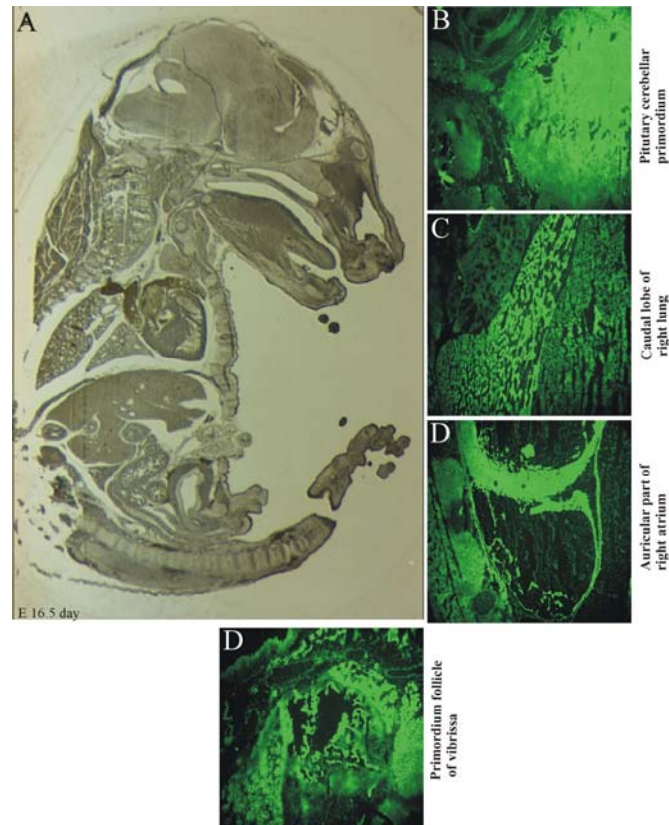


Figure 3.27: CAP2 expression in a mouse embryo at day 16. A cryosection of the embryo was fixed with paraformaldehyde and permeabilised with 0.5% Triton X-100. The section was incubated with CAP2 specific antibody after quenching the peroxidase activity and blocking. It was then incubated with a secondary anti-rabbit IgG antibody conjugated to FITC. Panel A shows the mouse embryo at day 16 just depicting the different parts of the embryo (taken from S. Abraham, 2004); B, pituitary cerebellar primordium (brain); C, caudal lobe of right lung; D, auricular part of the right atrium (heart); E, primordium follicle of vibrissa (upper lip).

3.22 Localization of CAP2 in PAM212 (mouse keratinocytes)

Western blot analysis (Figure 3.8) indicated an expression of CAP2 in PAM212 cells derived from mouse keratinocytes. Here we studied the subcellular distribution of the protein.

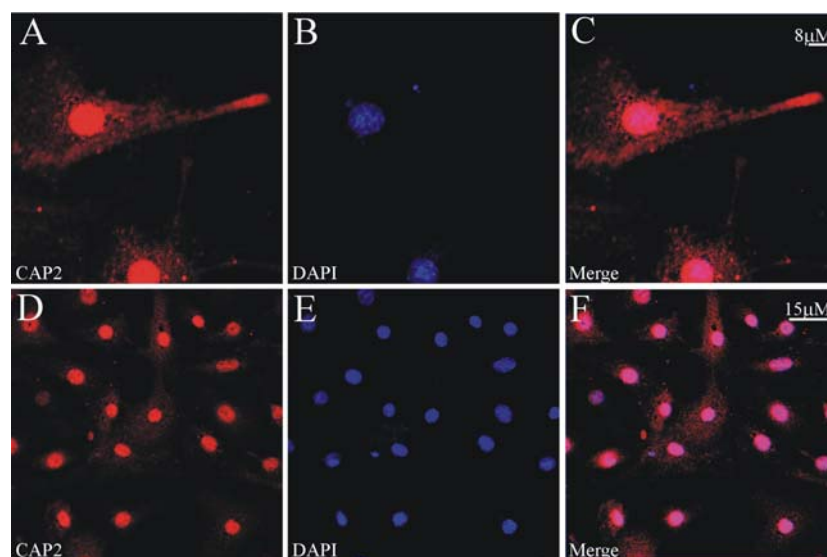


Figure 3.28: Localization of CAP2 in PAM212 cells. PAM212 cells were fixed with paraformaldehyde and permeabilised with 0.5% Triton X-100, stained with CAP2 specific antibodies, then probed with a secondary anti rabbit IgG antibody conjugated to Alexa 568 along with DAPI. The panels A and D show the CAP2 staining, B and E represents the DAPI staining and C and F are the overlay images. These images were taken by confocal microscopy.

In most of the cells a strong nuclear staining was observed (Figure 3.28). In addition, CAP was also located in the cell body and at the leading edge (Figure 3.28 A). In D an overview is shown, which shows the prominent nuclear localisation in nearly all of the cells.

To rule out the possibility of nuclear staining of CAP2 due to an artefact of fixing, we used methanol-acetone as a different fixation method. We again observed that CAP2 localises to the nucleus (Figure 3.29 A, D and G). In some of the cells CAP2 localisation was also prominent in the cytosol in addition to the nuclear staining (Figure 3.29 A and G). For control we used a tubulin specific antibody (Figure 3.29 B, E and H) showing the typical filamentous pattern of tubulin distribution. We also observed that CAP2 partially colocalised with tubulin indicated by the arrowheads (Figure 3.29 C, F and I). The significance of this finding is unknown.

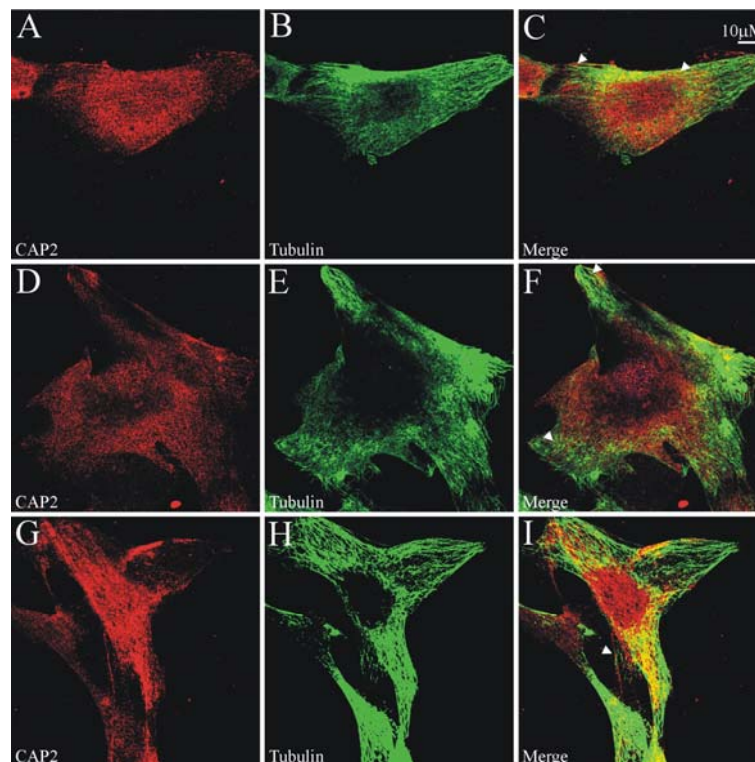


Figure 3.29: Localization of CAP2 in PAM212 cells fixed with methanol. The PAM212 cells were fixed with methanol-acetone, costained with CAP2 polyclonal and tubulin monoclonal antibodies, then probed with secondary anti rabbit IgG antibody conjugated to FITC and anti mouse IgG antibody conjugated to Alexa 568, respectively, along with DAPI. The panels A, D and G show the CAP2 staining, B, E and H represent the tubulin staining and C, F and I are the overlay images. These images were taken by confocal microscopy.

3.23 CAP2 localisation in PAM212 cells fixed with paraformaldehyde

We also studied the CAP2 colocalisation with the actin network in PAM212 cells. For this we had to use paraformaldehyde fixation.

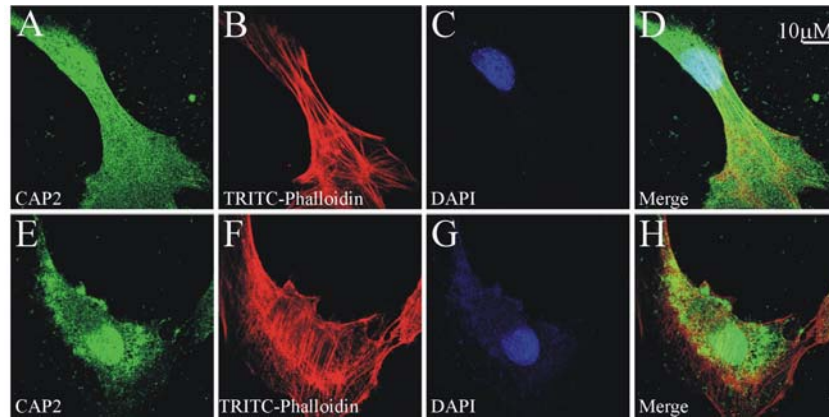


Figure 3.30: Localisation of CAP2 in PAM212. The PAM212 cells were fixed with paraformaldehyde and stained with CAP2 specific antibodies and then probed with a secondary anti rabbit IgG antibody conjugated to FITC along with DAPI and TRITC-Phalloidin. The panels A and E shows the CAP2 staining, B and F represents the F-actin staining and D and H are the overlay images. The images were taken by confocal microscopy.

We observed a CAP2 localisation to the nucleus (Figure 3.30 A and D) and also a distribution throughout the cytosol where it occasionally localised along actin fibers.

3.24 Subcellular fractionation of PAM212 cells

To confirm the results obtained by the immunofluorescence studies we performed a subcellular fractionation of PAM212 cells and subjected the cell lysates to differential centrifugation. The proteins of the different fractions were separated by SDS-PAGE and analysed in western blots using CAP2 antibodies and a monoclonal antibody specific for emerin, a protein of the inner membrane of the nucleus.

We observed CAP2 in the nuclear pellet fraction of PAM212 cell lysates (2 K) and in the 12 K pellet and supernatant. The nuclear envelope protein emerin was only observed in the 2K pellet fraction and in the whole cell lysate. In contrast, when we overexpressed CAP2 in HEK 293 cells the protein was present only in the cytosol (data not shown). The significance of the localization of CAP2 to the nucleus is yet to be understood.

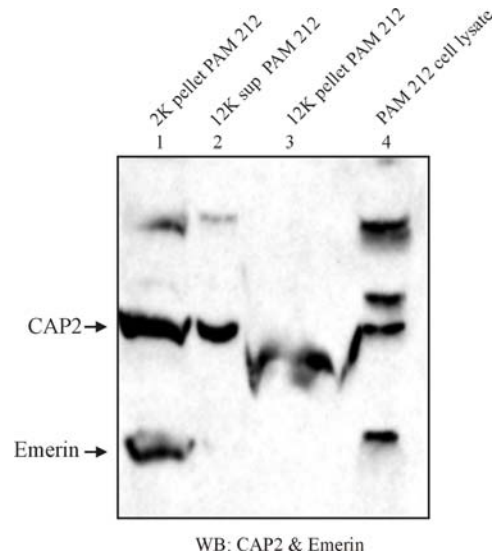


Figure 3.31: Cell fractionation study of PAM212 cells. The PAM212 cell lysate was subjected to differential centrifugation. The nuclei, cytosol and the cytoplasmic membranes were isolated and separated on 12% SDS polyacrylamide gels and blotted onto nitrocellulose membranes. The blot was incubated with CAP2 and emerlin specific antibodies. The position of the proteins are indicated. The bands seen above CAP2 are non-specific bands coming from the emerlin antibody.

3.25 Influence of drugs affecting the cytoskeleton on the subcellular distribution of CAP2

The fact that CAP2 partially colocalises with actin (Figure 3.30) and that actin interacts with CAP2 (M. Leichter, 2002; Huberstey et al., 1996) and partially colocalises with cytoskeletal components such as microtubuli prompted us to examine the effect of the actin depolymerising drug latrunculin B and the microtubule disturbing drug colchicin on the localisation of CAP2.

3.25.1 Nuclear localisation of CAP2 is not affected by a drug disrupting the microfilament cytoskeleton

The actin cytoskeleton was disturbed using latrunculin B, a microfilament-disrupting drug that binds to G-actin and prevent its polymerisation (Wakatsuki et al., 2001). PAM 212 were treated with the drug at 2.5 μm concentration for 5, 10 and 15 min, fixed with 3% paraformaldehyde and permeabilised with Triton X-100 for 5 min. We observed no alteration of the CAP2 distribution, whereas the filamentous actin network was no longer present. Also, the nuclear staining of CAP2 was retained (Figure 3.32).

3.25.2 Nuclear localisation of CAP2 is affected by a drug disrupting the microtubule cytoskeleton

We have previously noted a colocalisation of CAP2 with microtubules. When we disrupted the microtubule cytoskeleton using colchicin at 12.5 μ M concentration and fixed the cells after 20, 40 and 60 minutes of colchicin treatment,

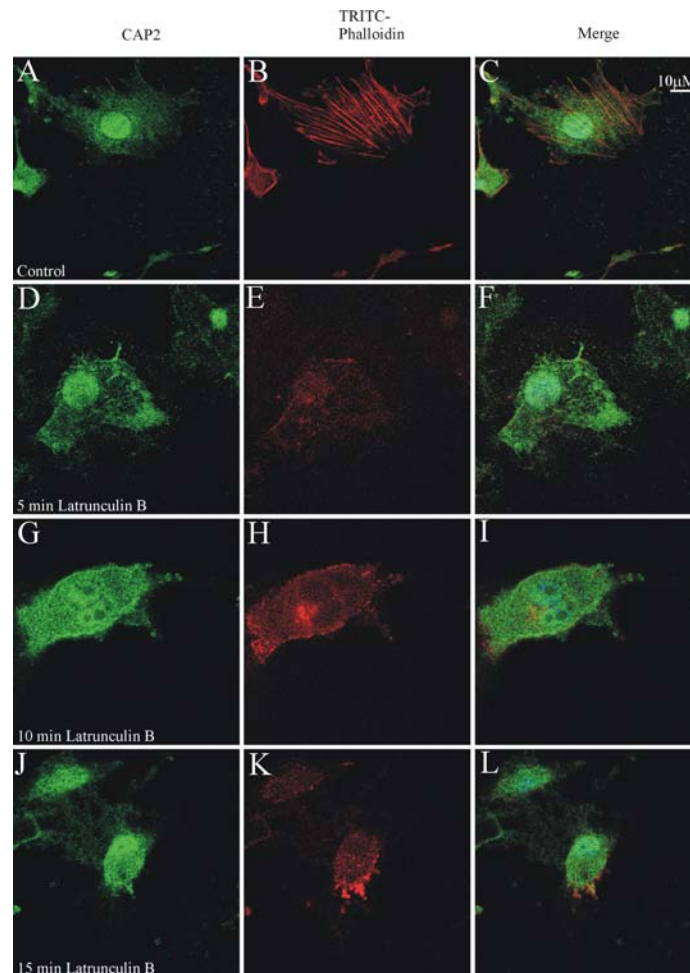


Figure 3.32: Latrunculin treatment of PAM212 cells. Panels A-C show untreated (control) PAM212 cells and panels D-F, G-I and J-L display cells after a 5, 10 and 15 min treatment with latrunculin B (2.5 μ m) respectively. Cells were fixed in 3% paraformaldehyde and incubated with the CAP2 antibodies and anti-rabbit FITC conjugated secondary antibody. F-actin is stained with phalloidin coupled to TRITC. Nuclei are stained with DAPI. Images were obtained with a confocal microscope.

In contrast to untreated cells (Figure 3.33 A-C), which display a nicely organized microtubule cytoskeleton the colchicin treated cells (Figure 3.33 D-L) showed a disrupted microtubule cytoskeletal network. The nuclear staining pattern of CAP2 remained unaffected at 20 min of colchicin treatment. (Figure 3.33 D, E and F). At 40 min of colchicin treatment we observed a diffused expression of CAP2 all over the cell indicating that CAP2 localisation is getting disturbed and at 60 min of colchicin treatment. (Figure 3.33 J, K and L) CAP2 presence in the nucleus was strongly reduced indicating that nuclear localisation of CAP2 was affected. From these results we conclude that CAP2 localisation is dependent on the microtubular network.

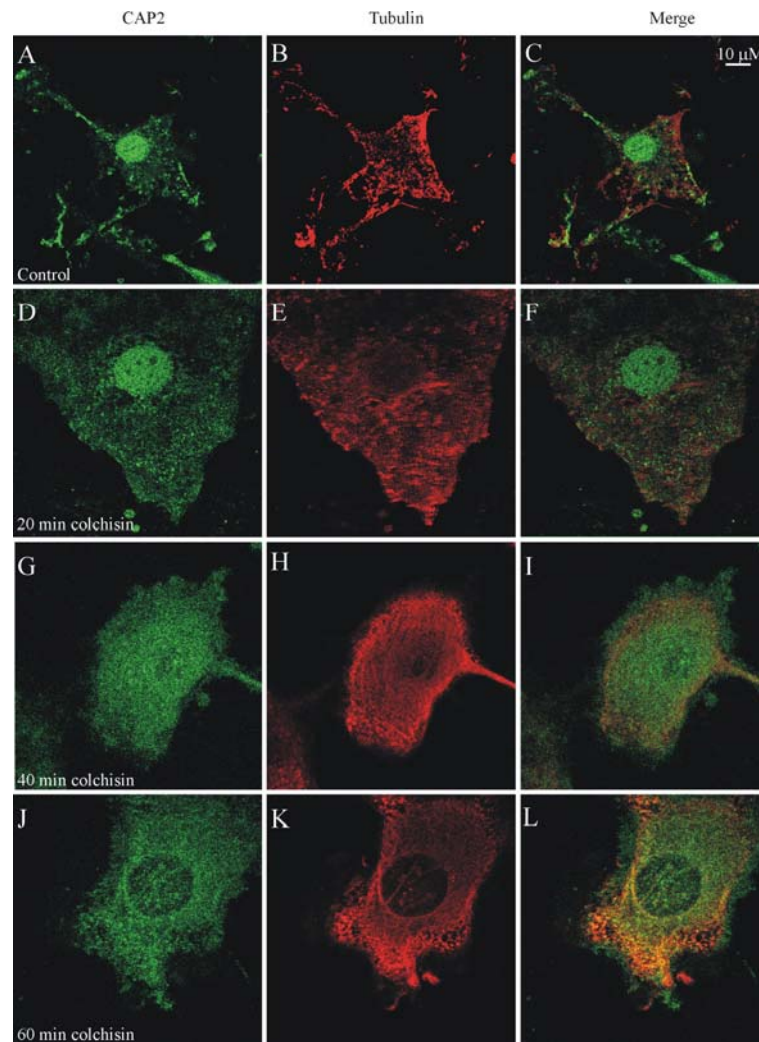


Figure 3.33: Colchicin treatment of PAM212 cells. PAM212 cells were treated with colchicin ($12.5 \mu\text{M}$) for 20, 40 and 60 min and fixed with methanol. Incubation was with the polyclonal CAP2 specific antibodies and anti- α -tubulin mouse monoclonal antibodies. Anti-rabbit-FITC and anti-mouse-Cy3 were used as secondary antibodies. Images were taken by confocal microscopy.

3.26 CAP2 localises also at the nuclear membrane

The nuclear envelope is composed of two membranes, the outer nuclear membrane, which is continuous with the endoplasmic reticulum, and the inner nuclear membrane. In order to examine a possible localisation and the exact topology of CAP2 at the nuclear envelope we performed permeabilisation studies. PAM212 cells were permeabilised with $40 \mu\text{g/ml}$ digitonin for 5 minutes or with 0.5% Triton X-100 separately. Triton X-100 permeabilises both the plasma membrane and also the nuclear membrane, while a short incubation with digitonin permeabilises only the plasma membrane and leaves the nuclear membrane intact. Thus the entry of antibodies only to the cytoplasm and not to the nucleoplasm allows the identification of cytoplasmic and outer nuclear membrane components. PAM212 cells were fixed with paraformaldehyde and treated with digitonin for different times to optimise the permeabilisation conditions. For controlling the permeabilisation procedure, we co-

immunostained the cells for emerin, which is an inner nuclear membrane protein and also located in the inner aspect of the nucleus. After 5 minutes of digitonin treatment,

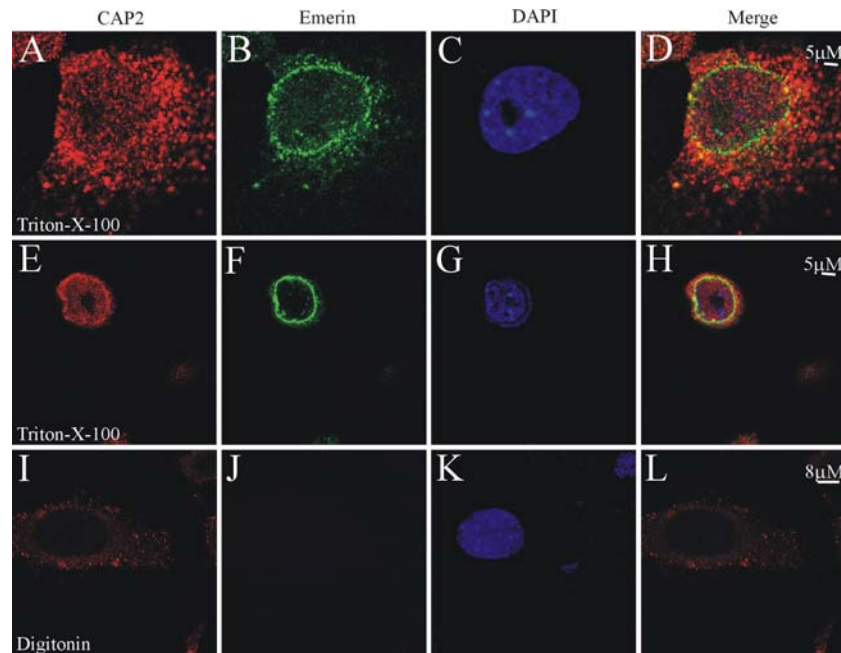


Figure 3.34: Permeabilisation of PAM212 cells with Triton X-100 and digitonin. PAM212 cells were fixed with 3% paraformaldehyde and permeabilised with the detergents Triton X-100 or digitonin for 5 min. A-H shows a Triton X-100 permeabilised cell and panels I-L show a cell after digitonin treatment. Images were taken by confocal microscopy.

we could observe only cytosolic staining of CAP2 (Figure 3.34 I) in digitonin treated cells. Emerin staining was completely absent confirming its presence at the inner aspect of the nuclear envelope (Figure 3.34 J). DAPI staining of the nucleus can be seen in panel K. Panel L shows the merged image of panels I-K where we can observe that after digitonin treatment CAP2 and emerin staining are absent from the nucleus and the inner nuclear membrane. In panels A-H, Triton X-100 permeabilised cells however, displayed nuclear, nuclear membrane and cytosol staining of CAP2 and inner nuclear membrane staining of emerin. The overlay images (Figure 3.34 D and H) show the partial colocalisation of CAP2 with emerin, which indicates that CAP2 also localises at the inner nuclear membrane. However the presence of CAP2 at the outer nuclear membrane cannot be ruled out. Taken together, CAP2 was localised not only to the nucleoplasm but also found to be associated with both inner and outer nuclear membranes.

3.27 An overview of nuclear staining in PAM212 cells

We consistently observed nuclear expression of CAP2 in PAM212 cells. However we also noticed cells where a nuclear localisation of CAP2 was absent. We therefore carried out a statistical analysis and counted about fifty cells from each staining which we had performed and observed that around 95 % of all cells showed a nuclear localisation of CAP2 (Figure

3.35), in 5 % of the cells CAP2 was purely cytosolic (Figure 3.35). However all the cells expressed CAP2 in the cytosol irrespective of the nuclear localisation. The arrowheads indicate the expression of CAP2 in the nucleus and arrows indicate the absence of CAP2 expression in the nucleus.

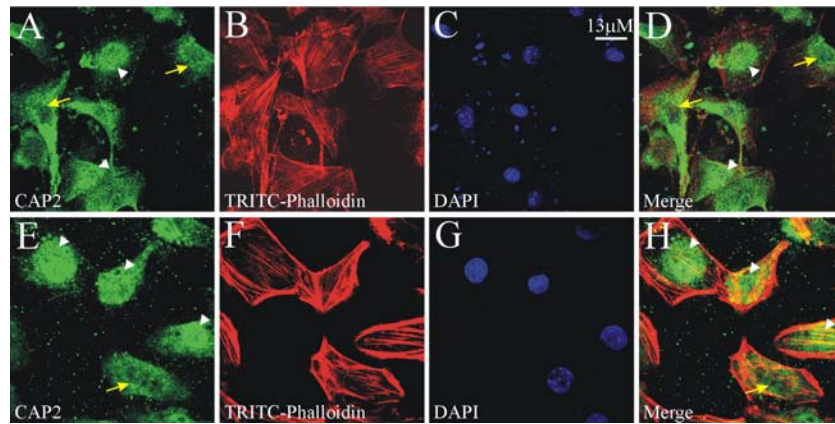


Figure 3.35: Overview images of CAP2 localisation in PAM212 cells. The PAM212 cells were fixed with paraformaldehyde and permeabilised with 0.5% Triton X-100, stained with CAP2 specific antibodies, then probed with a secondary anti rabbit IgG antibody conjugated to FITC along with TRITC-Phalloidin and DAPI. The panels A and E shows the CAP2 staining, B and F represents F-actin staining, C and G show the DAPI staining and panels D and H are the overlay images. The images were taken by confocal microscopy.

3.28 Expression of CAP2 in primary mouse keratinocytes

Since we observed the nuclear expression of CAP2 in PAM212 cells, which are derived from mouse keratinocytes, we wanted to investigate the localisation of CAP2 in primary mouse keratinocytes. We costained primary mouse keratinocytes with CAP2 specific antibodies and anti tubulin antibody as we had observed the partial colocalisation of CAP2 with tubulin in PAM212 cells. In the confocal images (Figure 3.36) we observed CAP2 in the nucleus (Figure 3.36 A, E and I) as well as in the cytosol, the tubulin staining gave a filamentous pattern (Figure 3.36 B, F and J). In the overlays in D, H and L we can observe that a partial colocalisation of CAP2 with tubulin at certain regions and around the nucleus in some cells (HandL) whereas in some cells which are represented by panel D the CAP2 expression is confined to the nucleus only.

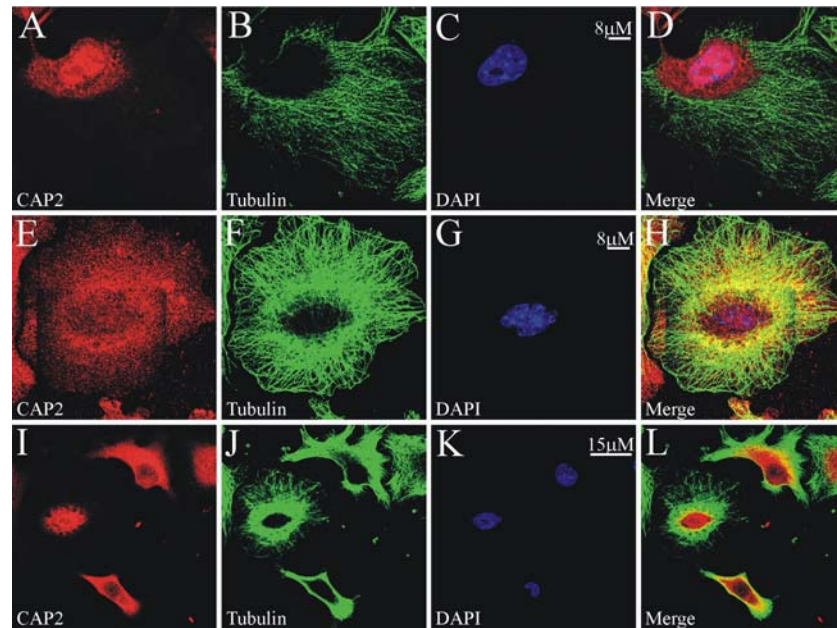


Figure 3.36: Localization of CAP2 in primary mouse keratinocytes. The primary mouse keratinocytes were fixed with methanol-acetone, costained with CAP2 and tubulin specific antibodies, then probed with secondary anti rabbit IgG antibody conjugated to Alexa 568 and anti mouse IgG antibody conjugated to Alexa 488, respectively, along with DAPI. The panels A, E and I show the CAP2 staining, B, F and J represent the tubulin staining, C, G and K, DAPI staining, and panels D, H and L, overlay images. These images were taken by confocal microscopy.

The results obtained here are comparable to with the result obtained with PAM212 cells. The panel I-L shows an overview of CAP2 localisation in primary mouse keratinocytes with some cells showing no CAP2 in the nucleus, which is similar to the findings observed with PAM212 cells.

3.29 Expression of CAP2 in primary human keratinocytes

We also performed immunofluorescence analysis of CAP2 in human keratinocytes. Surprisingly CAP2 localisation was confined to the cortex and the cytosol unlike the situation in mouse keratinocytes where we observed CAP2 was as also in the nucleus. The staining of cytosol and cortex was of a punctate pattern. The punctate pattern could be due to the presence of CAP2 in podosome like structures. This will be further investigated.

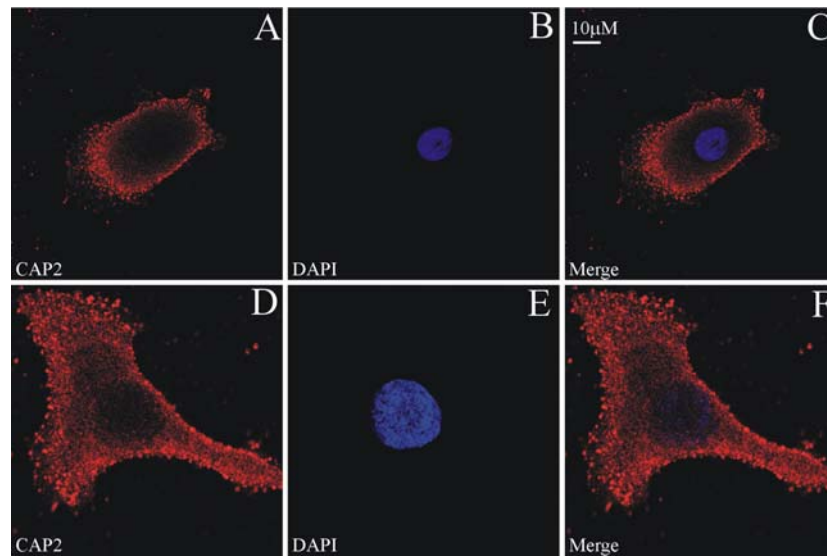


Figure 3.37: Localization of CAP2 in primary human keratinocytes. The primary human keratinocytes were fixed with paraformaldehyde and permeabilised with 0.5% Triton X-100, stained with CAP2 specific antibodies and probed with secondary anti rabbit IgG antibody conjugated to Alexa 568 along with DAPI. The panels A and D shows the CAP2 staining, B and E represents the DAPI staining and panels C and F are the overlay images. The images were taken by confocal microscopy.

3.30 Role of CAP2 in wound healing

Since the CAP2 expression was observed in the PAM212 cells, a mouse keratinocyte derived cell line, and keratinocytes play a very important role in the wound healing process, we studied its role in wound healing. Towards that we emulated the wound healing process in PAM212 and rat VSM cells on the cover slips, where we generated a wound by scratching the confluent monolayer cells on the cover slips.

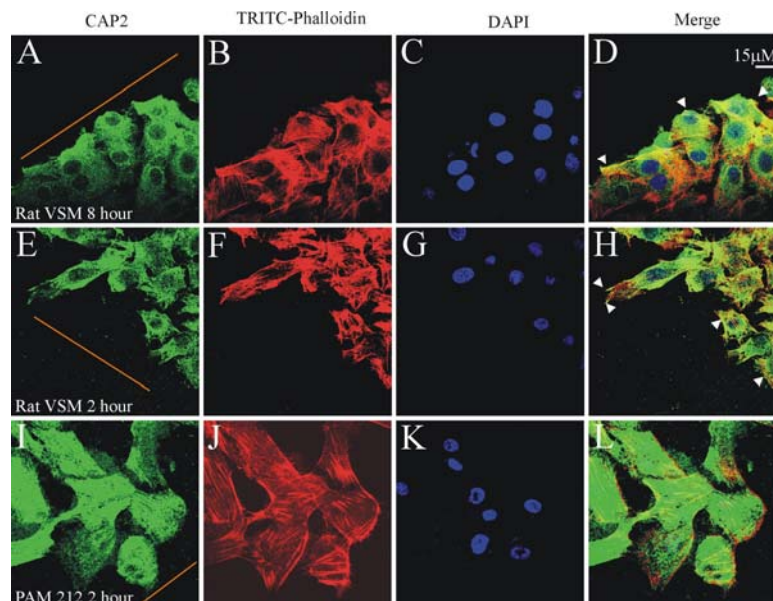


Figure 3.38: Overview images of CAP2 localization during the wound healing process in rat VSM and PAM212 cells. The rat VSM and PAM212 cells were fixed with paraformaldehyde and permeabilised with 0.5% Triton X-100, stained with CAP2 specific antibodies, then probed with secondary anti rabbit IgG antibody

conjugated to FITC along with TRITC-Phalloidin and DAPI. The panels A, E and I show the CAP2 staining, B, F and J represent F-actin, C, G and K show the DAPI staining and panels D, H and L are the overlay images. The orange line indicates the position of the wound. These images were taken by confocal microscopy.

After scratching, the cells were fixed at different time intervals and analysed by immunofluorescence. CAP2 colocalises with actin at certain regions of the cells where the wound was set. The arrowhead indicates the position at which the colocalisation was observed in the rat VSM and PAM212 cells, respectively.

3.31 CAP2 interacts with ACF7

As CAP2 is expressed in different kinds of tissues like heart, brain, skeletal muscle and skin and in different cells like glia cells, rat VSM and keratinocytes, it might play a different role in these different tissues and cell lines. To assign a role to CAP2; the identification of an interacting protein will throw a light and lead to the function of CAP2 in these tissues. For *Drosophila* CAP a meeting report was available (MBC 14, 2003, 1105, page 198a) that described that Short Stop protein binds to CAP via its EF-hand. Short Stop is allelic to kakapo which is known as ACF-7 in higher eukaryotes. ACF7 and Short Stop belong to the plakins family. Plakins are an emerging family of sequence-related cross-linker proteins that include plectins, the bullous pemphigoid antigen-1 proteins (BPAG1s), ACF7 (referred to as kakapo in lower eukaryotes), desmoplakin, envoplakin, and periplakin. Plakins are enormous proteins (200-700 kD) that anchor cytoskeletal networks to each other and/or to cellular structures such as adhesive junctions (Fuchs et al., 2001).

Tools to test for an ACF7 interaction are available in our group through Dr. Iakowos Karakesisoglou. A human Trabeculin (hACF7) GFP-ACF7 construct, GFP-C-ACF7, which contains the last 387 amino acids including the EF hands (amino acids 5308-5695) was coexpressed with Myc-CAP2 in HEK293 cells and an immunoprecipitation was performed using the CAP2 antibodies and the immunoprecipitate probed for the presence of the GFP-ACF7 fusion protein. For control we probed for the presence of coronin3 and coronin7.

In the immunoprecipitate we detected CAP2 and the GFP-ACF7 polypeptide whereas in the total homogenate CAP2 and GFP-ACF7 were detected but not coronin 3 and 7 which were only seen in the cell homogenate and thus served as a control for the specificity of the immunoprecipitation (Figure 3.38). The result from the immunoprecipitation experiment confirmed that CAP2 binds to ACF7 directly, which corresponds to the reported interaction for CAP of *Drosophila*. An interaction of mouse CAP1 with ACF7 was not tested. The significance of the binding of CAP2 to ACF7 is yet to be understood.

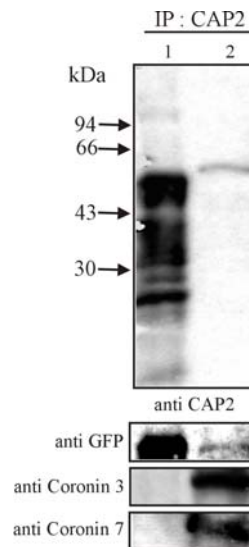


Figure 3.39: CAP2 binds to the C-terminus of ACF-7 in an immunoprecipitation experiment. Lane 1 represents the immunoprecipitate performed with protein A agarose beads carrying the CAP2 antibodies and homogenates of HEK293 cells coexpressing GFP-C-ACF7 and Myc-tagged CAP2. The lane 2 represents the homogenate used for the experiment. The proteins were separated on a 12% SDS polyacrylamide gel and the resulting blot was probed for the presence of CAP2 (control for a successful immunoprecipitation), the GFP-ACF7 fusion (experimental) and coronin 3 and 7 (negative control).

3.32 CAP2 partially colocalises with ACF7 in COS7 cells

To further confirm the results obtained from the immunoprecipitation studies (section 3.33) we performed immunofluorescence studies in COS7 cells. We used the same GFP-ACF7 construct as above and transiently coexpressed GFP C-ACF7 and Myc-CAP2 in COS7 cells. The cells were fixed with paraformaldehyde and permeabilised with 0.5% Triton X-100 and analysed for a CAP2 and ACF7 colocalisation.

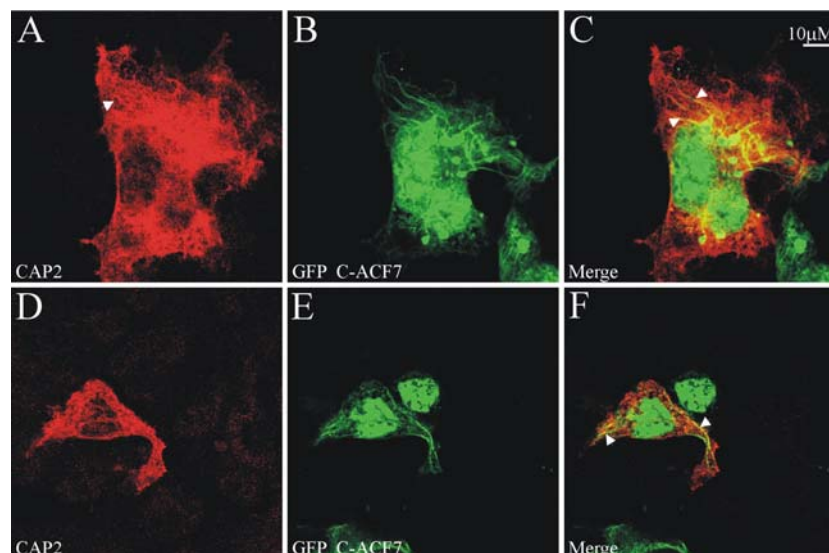


Figure 3.40: Expression of Myc-CAP2 and GFP-C-ACF7 in COS7 cells. The COS7 cells were fixed with paraformaldehyde and permeabilised with 0.5% Triton X-100, stained with CAP2 specific antibodies, then probed with secondary anti rabbit IgG antibody conjugated to Alexa 568 along with DAPI. The panels A and D show the CAP2 staining, B and G represent the GFP-C-ACF7 and C and F are the overlay images. The images were taken by confocal microscopy.

—

Myc-CAP2 was mainly found in the cytosol, where we observed a very weak filamentous pattern indicated by the arrowheads (Figure 3.40 A, D). GFP-C-ACF7 was strongly enriched in the nucleus and was also present in the cytosol, where a strong filamentous pattern of staining was observed (Figure 3.40 B, E). The panels C and F show the overlay images where a partial colocalisation of CAP2 with GFP-C-ACF7 was noted supporting the results obtained by immunoprecipitation studies. It may therefore well be that CAP2 interacts with ACF7.

3.33 Expression of ACF-7 in PAM212 cells

Since we observed CAP2 interaction with ACF7, we studied the localisation of endogenous ACF7 in PAM212 cells. Two different ACF7 antibodies were available, which were raised against polypeptides from two different regions of the huge ACF7 protein. The antibodies raised against the rod domain are designated as Rod ACF-7 and the antibodies raised against another part of the protein is designated as ACF-7, which is an isoform 3 specific. The PAM212 cells were separately stained with both the antibodies and then probed with secondary anti rabbit IgG antibody conjugated to Alexa 568 along with DAPI.

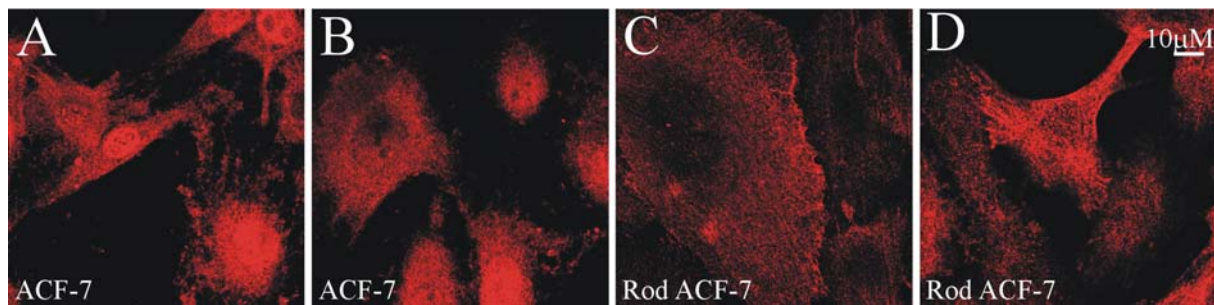


Figure 3.41: Expression of ACF7 in PAM212 cells. The PAM212 cells were fixed with paraformaldehyde and permeabilised with 0.5% Triton X-100 and stained with ACF-7 and Rod ACF-7 antibodies, then probed with secondary anti rabbit IgG antibody conjugated to Alexa 568. The panels A and B show the ACF-7 staining, C and D represent the Rod ACF-7 staining. The images were taken by confocal microscopy.

The confocal images (Figure 3.41) revealed that when PAM212 cells were stained with the ACF-7 antibodies, an ACF7 labeling was observed in the nucleus and in the cytosol. This pattern resembles the one of CAP2 in PAM212 cells. We observed that even the pattern of staining was similar for both proteins because the nuclear staining was absent in some cells as in the case of CAP2 (Figure 3.41 B). On the contrary when stained with Rod ACF-7 antibodies, the expression of ACF7 was confined to the cytosol (Figure 3.41 C) however a faint nuclear expression was observed in few cells. Here the staining showed a filamentous pattern, which was weaker in the case of the cells stained with the ACF-7 antibodies.

3.34 Expression of ACF-7 in primary mouse keratinocytes

We followed these findings up in primary mouse keratinocytes and stained them with ACF-7 and Rod ACF-7 antibodies separately.

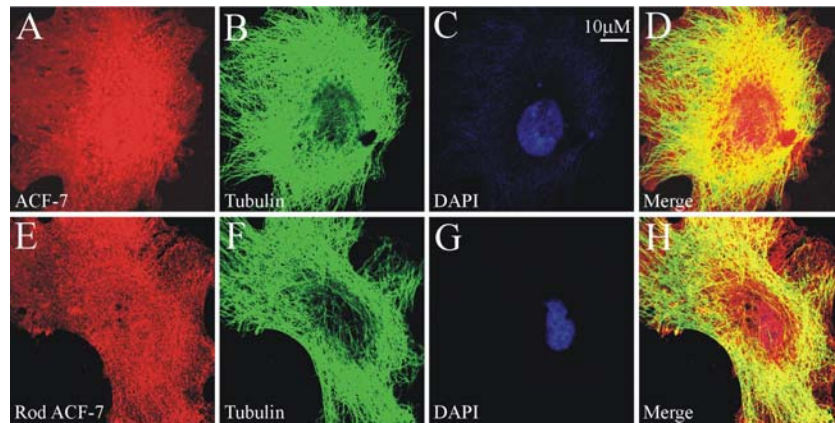


Figure 3.42: Expression of ACF7 in primary mouse keratinocytes. The primary mouse keratinocytes were fixed with paraformaldehyde and permeabilised with 0.5% Triton X-100 and costained with anti tubulin (B, F), ACF-7 (A) and Rod ACF-7 (E) antibodies, probed with secondary anti mouse and anti rabbit IgG antibodies conjugated to Alexa 488 and Alexa 568 along with DAPI respectively. B and F represents the tubulin staining. C and G represent the DAPI staining and D and H are the overlay images. The images were taken by confocal microscopy.

When stained with the ACF-7 antibody ACF7 in primary mouse keratinocytes was found to be similar to that of PAM212 staining (Figure 3.42 A), ACF7 labeling was observed in the nucleus and in the cytosol. However the staining pattern was more or less similar in both cell types. The ACF7 staining obtained with the Rod ACF-7 antibody was opposite to the one obtained with the ACF-7 antibody in PAM212 cells and the protein was observed both in the cytosol and in the nucleus (Figure 3.42 E). The staining pattern was more filamentous when compared to PAM212 cells. The overlay images (Figure 3.42 D and H) of tubulin and ACF7 (both the antibodies) shows a colocalisation and the pattern of staining and the overlay was similar to that of the CAP2 staining in primary mouse keratinocytes.

3.35 Generation of a CAP2 mouse mutant

Gene targeted mice are a powerful tool for studying the functional aspects of a protein. Gene targeting, introduction of site-specific modifications into the mouse genome by homologous recombination, is generally used for the production of mutant animals to study the gene function *in vivo*. In order to get further insight into the function of CAP2, a mouse knock out mutant is being generated in our lab.

3.35.1 Analysis of the structure of the mouse CAP2 gene

The CAP2 gene is located on chromosome 13 at the position A5 (13A5) Locus ID 67252. The gene has 12 exons spread over a length of around 132 kb. The introns are of varying length. The largest intron is around 50 kb in length and the smallest is 93 bases. The size of the first intron is around 5.54 kb, the intron between the 2nd and the 3rd exon has 29.53 kb. The intron between the 3rd and the 4th exon is the largest one extending over 50 kb. The length of the intron between the 4th and the 5th exon is 300 bases. The distance between the 5th and the 6th exon is about 5 kb. 20kb is the length between the 6th and the 7th exon. The 7th exon and the 8th exon are separated by a 2 kb intron. The length of the intron between the 8th and the 9th is 1.8 kb. The smallest intron size is 93 bases situated between the 9th and the 10th exon. Around 6.5 kb are present between the 10th and the 11th exon. The boundary between the 11th and the 12th exon is 1.6 kb. The starting codon ATG is located in the first exon. The exons and their intron boundaries are given in Table 3.1. We decided to target the 4th and the 5th exon by inserting a neomycin cassette in the middle of exon 4 so that the intron-exon transition is ablated and the transcription will come to an end. We decide to take out two exons in order to disturb the CAP2 protein as much as possible. Furthermore the intron is of a small size of only 300 bases. So it was convenient to remove the 5th exon as well. Since the first ATG is not ablated, the transcription will start but will come to a stop after the 3rd exon.

Sequence at intron exon boundary

Exon no	5' splice donnar	5' splice acceptor	Exon size (in bp)	Intron size (in bp)
1	CTTTC TAG /AATGAC	ATGGAG GT AGGGCC	121	
2	TTCAC AG /GTGTGG	ACTCAC GT GAGTGC	101	5546
3	GTCCGC AG /GCAGAA	CAAGAG GT AAGAGC	78	30258
4	GCCCGC AG /AATGAA	GCCGTG GT GAGTTA	144	49577
5	TTTCTC AG /TCCCCC	GCACAG GT ATGTAT	86	324
6	TGAGGA AG /CGATCT	CAGTAA GT ACCACG	106	5100
7	TCCCAC AG /GGTCCT	CTAAG GT AAGA AA	190	20409
8	CTTCCT AG /GGCTCC	AGAAGT GT AAGTAT	172	2037
9	ACCTTT AG /GAATAC	CTGTGC GT AGGCAA	123	1799
10	TCTTT AG /ATAACT	ATCCAG GT GAGCAG	83	92
11	CCCCT AG /GTAATG	GATTAT GT GAGTAC	141	6569
12	CTCCAG AG /AGAGAA	GAAATA GT	95	1620

Table 3.1: Intron-exon boundaries and sizes of introns and exons of the mouse CAP2 gene.

The possible acceptor from exon 3, in case of a splicing to form an in-frame protein, will be to exon 7. Such a spliced variant of CAP2 will be lacking the middle 115 amino acids region of the N-terminal domain, which may severely affect the functional property of the translated protein.

Prior to the generation of a targeting construct, 10 kb intronic sequences upstream of 4th exon and down stream of the exon 5th were tested against the mouse genomic database to exclude

the presence of any repetitive sequence or duplicated sequence. The analysis indicated no repetitive sequence in the intended part of vector generation.

3.35.2 Construction of the targeting vector (CAP2 KO)

For the vector construction, genomic DNA was isolated from IB10 mouse embryonic stem cells of the SV126 strain. A schematic diagram of the target vector is given in Figure X. For the 5' arm, a 4.506 kb genomic fragment at the 5' side of the 4th exon including a short stretch of bases from the 4th exon itself was amplified with primers which have SacII restriction sites using a Pfu Turbo DNA polymerase and cloned into the Neo-pBluescript vector, a pBluescript plasmid carrying a 1.8 kb EcoRV-NotI fragment containing the neomycin resistant cassette. This plasmid served as the vector backbone. The 5' arm was cloned into Neo-pBluescript using SacII to the 5' side. The 3' arm was designed downstream of exon 5. The 3' arm was amplified from the ES cell genomic DNA with primers carrying ClaI and Sall restriction sites with a SmaI site located just 30 bases to the 5' side of the 3' arm and cloned first into pGEM-T easy. The 3' arm was retrieved from the pGEM-T easy using SmaI and Sall and ligated to the 3' arm-Neo-pBluescript. All the fragments were sequenced and the cloning directions were confirmed.

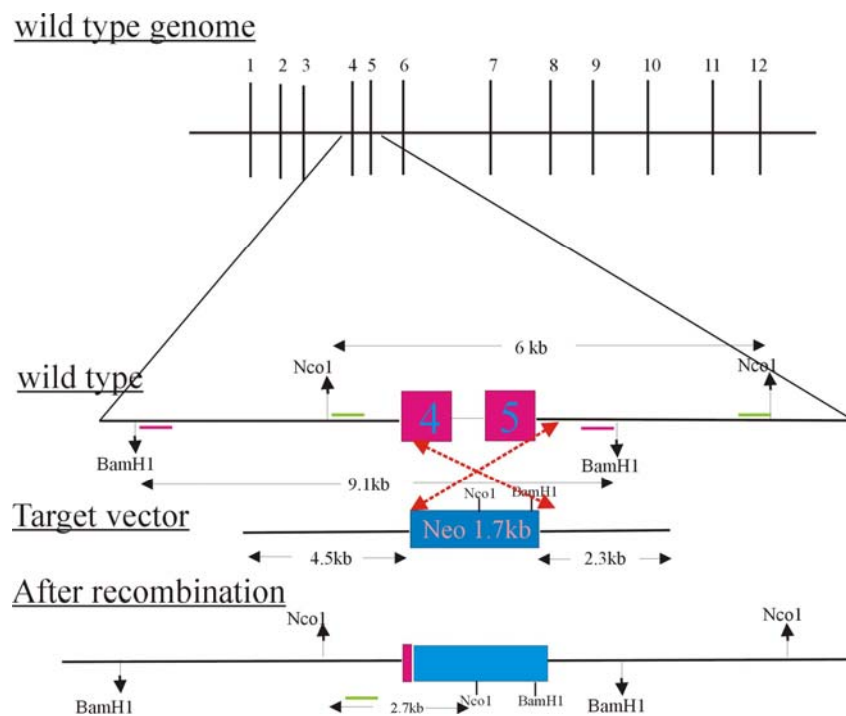


Figure 3.43: Schematic representation of the targeting vector and the recombination events. The perpendicular lines 1 to 12 in the wild type genome represent the 12 exons of the CAP2 gene. Wild type shows the 13 kb length upstream of 4th exon to the down stream of 5th exon. The target vector was linearised with Sall. Dotted arrows in orange depict the event of homologous recombination. The red line and the green line represent

the probes of the 5' arm (left arm) and the 3' arm (right arm) respectively. After recombination, depicts the integration of the Neomycin cassette in the genome.

Two external probes were generated for each arm of the target vector, which could be used for the screening of clones and also for checking the recombinant clones. These probes were tested for the genomic digestion pattern and for the specificity of the probes. Southern blotting after digestion of genomic DNA with different enzymes has given the expected pattern of bands. The probes detected specifically single bands at the expected sizes (Figure 3.43 A). After recombination event the possible fragments detected by the individual probes of each arm is shown in the tables below. The probes of the left arm (5' arm of the vector) recognising the fragments after recombination is shown in table 3.2. The recognising fragments by the 3'arm probes (right arm) are in the table 3.3.

BamHI digest: probes of 5' arm (left arm) of the target vector

	5'probe	3'probe
Wild type	9.1kb	9.1kb
Recombinant	9.1kb	1.1kb

Table 3.2: Sizes of wild type and knockout bands with 5' and 3' probes of the left arm (5' arm of the target vector when digested with BamHI).

NcoI digest: probes of 3'arm (right arm) of the target vector.

	5' probe	3' probe
Wild type	6 kb	6 kb
Recombinant	2.74 kb	4.2 kb

Table 3.3: Sizes of wild type and knockout bands with 5' and 3' probes of the right arm (3' arm of the target vector when digested with NcoI).

3.35.3 ES cell transfection and screening

The target vector was linearised with Sall and 40 µg of purified plasmid DNA were transfected into ES cells from both the IB-10 and R-1 lineage. The clones were selected using G418 for a period of 8 days after transfection. Neomycin resistant clones were picked and grown in 24 well plates. One part of the cells was frozen and another part used for isolating genomic DNA. NcoI was chosen for digesting the genomic DNA. Since NcoI was chosen, we used the 5'probe of the right arm (3'arm of the target vector). The expected sizes of the signals with both wild type and recombinant DNA are given in the Tables above.

We have done two ES cell transfection and more than 800 clones which showed resistance to neomycin were picked and analysed by Southern blotting. Preliminary screening was done with the 5' probe of the right arm (3' arm of the vector) and out of 800 clones, we have analysed so far 110 clones and only one clone (98 in lane 2 of Figure 3.44 C) gave the recombinant band of 2.7 kb in addition to the wild type band of 6 kb (Figure 3.44 C).

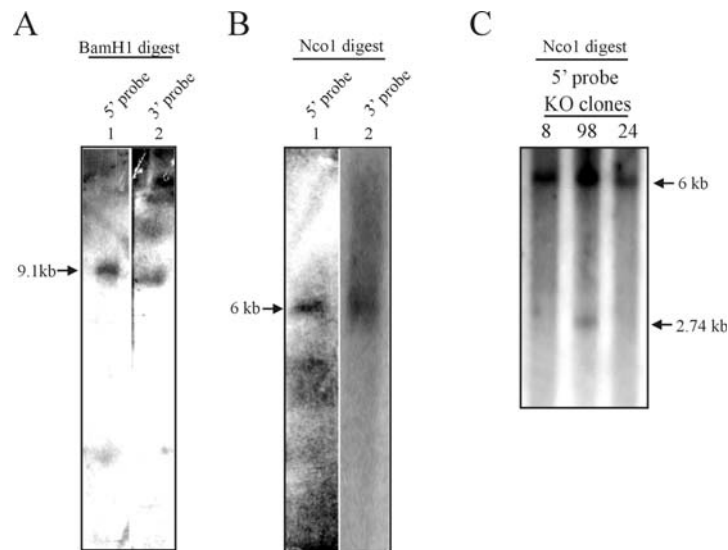


Figure 3.44: Southern blot analysis of genomic DNA and Es cell clones. 10 μ g of genomic DNA digested with the appropriate enzyme were loaded onto an agarose gel (0.9 % agarose), separated by electrophoresis, denatured and transferred onto a nitrocellulose membrane and hybridized with 32 P labelled probes generated by PCR. In (A) Lane1, genomic DNA digested with BamHI hybridized with the 5' probe of the BamHI fragment, Lane 2, same as lane 1 but hybridized with the 3' probe of the genomic BamHI fragment. (B) Lane 1, genomic DNA digested with NcoI was hybridized with the 5' probe of the NcoI fragment. Lane 2, same as lane 1 but hybridized with the 3' probe of the NcoI derived genomic fragment. In panel C, clones resistant to neomycin (8, 98 and 24) were digested with NcoI and probed with the 5' probe of the NcoI fragment. The clone number 98 gives two bands at the expected sizes.

These clones will be analysed further for the recombination events with different enzymes and with the neomycin probe to exclude a random integration into other sites before they will be used for injection.

DISCUSSION

4 DISCUSSION

The actin cytoskeleton plays a critical role in many different cellular processes, including polarity, morphogenesis, motility, endocytosis and intracellular transport. Various intra- and extracellular signals regulate the structure and dynamics of the actin cytoskeleton through an array of actin binding proteins. One central family of cytoskeletal regulators is the cyclase associated proteins (CAP), which are conserved actin monomer binding proteins found in all eukaryotes studied so far. The original CAP was isolated as a component of the *Saccharomyces cerevisiae* adenylyl cyclase complex that serves as an effector of Ras during nutritional signalling. CAPs are multifunctional molecules that contain domains involved in actin binding, adenylyl cyclase association in yeast, SH3 binding, and oligomerization (Hubberstey et al., 1996). Unlike yeast, *Drosophila* and *Dictyostelium*, mammals have two homologues namely CAP1 and CAP2. CAP2 has 42-50% homology to all the species of CAP and to its homologues at the nucleotide level. Furthermore, CAP2 has all the domains, which are present in all the other CAPs.

4.1 Comparison of the CAP2 protein sequence with its homologues

The protein alignment reveals that CAP2 is having significant homology and similarity to CAP1 of mouse. Apart from that CAP2 has similar characteristic features in its protein sequence as CAP1 of mouse and CAP of *S. cerevisiae*, where a similar domain structure was determined. CAP2 has an amino terminal and a carboxyl terminal domain which is highly conserved in all CAPs and a proline rich region which is known to have a role in the localisation of the protein. Closer examination of the amino-terminal sequences of CAP reveals the presence of a heptad repeat region ($\alpha XX\alpha XXX$; where α represents a hydrophobic residue). Heptad repeats are thought to form α -helices that wind around each other to form a coiled coil structure. Coiled coils are highly versatile motifs involved in oligomerization and protein-protein interactions (Burkhard et al., 2001). This conserved N-terminal motif was termed as the 'RLE motif' by other researchers. The RLE motif is identical to the 'CAP signature' motif identified in the ExPASy protein motif database. It was suggested that this motif has diverged functionally during evolution but may still be critical for CAP function in all the organisms. Perhaps the coiled coil regions in other signalling proteins interact with the CAP RLE motif in higher eukaryotes. On the contrary to the conserved N-terminal motif, the N-terminal domains as such are the least structurally conserved regions from human to yeast CAP. As in the human protein, the N-terminus of mouse CAP2 is least conserved with its counterpart in CAP1 (Yu et al., 1994). Apart from this CAP2 has a WH2 domain similar to

that found in CAP of different organisms. WH2 domains are signature actin-binding motifs that show a strong preference for binding ATP-actin monomers (Paunola et al., 2002). The WH2 domain of CAP2 resides at 20 amino acids after the middle towards the C-terminus of the protein. Recent reports coming from Srv2/CAP suggest that CAP preferentially binds to the ADP-actin monomers rather than ATP-actin monomer (Mattila et al., 2004) wherein it was shown that mutations in WH2 domain residues, which are critical for actin-binding caused no significant effect on the ADP-actin binding affinity, however a small reduction in the affinity of binding to ATP-actin. The possibility of a difference in the affinity to bind to actin by the WH2 domains of the CAP family protein might come from the fact that all CAP family members contain a small insertion of 3-4 residues located near the key actin-binding site at the N-terminal α -helix in WH2 domains (Hertzog et al., 2004). Such insertions are not found in the other WH2 domain containing proteins (Paunola et al., 2002). The small change in the WH2 domain, which is specific to the CAP family, might play a specific role in the specific functions of CAP in some specific tissues. This theory may hold good even in the case of CAP2 which might have a specific function in specific tissues.

4.2 CAP2 tissue distribution and its role

The Expression of CAP2 transcripts appear to be tissue specific unlike the one of CAP1, which is expressed ubiquitously. It has been reported also in rat that CAP2 expression is tissue specific and that it is expressed only in some tissues unlike the CAP1 of rat (Vojtek and Cooper, 1993; Zelicof et al., 1993; Swiston et al., 1995).

One more feature of CAP2 is the presence of two transcripts in contrast to CAP1, which is having only one transcript. The result we obtained was in line with the findings of Bertling et al. (2004) who also observed two transcripts and reported that the two signals might be the consequence of the selective use of two polyadenylation signals. Taken together the results from our northern and western blot analyses were in agreement with the findings of Bertling et al. They were able to detect a CAP2 transcript in testis; likewise we detected a mRNA in our northern blot analysis but did not detect a signal at the protein level. They also reported that in the testis the signal detected was from a splice variant of CAP2.

The expression of CAP2 in heart, skeletal muscle and brain was strong. Similar results were also reported by Bertling et al. (2004), who in addition found a very weak expression in lung and liver. We were unable to detect the signals for CAP2 in adult mice in lung and liver. On the contrary, our embryo staining revealed a moderate expression of CAP2 in lung of E16.5. It appears that the level of CAP2 expression in lung might be reduced during the transition

stages of embryo to the newborn and to the adulthood. In the skeletal muscle, CAP2 shows a striated pattern of distribution. It is however not localized to the Z-band which is obvious from our staining as it is not colocalizing with desmin, which is located in the Z-discs. Rather, CAP2 might be located in the neighbouring I-, A- or M- bands. Moreover CAP2 is more abundant in skeletal muscle than CAP1 (Korte 2004). These findings point to a specific role for CAP2 in the skeletal muscle.

The strength of skeletal muscle is directly proportional to its cross-sectional area. The strength of a body, however, is determined by a number of biomechanical principles (the distance between muscle insertions and joints, muscle size, and so on). Muscles are normally arranged in opposition, so that as one group of muscles contract, another group relaxes or expands. Skeletal muscles are used to facilitate movements by applying force to bones and joints via contraction. They generally contract voluntarily (via nerve stimulation), although they can contract involuntarily. The muscle consists of actin and myosin plus some regulatory subunits. These are the components of each muscle cell that actually produce force. The rest of the machinery plays a supporting or repair function. Hence the muscle is the important machinery for the contractile movements, wherein the actinomyosin complex is involved in. The expression of CAP2 in skeletal muscle, its possible association with myofibrillar region and its association with actin as reported by Huberstey et al. (1996) give an indication that CAP2 might play a role in the formation or regulation of the actinomyosin complex. Further investigation is required to exactly localize the CAP2 protein in the skeletal muscles, preferably by immuno-electronmicroscopy, and to ascertain the role it might play in the above mentioned process.

In the heart the expression of CAP2 was detected in capillary walls around the RBCs, endothelial cells of the heart and in the sarcomeres where we again observed a striated pattern of staining. The exact localisation of CAP2 in heart is discussed in the next section. The expression of CAP2 in heart was also observed at embryonic stage E16.5, Bertling et al. (2004) reported that the CAP2 expression was restricted only to the developing heart and muscle tissue at E 10.5.

From our northern blot analysis we were not able to detect the mRNA of CAP2 in brain, but we were able to detect a strong expression of CAP2 at the protein level. The results were similar to that of the findings of Bertling et al. (2004). It is quite interesting to mention that like in the case of skeletal muscle, the expression of CAP1 in brain was less compared to the other tissues (Korte, 2004). The expression of CAP2 was uniform throughout the brain as observed in our western blot analysis. On contrary to the data from the adult brain we were

able to detect a very weak expression of CAP2 in the cerebellum and in the brain stem of the newborn mice. We observed a strong staining in the cortex of the cerebrum and a weak expression in the grey matter in case of the newborn, whereas the expression of CAP2 was found in the molecular layer and was absent in the grey layer in adult mice thus suggesting that the CAP2 expression gradually increases outwards of the white matter into the cortex. These results also revealed that CAP2 might play a role in the differentiation of neurons. Neurons originate in the white and grey matter and migrate outwards to the cortex implicating that the differentiated neurons with their axons are migrating to the cortex of both cerebellum and the cerebrum. The expression of CAP2 increases in the differentiated neurons as we observed a strong staining of the cerebellar cortex in the adult mice. Unfortunately we could not detect CAP2 expression in any of the neuronal cell lines we checked so far. A strong expression of CAP2 in the white matter of myelinated axons reveals that CAP2 is present in the glia cells and the rat cerebellar culture, which is discussed in the later sections. The immunofluorescence studies also revealed that CAP2 was expressed in the Purkinje cells. By contrast, CAP1 does not stain Purkinje cells (Korte, 2004). The E16.5 day also showed a moderate CAP2 expression in the cerebellum region which correlates with the studies carried out by Bertling et al. (2004) that reported a strong expression in the thalamic region of the brain at E18.5.

The expression of CAP2 was observed in skin by western blot analysis and confirmed by two different immunofluorescence studies. This is the first report that CAP2 is expressed in skin. We observed a strong expression of CAP2 in the basal layer of the epidermis and in the hair follicular regions. Further immunostainings revealed that CAP2 is present in the keratinocytes of the basal layer of the epidermis. In addition to the presence in the hair follicular region CAP2 was also found in the sebaceous glands of the skin. As CAP2 is present in the hair follicles, a highly proliferating region of keratinocytes, CAP2 might play a possible role in the proliferation of hair follicles and may be involved in the process of differentiation and migration of keratinocytes.

In conclusion, CAP2 is expressed in brain, heart and skeletal muscle, it may be weakly expressed in lung and in the testis, furthermore it is present in skin. These reports suggests that unlike CAP1, CAP2 is expressed in some specific tissues only and might play an important role in different cellular processes like morphogenesis, polarization, migration and endocytosis. CAPs are not the only proteins of this class of actin-binding proteins. There are reports of similar differential expression specificities for other mammalian actin binding

proteins such as ADF/cofilin, twinfilin and capping protein (Ono et al., 1994; Schafer et al., 1994; Vartiainen et al., 2003).

4.3 CAP2 associates with cardiac myofibrils

Myofibrils are made of three kinds of proteins namely, contractile protein (myosin and actin), regulatory proteins which turn contraction on and off (Troponin and tropomyosin) and structural proteins which provide proper alignment, elasticity and extensibility (titin, myomesin, nebulin and dystrophin). Thick filaments are composed of myosin, in which each molecule resembles two golf clubs twisted together. Myosin heads (crossbridges) extend towards the thin filaments. The thick filaments were held in place by the M line proteins. The thin filaments consist of actin, tropomyosin and troponin, which plays a role in regulating the muscle contraction. The thin filaments are held in line by Z-discs.

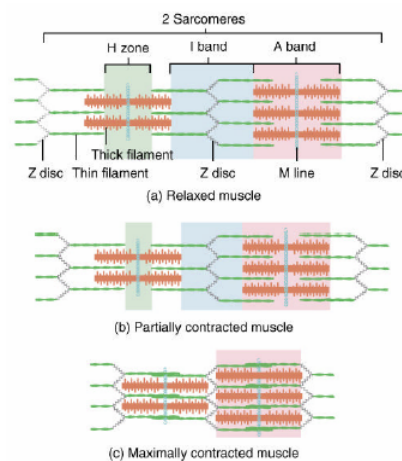


Figure 4.1: Schematic diagram showing the position of the A-, I-, Z- and M-line in the sarcomeres during the relaxed, partially contracted and fully contracted muscle.

Our immunofluorescence studies showed that CAP2 is associated with the M-line, wherein CAP2 co-localizes with myomesin, which is a M-band protein. (Grove et al., 1984). Recent reports suggest that the main components of M-band are the C-terminal kinase domain of the giant protein titin (Mayans et al., 1998), MM-CK creatinine kinase (Wallimann et al., 1977) and M-protein (Eppenberger et al., 1981). There are few more candidates, which are present in the M-band by virtue of interacting with the four major proteins. It will be interesting to screen for the interacting partners for CAP2 in the myofibrils to ascertain whether CAP2 is present in the M-band on its own or by virtue of the interaction with these proteins. One example of an M-band associated protein is murf2, which is present in the M-band through association with the kinase domain of titin (Centner et al., 2001). Murf 2 is a ring finger protein involved in several cellular processes including signal transduction, ubiquitination and

morphogenesis (Jackson et al., 2000; Spencer et al., 2000). A search for an interaction of CAP2 with the major M-band proteins may directly lead to the identification of a partner.

One more interesting point is that all the four proteins have immunoglobulin domains and it has been reported that these domains play a part in incorporating these protein into the M-band region. In myomesin, a N-terminal immunoglobulin-like domain is sufficient for it to targeting to the M-band (Auerbach et al., 1999). CAP is composed of alpha helices in its N-domain and beta-helices and beta-sheets in the C-domain. The crystal structure of the C-terminal dimerization and actin monomer-binding domain (C-CAP) reveals a highly unusual dimer, composed of monomers possessing six coils of right-handed beta-helices flanked by antiparallel beta-strands (Dodatko et al., 2004). For the N-terminus of *Dictyostelium* CAP it has been reported that it is composed of alpha helices where the core is formed by an alpha-helix bundle composed of six antiparallel helices, in stark contrast to the CAP C-terminal domain (Mavoungou et al., 2004). The unusual right-handed beta-helical fold present in C-CAP has been implicated in supporting a wide range of biological functions.

CAP2 is present in the myofibril and is associated with the M-band. The M-band is the transverse structure in the center of the sarcomeric A-band, which is responsible both for the regular packing of thick filaments and for the uniform distribution of the tension over the myosin filament lattice in the activated sarcomere. Although some proteins from the Ig-superfamily, like myomesin and M-protein, are the major candidates for the role of M-band bridges, the exact molecular organisation of the M-band is not clear. However, the protein composition of the M-band seems to modulate the mechanical characteristics of the thick filament lattice, in particular its stiffness, adjusting it to the specific demands in different muscle types (Agarkova et al., 2003). CAP2 localisation in the M-band is an exciting aspect and further studies are required to ascertain the role of CAP2 in these complex structures.

4.4 Overexpression of CAP2 in mammalian cells

The overexpression of GFP-CAP2 and Myc-CAP2 fusion proteins showed a diffused cytosolic localisation and colocalisation of CAP2 with cortical actin structures which was in line with the results obtained by M Leichter (2002). In budding yeast and *Dictyostelium* Srv2/CAP localize to the cortical actin cytoskeleton (Freeman et al., 1996; Noegel et al., 1999). However, the subcellular localisation of mammalian CAPs has remained elusive. Studies with tagged versions and followed by immunofluorescence analysis showed that CAP1 localises to the dynamic regions of the cortical actin cytoskeleton in C3H-2K fibroblasts (Moriyama and Yahara, 2002). On the other hand, studies with monoclonal

antibodies against human CAP1 suggested that, in addition to cortical actin structures, this protein also localises to actin stress-fibers in Swiss 3T3 fibroblasts (Freeman and Field, 2000). The localisation of CAP1 in cultured NIH3T3 and B16F1 cells showed diffused cytoplasmic localisation, but it was also concentrated at actin-rich membrane ruffles and weakly staining stress-fibers of NIH3T3 cells (Bertling 2004). Therefore we can conclude that overexpression of CAP2 and CAP1 has similar effects in cell lines but overexpression of CAP/Srv2 in plants results in defects in actin filament structures and problems in cell growth and division (Barrero et al., 2002). The other interesting point is that the localisation of CAP1 was dependent on its N-terminal region with which it associates with actin in the presence of cofilin very effectively and in the case of CAP2 as well it holds good that the N-terminal region helps in actin-modulating function (Moriyama et al., 2002). In *Dictyostelium* it was reported that the localisation of CAP at the anterior and posterior edges of cells require its N-terminal domain but not its C-terminus (Noegel et al., 1999). Taken together, the function of the N-terminus of CAP is conserved and has a similar role from *Dictyostelium* to man (Moriyama et al., 2002) including CAP2 of mouse.

4.5 CAP2 interacts with CAP1

Our immunoprecipitation results showed that CAP2 interacts with CAP1. These findings extend the ones obtained for human CAP1 and CAP2 (Hubberstey et al., 1996). The results obtained by us and findings of the others suggest that the interaction has been conserved in mammals. Furthermore, it was reported that CAP is capable of interacting with other CAP molecules or with CAP2 in vivo. This suggests that CAP may form large complexes with itself or with other homologues. These may be probably dimers, although higher order structures have not been excluded. In fact, a number of previous studies have shown that CAP exists in a high molecular weight complex in cell extracts and that purified CAPs oligomerise via interacting within and between their N and C-termini. Moreover, a recent report indicated that CAP is found in a complex containing only actin and CAP is in a 1:1 M ratio in *S. cerevisiae* (Balcer et al., 2003). It was suggested that the complex contains six actin monomers and six CAP molecules organized into a macromolecular complex involving intra- and inter-molecular interactions between the domains. The amino terminus and carboxy terminus can interact with each other as well as within themselves which suggests that CAP may form a parallel dimer in which the amino terminus interacts with the carboxy terminus to potentially block actin binding. Alternatively, antiparallel dimers that interact between the amino and carboxy terminus, which then fold over to interact with themselves, may exist (Fig.

4.2). Since the poly-proline domain resides essentially in the middle of the protein, both models allow for the poly-proline SH3 interacting domain to be free to bind target proteins like ABP1 and render proper localisation to the CAP molecule, though other domains may be involved.

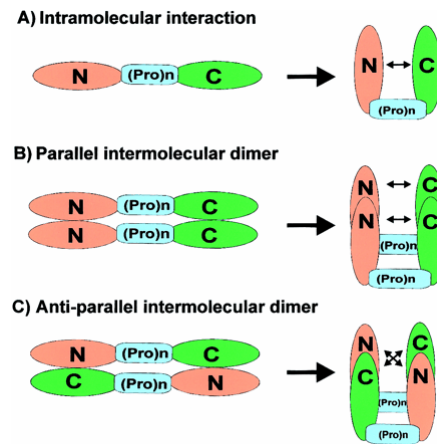


Figure 4.2: Model for CAP multimerisation: a schematic representation of CAP consisting of the amino-terminal domain (orange), poly-proline region (blue), and carboxy-terminal actin binding domain (green). The figure is taken from Hubberstey and Mottillo 2002, *FASEB J.* 16, 487-499.

4.6 CAP2 and its interacting partners

Our results showed that the N-terminal CAP2 interacts with the myosin light chain alkali 3, a non-muscle isoform, in the skin (MLC 3 nm). It has been reported that actin interacts not only with the N-terminus of MLC_1F but also with the N-terminal sequences of the essential light chain isoforms of slow myosin (Nieznanaska et al., 2002). Furthermore, the same author reported that the long isoform of the essential light chain can induce two different effects in the muscle cells, first it is associated with a mechanical lowering of the cross bridge cycling rate resulting from the attachment of the myosin head to the actin by the N-terminal part of essential light chains, second, it is associated with the introduction of a positive charge by the N-terminus of essential light chain into the thin filament suggesting a conformational change in the thin filament and thus playing a role in regulating the thin filaments. Since CAP2 is present in the striated muscle cells and is associated with M-bands, where proteins present in that region - as discussed in the above section - play a structural role in keeping the thick filaments in order, the interaction with essential myosin light chain give us a clue that CAP2 might bind to the myosin light chain of the thick filament not only holding them in position but also may play a role through the myosin light chain regulating the thin filaments.

Our findings that CAP2 interacts with ACF-7 suggest that the functional aspects of the CAPs are conserved from fly to mammals, with the report from *Drosophila* showing that CAP interacts with short stop in a calcium dependent manner through its EF-hand domain residing at its C-terminus, a meeting report was available (MBC 14, 2003,1105, page 198a). Short stop is a spectraplakins, which form a subfamily of plakins (Fuchs and Karakesisoglou 2001; Leung et al. 2002; Roper et al., 2002). The plakins family, which includes mammalian ACF7 and neuronal BPAG1, *Drosophila* Kakapo/shot, and *C. elegans* vab10, is characterised by their unusual capacity to simultaneously bind F-actin and microtubules (Yang et al., 1999; Svitkina et al., 1996; Andrä et al., 1998; Karakesisoglou et al., 2000 and Sun et al., 2001). ACF7 appears to confer stabilising effects in two ways, by both direct microtubule binding and by microtubule-F-actin crosslinking, and is therefore able to respond versatilely to positional information within cells and modify microtubule dynamics to spatially organise the cytoplasm (Kodama et al., 2003). In our study we observed that CAP2 colocalises with microtubules in primary keratinocytes and is affected in its distribution by microtubule disrupting drugs. This interaction might be a direct one or be mediated by ACF7. Taken together, by binding to ACF7 and associating with the microtubules CAP2 might also play a role in regulating the microtubule-F-actin.

Apart from these interacting partners CAP is also known to interact with at least three other actin-binding proteins, Abp1 (Freeman et al., 1996; Lila and Drubin, 1997; Balcer et al., 2003), cofilin (Moriyama and Yahara, 2002), and profilin (Drees et al., 2000). CAP interacts with itself and forms a complex with actin. This complex promotes the cofilin-dependent turnover of actin filaments in vitro and in vivo (Moriyama and Yahara, 2002; Balcer *et al.*, 2003; Bertling *et al.*, 2004). Similar interactions have been noted for CAP2 as it binds to actin and interacts with its counter part CAP1 (Hubberstey et al., 1996) and binds to cofilin as well (Moriyama and Yahara 2002). CAP2 might have a different interacting partner depending on in which process it is involved in and as discussed above section CAP2 might have many more tentative potential candidates as its interacting partners. However the mechanism by which it interacts and how it gets involved in different cellular process is still a mystery.

4.7 CAP2 in PAM212 and other primary cell culture

CAP2 is expressed in PAM212 cells, which are derived from mouse keratinocytes. This was the only cell line in which CAP2 was expressed out of many other cell lines we have checked so far. Interestingly, CAP2 was localised in the nucleus as well as in the cytosol. In general

CAP molecules are cytosolic in nature. The nuclear localisation could also be confirmed by cell fractionation experiments. CAP2 does not contain a typical nuclear localisation signal and the mechanism of its translocation is not known. Also, the role of CAP2 in the nucleus is speculative. However, its binding partner actin is a constituent of the nucleus and recent reports proved that it is universally existent in the nuclei of many cell types. Actin, actin-binding proteins and as well as actin-related proteins are necessary for the mediation of the conformation and function of nuclear actin, including the transformation of actin between G-actin (unpolymerised) and F-actin (polymerised), chromatin remodelling, regulation of gene expression, RNA processing and as well as RNA transport (Rando et al., 2000; Hofmann et al., 2001; Percipalle et al., 2001). An increasing number of actin-binding proteins has been reported to shuttle between nucleus and cytoplasm. Already in 1993, Onoda *et al.* showed that CapG (Mbh1 or gCap39), a ubiquitous 39-kDa barbed end F-actin-binding protein particularly abundant in macrophages (Johnston et al., 1990), is a nuclear and cytoplasmic protein. CapG does not contain a canonical nuclear localization signal, but it has been suggested that phosphorylation of CapG may be involved in controlling the subcellular localization of the protein (Onoda et al., 1993). Another protein with a dual localisation is Cofilin. Cofilin is a major actin depolymerising protein, and its nuclear translocation is regulated by phosphorylation in some cells (Ohta et al., 1989; Samstag et al., 1996; Nebl et al., 1996; Nagaoka et al., 1996). Cofilin has a preference for ADP-actin. A very recent report showed that Srv2/CAP binds with strong preference to ADP-actin monomers compared with ATP-actin monomers and directly competes with cofilin for binding to ADP-actin. This explains how Srv2 can recycle ADP-G-actin from a cofilin-bound state and release monomers after they have undergone nucleotide exchange. Srv2 also blocks ATP-actin monomer addition to the barbed ends of filaments, suggesting that *in vivo* Srv2 acts as a middleman and there is a handoff to other actin monomer binding proteins with a higher affinity for ATP-G-actin such as profilin (Mattila et al., 2004). It has also been reported that CAP 2 binds to cofilin. So CAP2 might take up the job of actin turnover in certain specific tissues and in specific locations like in nucleus in certain types of cells. Furthermore, from the sequence analysis we know that CAP2 has potential phosphorylation sites. CAP2 localisation could thus be regulated in a similar manner as the one of cofilin. Another possibility of taking CAP2 into the nucleus could be with ACF7 which has an NLS.

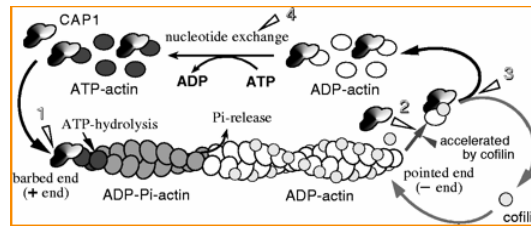


Fig 4.3: A schematic model of cooperation between CAP1 and cofilin in promotion of actin dynamics. The working steps of CAP1 are indicated by open arrowheads. (1) CAP1 facilitates the addition of Mg-ATP-actin monomer onto the barbed end of actin filament. Cofilin-induced severing also contributes to this step by increasing the number of barbed ends. (2) CAP1 accelerates subunit release at the pointed end and enhances the more potent, analogous effect of cofilin. (3) CAP1 relieves the inhibitory effect of cofilin on nucleotide exchange of ADP-actin. (4) CAP1 accelerates nucleotide exchange on G-actin. Taken from **Moriyama and Ichiro Yahara JCS 115, 1591-1601 (2002)**.

One more possibility of CAP2 transport into the nucleus is by the new protein import pathway, which was identified for the shuttling of hnRNP K protein, which contains a novel shuttling domain (termed KNS), which has many of the characteristics of M9. M9 was identified initially as the A1 nuclear localisation signal (NLS) as placement of M9 on normally cytoplasmic reporter proteins results in nuclear localisation (Siomi and Dreyfuss 1995; Weighardt et al., 1995) and also supplies the A1 nuclear export (Michael et al., 1995), in that it confers bi-directional transport across the nuclear envelope. KNS-mediated nuclear import is dependent on RNA polymerase II transcription, and a classical NLS can override this effect. Furthermore, it has been reported that KNS accesses a separate import pathway distinct from either classical NLSs or M9 (Michael et al., 1997).

We confirmed the nuclear localisation of CAP2 also in primary mouse keratinocytes and found here also a colocalisation of microtubuli with CAP2 as in the case of PAM212 cells. CAP2 interacting partner ACF7 also showed similar localisation and colocalisation pattern with microtubuli give us further evidence, apart from our biochemical and immunofluorescence that CAP2 indeed interacts with ACF7.

In primary human keratinocytes, however, nuclear staining was absent and we observed a punctate pattern of staining around the cortex. One explanation is that the epitope, which recognises CAP2, might be masked inside the nucleus in the human keratinocytes. Similar findings were reported for an antibody recognising nuclear actin (Gonsior et al., 1999). As we had observed CAP2 expression in the white matter region of the brain, we stained primary glia cells from rat and observed a diffuse cytosolic staining in some cells and also observed CAP2 in the nucleus of some cells. Nuclear staining was also obtained in case of the rat cerebellar cultures.

Interestingly, we observed CAP2 expression in primary cardiomyocytes isolated from E17 to E19 mice where it partially colocalised with Troponin I (cTnI), which is used as a marker for the cardiomyocytes. Troponin is a globular protein complex consisting of three subunits, (1) troponin C (TnC), the Ca^{2+} binding subunit; (2) troponin I (TnI), the inhibitory subunit; and (3) troponin T (TnT), the subunit that binds to tropomyosin (Ebashi et al., 1968). It has long been appreciated that TnI plays an indispensable role in Ca^{2+} regulation of the thin filament. TnI can be considered as the molecular switch of the thin filament regulatory system (Farah and Reinach, 1995). In further studies we will test whether CAP2 interacts directly with Troponin I.

The other important point to be noticed here is the nuclear localisation of CAP2 in primary cardiomyocytes apart from the weak cytosolic staining. We also observed the same localisation in the cardiomyocyte cell line HL-1. It has been described that proteins associated with the Z-disc, I-band and M-band can translocate and shuttle from the cytosol to the nucleus. One such report is available for MURF2, a member of the MURF family of muscle-specific RING/B-box zinc-finger proteins, which localises at the sarcomeric Z- and M-bands of cardiomyocytes (Centner et al., 2001; Spencer et al., 2000). MURF2 is largely diffusely distributed in the cytosol but notably found in a speckled pattern in the nucleus and colocalises with proteins involved in SUMO-regulated nuclear transport like Ran GAP (Pizon et al., 2002). The diffused cytosolic staining suggests a mobile pool of protein. As CAP2 also shows a diffused cytosolic staining and has a speckled pattern of staining inside the nucleus and is associated with the M-band, we speculate that it translocates to the nucleus like MURF2. Taken together CAP2 has a triple cellular localisation: it partially colocalises with microtubules, at M-bands and in the nucleus where it might have different roles and might translocate in to the nucleus in one of the speculative ways discussed above. Further investigation is required to throw a light on its nuclear localisation and its role in the nucleus.

The nuclear localisation of CAP2 was not observed in all the cells of a population. We found for PAM212, primary mouse keratinocytes, rat VSM cells and HL-1 that ~5% of the cells did not exhibit nuclear CAP2 stain. This phenomenon is not yet understood. Possible explanations for this may be, that due to a stress response the CAP2 localisation in some cells was altered. In wound healing experiments carried out in rat VSM and PAM212 cells CAP2 partially colocalises with F-actin at certain points of the lamellipodia in the cells at the time of wound closure.

Summarising the various findings on CAP2 it may be concluded that CAP2 could have different roles altogether in different tissues and at different stages in the life of a cell.

4.8 Genomic analysis of CAP2 and its Knockout

From the previous studies we know that CAP is involved in different cellular processes and the ablation or knock out causes a typical phenotype associated with the loss of Srv2 in budding yeast. Deletion of its C-terminus in yeast led to severe defects in the actin cytoskeleton and abnormalities in cell morphology such as cell swelling and a random budding pattern. These phenotypes were partially suppressed by overexpression of the actin monomer-binding protein profilin (Gerst et al., 1991; Vojtek et al., 1991). The loss of Srv2/CAP in *Dictyostelium*, *Drosophila*, and mammalian cells also resulted in an accumulation of abnormal actin filament structures and defects in actin-dependent cellular processes such as motility and endocytosis (Baum et al., 2000; Benlali et al., 2000; Noegel et al., 2004; Bertling et al., 2004). In addition, overexpression of Srv2/CAP in plants results in defects in actin filament structures and problems in cell growth and division (Barrero *et al.*, 2002). Towards dissecting the role of CAP2 in different cellular processes we performed an analysis of the CAP2 gene and found that the CAP2 coding regions are distributed along the length of 132 kb on the chromosome 13 and located at 13A5. Even though CAP2 has 90% identity with the CAP1 coding sequence of mouse, its genomic organisation is different from the CAP1 gene. In the CAP1 gene 12 exons are spread over a length of only around 28 kb, furthermore the gene is mapped to the chromosome 6. Since the genome structure of CAP2 and its expression pattern is quite different from CAP1, it could be that CAP2 has a specific role in those different tissues. To investigate and shed a light on the above aspects we chose to carry out a knock out of the CAP2 gene and study its functions and its role in the above-mentioned aspects.

4.9 Future directions

Apart from the leads we generated analysing CAP2 and knock out mice analysis, since there are some indications that CAP is regulated by phosphoinositides. Phosphoinositides generally play a critical role not only in generating second messengers but also in modulating a variety of cellular functions including cytoskeletal organization and membrane trafficking. Many inositol lipid kinases and phosphatases appear to regulate the concentration of a variety of phosphoinositides in a specific area, thereby inducing spatial and temporal changes in their

availability. For example, local concentration changes in phosphatidylinositol 4,5-bisphosphate (PI(4,5)P₂) in response to extracellular stimuli cause the reorganisation of actin filaments and a change in cell shape. PI(4,5)P₂ uncaps the barbed end of actin filaments and increases actin nucleation by modulating a variety of actin regulatory proteins, leading to de novo actin polymerisation. PI(4,5)P₂ also plays a key role in membrane trafficking processes. (Takenawa and Itoh, 2001). Apart from that it has been shown that phosphatidylinositol 4,5-bisphosphate (PIP₂) can promote the availability of monomeric actin for polymerisation. Addition of PIP₂ at a high molar ratio of CAP to PIP₂ (1:40) inhibited sequestration of actin, suggesting that PIP₂ negatively regulates the CAP-actin interaction, causing release of G-actin from CAP and consequently F-actin assembly. The carboxy terminal domain alone was unaffected by PIP₂ addition, implying that the phospholipid binding site resides within the amino terminal or proline rich domains (Gottwald et al., 1996). The negative effect of PIP₂ on the CAP-actin interaction correlates with the positive effect of PIP₂ on activating WASp, a regulator of actin assembly, which can stimulate actin nucleation by the Arp2/3 complex (Higgs and Pollard, 2000). From the multiple alignments we know that CAP2 has a SH3 domain as they are present in other CAPs and a region, which shows similarity to the verprolin homology domain (LKKAET) (Vaduva et al., 1997). The SH3 domain of human c-Abl interacted with human CAP in an overlay assay, but in this case the P1site was necessary for protein-protein interaction (Freeman et al., 1996). It has been shown that c-Abl plays an important role in signalling actin reorganisation (Lanier et al., 2000) whereas CAP also plays a role in actin sequestering. So we are interested in studying the regulation of CAP2, in particular its relation with PIP₂ and ascertain its possible indirect or direct interaction with PIP₂ and also look for interaction of CAP2 with other proteins through its SH3 domain.

Summary Zusammenfassung

5 Summary

Cyclase associated protein (CAP) is a bifunctional protein having an N-terminal adenyl cyclase binding domain and a C-terminal actin-binding domain. In-between these two domains there is a proline rich SH3 domain presumably involved in the localization of CAP. CAP is expressed widely and has been found in yeast, *Dictyostelium*, *Drosophila*, rat, mouse and humans. Two homologues of CAP have been identified in higher eukaryotes, CAP1 and CAP2. Although CAP proteins have been studied for more than a decade and are present in all organisms, many questions remain about the mechanisms of CAP function. The roles of mammalian CAP2 proteins have not been investigated extensively. In our study we showed that CAP2 has 2 transcripts of 3 and 3.5 kb unlike the ubiquitously expressed CAP1, homologue of CAP2 in mice. In contrast to CAP1, CAP2 is expressed in a tissue specific manner. We found that CAP2 is present in relatively moderate levels in brain, heart and skeletal muscle and lower levels in skin. Furthermore, we investigated the expression pattern in more detail in these tissues and found that CAP2 is present in all parts of the adult brain but is detected only in the cerebellum and brain stem in the newborn mice and expressed only in the cerebellar region of the brain in embryos of E16. In brain CAP2 was expressed uniformly in the cortex and also found in the Purkinje cells and in the myelinated axons of the white matter. In skeletal muscle we observed a striated pattern. CAP2 was strongly expressed in the heart where it was present in cardiomyocytes, endothelial cells and the capillary wall of the blood vessels. We observed a striated pattern, which correlated with an association of CAP2 with the M-bands. In the skin CAP2 was expressed in the basal epidermal layers and in the hair follicle region and was found in the sebaceous glands. CAP2 was also expressed in the keratinocytes in skin.

Immunofluorescence studies with PAM212, a mouse keratinocyte cell line, and primary mouse keratinocytes revealed that CAP2 was surprisingly localized in the nucleus. Cell fractionation experiments performed with PAM212 cells confirmed the presence of CAP2 in the nucleus. In the case of primary mouse keratinocytes CAP2 was also localised to the nucleus apart from its presence in the cytosol. In contrast in human keratinocytes CAP2 localised to the cell cortex and present in patches. Immunofluorescence studies and experiments with drugs affecting the cytoskeleton revealed that CAP2 was partially associated with F-actin and the microtubules. The nuclear localization was dependent on the microtubular cytoskeletal network and independent of the actin cytoskeleton.

Overexpression studies in HEK293 cells using EGFP and Myc fusion proteins showed that CAP2 is cytosolic and was associated with lamellipodia. Unlike our overexpression studies, the immunofluorescence studies with HL-1, a cardiomyocyte cell line, and with primary cardiomyocytes of embryonic stages E17 and E19 showed that CAP2 was localized to the nucleus as in the PAM212 cells. In cardiomyocytes, CAP2 colocalised partially with Troponin I.

In order to investigate the interaction with its homologue CAP1, cotransfection of GFP-CAP1, Myc-CAP2 into HEK293 cells followed by immunoprecipitation experiments was performed. The results revealed that CAP2 interacts with CAP1. While investigating the interaction of CAP2 with other proteins, we found that ACF7, an F-actin crosslinking protein interacts with CAP2 in immunoprecipitation studies carried out on HEK293 cells, coexpressing GFP-C-ACF7 and Myc-CAP2. We further found that the domain of CAP2 interacts with myosin light chain alkali (MLC3nm) in skin lysate.

In a wound healing assay CAP2 colocalised with F-actin at certain places suggesting CAP2 plays a role in wound healing. Using a conventional knock out strategy we are currently generating a mice knock out strain of CAP2 in order to learn more about the functions of this protein.

ZUSAMMENFASSUNG

CAP (Cyclase Associated Protein) besteht aus einer N-terminalen Domäne, die in Hefe an Adenylatzyklase binden kann, und einer C-terminalen Domäne, die für die Bindung an G-Aktin von Bedeutung ist. Beide Bereiche werden durch eine Prolin-reiche Sequenz getrennt, die, wiederum in Hefe, die Lokalisation im Zellkortex bestimmt und an SH3-Domänen binden kann. In Säugern gibt es zwei CAP Formen, CAP1 und CAP2, die durch unterschiedliche Gene kodiert werden.

In dieser Arbeit wurde CAP2 untersucht. CAP2 ist im Vergleich zu CAP1 weniger stark exprimiert und zeigt eine hohe Gewebsspezifität. Es wurde nur in Gehirn, Herz, Skelettmuskel und der Haut gefunden. Seine Verteilung in diesen Organen wurde im Embryo und im adulten Organismus detailliert untersucht. Bemerkenswert ist die Verteilung im Skelettmuskel. Hier wurde eine Bänderung beobachtet wie sie für die Elemente des kontraktiven Apparates charakteristisch ist. Koimmunfärbungen mit Antikörpern gegen verschiedene Muskelproteine haben dann eine Zuordnung zur M-Bande ergeben.

Eine weitere ungewöhnliche Färbung wurde beobachtet bei der Analyse der subzellulären Lokalisation. In PAM212 Zellen, einer Maus Keratinozyten Zelllinie, und in primären Maus Keratinozyten ist CAP2 im Zellkern lokalisiert. Diese Lokalisierung konnte in Zellfraktionierungsexperimenten bestätigt werden. Die gleiche Verteilung wurde auch in HL-1 Zellen, einer Kardiomyozyten Zelllinie, und in primären embryonalen Kardiomyozyten beobachtet. Allerdings ist die Kernlokalisation nicht in allen Zellen zu beobachten. Die Ursache für die wechselnde Lokalisation ist nicht bekannt. CAP2 könnte auf Grund dieser Befunde zu einer neuartigen Klasse von Proteinen gehören, die zwischen Zytosol und Zellkern hin- und herwandert. Bekanntestes Beispiel ist hierfür β -Catenin.

Mit der leichten Kette des Myosins und dem Protein ACF7, einem Protein, das Zytoskelettelemente verbindet und das auch im Zellkern vorkommen kann, wurden mögliche Interaktionspartner von CAP2 identifiziert.

Schliesslich wurde ein Vektor konstruiert, mit dem das CAP2 Gen gezielt inaktiviert werden kann und mit dessen Hilfe im weiteren Verlauf der Untersuchungen die in vivo Funktion von CAP2 geklärt werden soll.

BIBLIOGRAPH

6 BIBLIOGRAPHY

- Agafonov, M.O., Deev, A.V., Kim, S.Y., Sohn, J.H., Choi, E.S. and Ter-Avanesian, M.D. (2003) A novel approach to isolation and functional characterization of genomic DNA from the methylotrophic yeast *Hansenula polymorpha*. *Mol Biol (Mosk)*, 37, 81-87.
- Alonso, L. and Fuchs, E. (2003) Stem cells of the skin epithelium. *Proc Natl Acad Sci U S A*, 100 Suppl 1, 11830-11835.
- Amberg, D.C., Basart, E. and Botstein, D. (1995) Defining protein interactions with yeast actin in vivo. *Nat Struct Biol*, 2, 28-35.
- Amberg, D.C., Basart, E. and Botstein, D. (1995) Defining protein interactions with yeast actin in vivo. *Nat Struct Biol*, 2, 28-35.
- Andra, K., Nikolic, B., Stocher, M., Drenckhahn, D. and Wiche, G. (1998) Not just scaffolding: plectin regulates actin dynamics in cultured cells. *Genes Dev*, 12, 3442-3451.
- Auerbach, D., Bantle, S., Keller, S., Hinderling, V., Leu, M., Ehler, E. and Perriard, J.C. (1999) Different domains of the M-band protein myomesin are involved in myosin binding and M-band targeting. *Mol Biol Cell*, 10, 1297-1308.
- Bahn, Y.S. and Sundstrom, P. (2001) CAP1, an adenylate cyclase-associated protein gene, regulates bud-hypha transitions, filamentous growth, and cyclic AMP levels and is required for virulence of *Candida albicans*. *J Bacteriol*, 183, 3211-3223.
- Balcer, H.I., Goodman, A.L., Rodal, A.A., Smith, E., Kugler, J., Heuser, J.E. and Goode, B.L. (2003) Coordinated regulation of actin filament turnover by a high-molecular-weight Srv2/CAP complex, cofilin, profilin, and Aip1. *Curr Biol*, 13, 2159-2169.
- Barrero, R.A., Umeda, M., Yamamura, S. and Uchimiya, H. (2002) Arabidopsis CAP regulates the actin cytoskeleton necessary for plant cell elongation and division. *Plant Cell*, 14, 149-163.
- Barrero, R.A., Umeda, M., Yamamura, S. and Uchimiya, H. (2002) Arabidopsis CAP regulates the actin cytoskeleton necessary for plant cell elongation and division. *Plant Cell*, 14, 149-163.
- Baum, B., Li, W. and Perrimon, N. (2000) A cyclase-associated protein regulates actin and cell polarity during *Drosophila* oogenesis and in yeast. *Curr Biol*, 10, 964-973.
- Baum, B. and Perrimon, N. (2001) Spatial control of the actin cytoskeleton in *Drosophila* epithelial cells. *Nat Cell Biol*, 3, 883-890.
- Benlali, A., Draskovic, I., Hazelett, D.J. and Treisman, J.E. (2000) act up controls actin polymerization to alter cell shape and restrict Hedgehog signaling in the *Drosophila* eye disc. *Cell*, 101, 271-281.

- Bertling, E., Hotulainen, P., Mattila, P.K., Matilainen, T., Salminen, M. and Lappalainen, P. (2004) Cyclase-associated protein 1 (CAP1) promotes cofilin-induced actin dynamics in mammalian nonmuscle cells. *Mol Biol Cell*, 15, 2324-2334.
- Broach, J.R. and Deschenes, R.J. (1990) The function of ras genes in *Saccharomyces cerevisiae*. *Adv Cancer Res*, 54, 79-139.
- Burkhard, P., Strelkov, S. V., Stetefeld, J. (2001) Coiled coils: a highly versatile protein folding motif. *Trends Cell Biol.*, 11, 82-88.
- Carlier MF, P.D. (1997) Control of actin dynamics in cell motility. *J Mol Biol*, 269, 459-467.
- CarlierMF. (1991) Actin: protein structure and filament dynamics. *J Biol Chem*, 266, 1-4.
- Casey PJ, M.J., Zhang FL, Higgins YB, Thissen JA. (1994) Prenylation and G protein signaling. *Recent Prog Horm Res*, 49, 215-238.
- Centner, T., Yano, J., Kimura, E., McElhinny, A.S., Pelin, K., Witt, C.C., Bang, M.L., Trombitas, K., Granzier, H., Gregorio, C.C., Sorimachi, H. and Labeit, S. (2001) Identification of muscle specific ring finger proteins as potential regulators of the titin kinase domain. *J Mol Biol*, 306, 717-726.
- Chomczynski, P.a.S., N. (1987) Isolation of RNA. *Anal. Biochem.*, 162, 156-159.
- Collard JG, H.G., Michiels F, Stam J, van der Kammen RA, van Leeuwen F. (1996) Role of Tiam 1 in Rac-mediated signal transduction pathways. *Curr Top Microbiol Immunol*, 213, 253-265.
- ColuccioLM. (1994) An end in sight: Tropomodulin. *J Cell Biol*, 127, 1497-1499.
- Davis, S., Lu, M.L., Lo, S.H., Lin, S., Butler, J.A., Druker, B.J., Roberts, T.M., An, Q. and Chen, L.B. (1991) Presence of an SH2 domain in the actin-binding protein tensin. *Science*, 252, 712-715.
- Dodatko, T., Fedorov, A.A., Grynberg, M., Patskovsky, Y., Rozwarski, D.A., Jaroszewski, L., Aronoff-Spencer, E., Kondraskina, E., Irving, T., Godzik, A. and Almo, S.C. (2004) Crystal structure of the actin binding domain of the cyclase-associated protein. *Biochemistry*, 43, 10628-10641.
- Drees, B.L., Sundin, B., Brazeau, E., Caviston, J. P., Chen, G.-C., Guo, W., Kozminski, K. G., Lau, M. W., Moskow, J. J., Tong, A., Schenkman, L. R., McKenzie, A., III, Brennwald, P., Longtine, M., Bi, E., Chan, C., Novick, P., Boone, C., Pringle, J. R., Davis, T. N., Fields, S., Drubin, D. G. (2000) A protein interaction map for cell polarity development. *J. Cell Biol*, 154, 549-576.
- Drees, B.L., Sundin, B., Brazeau, E., Caviston, J.P., Chen, G.C., Guo, W., Kozminski, K.G., Lau, M.W., Moskow, J.J., Tong, A., Schenkman, L.R., McKenzie, A., 3rd, Brennwald, P., Longtine, M., Bi, E., Chan, C., Novick, P., Boone, C., Pringle, J.R., Davis, T.N., Fields, S. and Drubin, D.G. (2001) A protein interaction map for cell polarity development. *J Cell Biol*, 154, 549-571.

- Drubin DG, M.K., Botstein D. (1988) Yeast actin-binding proteins: evidence for a role in morphogenesis. *J Cell Biol*, 107, 2551-2561.
- Ebashi, S., Kodama, A. and Ebashi, F. (1968) Troponin. I. Preparation and physiological function. *J Biochem (Tokyo)*, 64, 465-477.
- Eppenberger, H.M., Perriard, J.C., Rosenberg, U.B. and Strehler, E.E. (1981) The Mr 165,000 M-protein myomesin: a specific protein of cross-striated muscle cells. *J Cell Biol*, 89, 185-193.
- Farah, C.S. and Reinach, F.C. (1995) The troponin complex and regulation of muscle contraction. *Faseb J*, 9, 755-767.
- Fedor-Chaiken, M., Deschenes, R.J. and Broach, J.R. (1990) SRV2, a gene required for RAS activation of adenylate cyclase in yeast. *Cell*, 61, 329-340.
- Fenger, U., Hofmann, M., Galliot, B. and Schaller, H.C. (1994) The role of the cAMP pathway in mediating the effect of head activator on nerve-cell determination and differentiation in hydra. *Mech Dev*, 47, 115-125.
- Field, J., Vojtek, A., Ballester, R., Bolger, G., Colicelli, J., Ferguson, K., Gerst, J., Kataoka, T., Michaeli, T., Powers, S. and et al. (1990) Cloning and characterization of CAP, the *S. cerevisiae* gene encoding the 70 kd adenylyl cyclase-associated protein. *Cell*, 61, 319-327.
- Fowler VM, S.M., Miller PG, Flucher BE, Daniels MP. (1993) Tropomodulin is associated with the free (pointed) ends of the thin filaments in rat skeletal muscle. *J Cell Biol*, 120, 411-420.
- Freeman, N.L., Chen, Z., Horenstein, J., Weber, A. and Field, J. (1995) An actin monomer binding activity localizes to the carboxyl-terminal half of the *Saccharomyces cerevisiae* cyclase-associated protein. *J Biol Chem*, 270, 5680-5685.
- Freeman, N.L., Lila, T., Mintzer, K.A., Chen, Z., Pahk, A.J., Ren, R., Drubin, D.G. and Field, J. (1996) A conserved proline-rich region of the *Saccharomyces cerevisiae* cyclase-associated protein binds SH3 domains and modulates cytoskeletal localization. *Mol Cell Biol*, 16, 548-556.
- Freeman, N.L. and Field, J. (2000) Mammalian homolog of the yeast cyclase associated protein, CAP/Srv2p, regulates actin filament assembly. *Cell Motil Cytoskeleton*, 45, 106-120.
- Fuchs, E. and Karakesisoglou, I. (2001) Bridging cytoskeletal intersections. *Genes Dev*, 15, 1-14.
- Funayama N, N.A., Sato N, Tsukita S, Tsukita S. (1991) Radixin is a novel member of the band 4.1 family. *J Cell Biol*, 115, 1039-1048.
- Gerst, J.E., Ferguson, K., Vojtek, A., Wigler, M. and Field, J. (1991) CAP is a bifunctional component of the *Saccharomyces cerevisiae* adenylyl cyclase complex. *Mol Cell Biol*, 11, 1248-1257.

- Gertler R, K.-S.E., Blackwell CJ. (1995) enabled, a dosage-sensitive suppressor of mutations in the *Drosophila* Abl tyrosine kinase, encodes an Abl substrate with SH3 domain-binding properties. *Genes Dev*, 9, 521-533.
- Gieselmann, R. and Mann, K. (1992) ASP-56, a new actin sequestering protein from pig platelets with homology to CAP, an adenylate cyclase-associated protein from yeast. *FEBS Lett*, 298, 149-153.
- Gonsior, S.M., Platz, S., Buchmeier, S., Scheer, U., Jockusch, B.M. and Hinssen, H. (1999) Conformational difference between nuclear and cytoplasmic actin as detected by a monoclonal antibody. *J Cell Sci*, 112 (Pt 6), 797-809.
- Goode, B.L., Rodal, A.A., Barnes, G. and Drubin, D.G. (2001) Activation of the Arp2/3 complex by the actin filament binding protein Abp1p. *J Cell Biol*, 153, 627-634.
- Gottwald, U., Brokamp, R., Karakesisoglou, I., Schleicher, M. and Noegel, A.A. (1996) Identification of a cyclase-associated protein (CAP) homologue in *Dictyostelium discoideum* and characterization of its interaction with actin. *Mol Biol Cell*, 7, 261-272.
- Grove, B.K., Kurer, V., Lehner, C., Doetschman, T.C., Perriard, J.C. and Eppenberger, H.M. (1984) A new 185,000-dalton skeletal muscle protein detected by monoclonal antibodies. *J Cell Biol*, 98, 518-524.
- Halla. (1998) Rho GTPases and the actin cytoskeleton. *Science*, 279, 509-514.
- Hartwig J H, B.G.M., Carpenter C L, Janmey P A, Taylor L A, and Toker A, S.T.P. (1995) Thrombin receptor ligation and activated Rac uncap actin filament barbed ends through Phosphoinositide synthesis in permeabilized human platelets. *Cell*, 82, 643-653.
- Hertzog, M., van Heijenoort, C., Didry, D., Gaudier, M., Coutant, J., Gigant, B., Didelot, G., Preat, T., Knossow, M., Guittet, E. and Carlier, M.F. (2004) The beta-thymosin/WH2 domain; structural basis for the switch from inhibition to promotion of actin assembly. *Cell*, 117, 611-623.
- Higgins DG, S.P. (1988) CLUSTAL: a package for performing multiple sequence alignment on a microcomputer. *Gene*, 73, 237-244.
- HiggsHN., P. (2000) Activation by Cdc42 and PIP(2) of Wiskott-Aldrich syndrome protein (WASp) stimulates actin nucleation by Arp2/3 complex. *J Cell Biol*, 150, 1311-1320.
- Hoffmann, B., Zuo, W., Liu, A. and Morris, N.R. (2001) The LIS1-related protein NUDF of *Aspergillus nidulans* and its interaction partner NUDE bind directly to specific subunits of dynein and dynactin and to alpha- and gamma-tubulin. *J Biol Chem*, 276, 38877-38884.
- Hubberstey, A., Yu, G., Loewith, R., Lakusta, C. and Young, D. (1996) Mammalian CAP interacts with CAP, CAP2, and actin. *J Cell Biochem*, 61, 459-466.
- Hubberstey, A.V. and Mottillo, E.P. (2002) Cyclase-associated proteins: CAPacity for linking signal transduction and actin polymerization. *Faseb J*, 16, 487-499.

- Jackson, T.R., Kearns, B.G. and Theibert, A.B. (2000) Cytohesins and centaurins: mediators of PI 3-kinase-regulated Arf signaling. *Trends Biochem Sci*, 25, 489-495.
- Johnston, P.A., Yu, F.X., Reynolds, G.A., Yin, H.L., Moomaw, C.R., Slaughter, C.A. and Sudhof, T.C. (1990) Purification and expression of gCap39. An intracellular and secreted Ca²⁺(+)-dependent actin-binding protein enriched in mononuclear phagocytes. *J Biol Chem*, 265, 17946-17952.
- Karakesisoglou, I., Yang, Y. and Fuchs, E. (2000) An epidermal plakin that integrates actin and microtubule networks at cellular junctions. *J Cell Biol*, 149, 195-208.
- Kawamukai, M., Gerst, J., Field, J., Riggs, M., Rodgers, L., Wigler, M. and Young, D. (1992) Genetic and biochemical analysis of the adenylyl cyclase-associated protein, cap, in *Schizosaccharomyces pombe*. *Mol Biol Cell*, 3, 167-180.
- Kodama, A., Karakesisoglou, I., Wong, E., Vaezi, A. and Fuchs, E. (2003) ACF7: an essential integrator of microtubule dynamics. *Cell*, 115, 343-354.
- Korte, H. (2004) In vivo function of CAP1. *Biochemie 1*, Institute for biochemistry, Medical faculty, university of cologne, cologne.
- Kozak M. (1987) An analysis of 5'-noncoding sequences from 699 vertebrate messenger RNAs. *Nucleic Acids Res*, 15, 8125-8148.
- Kühn, R.M.T.a.R. (1997) *Laboratory protocols for Conditional Gene Targeting*. Oxford university Press, Newyork.
- LaemmliUK. (1970) Cleavage of structural proteins during the assembly of the head of bacteriophage T4. *Nature*, 227, 680-685.
- Lambrechts A, V.J., Jonckheere V, Goethals M, Vandekerckhove J, Ampe C. (1997) The mammalian profilin isoforms display complementary affinities for PIP2 and proline-rich sequences. *EMBO J*, 16, 484-494.
- Lanier LM, G.F. (2000) Actin cytoskeleton: thinking globally, actin' locally. *Curr Biol*, 10, R655-657.
- Lauffenburger DA, H.A. (1996) Cell migration: a physically integrated molecular process. *Cell*, 84, 359-369.
- Lehrach H, D.D., Wozney JM, Boedtke H. (1977) RNA molecular weight determinations by gel electrophoresis under denaturing conditions, a critical reexamination. *Biochemistry*, 16, 4743-4751.
- Leichter, M. (2002) Analysis of CAP homologues in Mouse. *Biochemie 1*, Institute for biochemistry, Medical faculty. university of cologne, cologne, p. 89.
- Leung, C.L., Green, K.J. and Liem, R.K. (2002) Plakins: a family of versatile cytolinker proteins. *Trends Cell Biol*, 12, 37-45.

Lila, T. and Drubin, D.G. (1997) Evidence for physical and functional interactions among two *Saccharomyces cerevisiae* SH3 domain proteins, an adenylyl cyclase-associated protein and the actin cytoskeleton. *Mol Biol Cell*, 8, 367-385.

Mattila, P.K., Quintero-Monzon, O., Kugler, J., Moseley, J.B., Almo, S.C., Lappalainen, P. and Goode, B.L. (2004) A high-affinity interaction with ADP-actin monomers underlies the mechanism and in vivo function of Srv2/cyclase-associated protein. *Mol Biol Cell*, 15, 5158-5171.

Mattila, P.K., Quintero-Monzon, O., Kugler, J., Moseley, J.B., Almo, S.C., Lappalainen, P. and Goode, B.L. (2004) A high-affinity interaction with ADP-actin monomers underlies the mechanism and in vivo function of Srv2/cyclase-associated protein. *Mol Biol Cell*, 15, 5158-5171.

Matviw, H., Yu, G. and Young, D. (1992) Identification of a human cDNA encoding a protein that is structurally and functionally related to the yeast adenylyl cyclase-associated CAP proteins. *Mol Cell Biol*, 12, 5033-5040.

Mavoungou, C., Israel, L., Rehm, T., Ksiazek, D., Krajewski, M., Popowicz, G., Noegel, A.A., Schleicher, M. and Holak, T.A. (2004) NMR structural characterization of the N-terminal domain of the adenylyl cyclase-associated protein (CAP) from *Dictyostelium discoideum*. *J Biomol NMR*, 29, 73-84.

Mayans, O., van der Ven, P.F., Wilm, M., Mues, A., Young, P., Furst, D.O., Wilmanns, M. and Gautel, M. (1998) Structural basis for activation of the titin kinase domain during myofibrillogenesis. *Nature*, 395, 863-869.

Meinert, M., Delmer, D. P. (1997) Changes in biochemical composition of the cell wall in cotton fiber during development. *Plant Physiol.*, 59, 1088-1097.

Michael, W.M., Siomi, H., Choi, M., Pinol-Roma, S., Nakielny, S., Liu, Q. and Dreyfuss, G. (1995) Signal sequences that target nuclear import and nuclear export of pre-mRNA-binding proteins. *Cold Spring Harb Symp Quant Biol*, 60, 663-668.

Michael, W.M., Eder, P.S. and Dreyfuss, G. (1997) The K nuclear shuttling domain: a novel signal for nuclear import and nuclear export in the hnRNP K protein. *Embo J*, 16, 3587-3598.

Mintzer, K.A. and Field, J. (1994) Interactions between adenylyl cyclase, CAP and RAS from *Saccharomyces cerevisiae*. *Cell Signal*, 6, 681-694.

Moriyama, K. and Yahara, I. (2002) Human CAP1 is a key factor in the recycling of cofilin and actin for rapid actin turnover. *J Cell Sci*, 115, 1591-1601.

Nachmias V T, G.R., Casella J F, BarronCasella E. (1996) Cap Z, a calcium insensitive capping protein in resting and activated platelets. *Febs Lett*, 378, 258-262.

Nagaoka, R., Abe, H. and Obinata, T. (1996) Site-directed mutagenesis of the phosphorylation site of cofilin: its role in cofilin-actin interaction and cytoplasmic localization. *Cell Motil Cytoskeleton*, 35, 200-209.

- Nebl, G., Meuer, S.C. and Samstag, Y. (1996) Dephosphorylation of serine 3 regulates nuclear translocation of cofilin. *J Biol Chem*, 271, 26276-26280.
- Nieznanska, H., Nieznanski, K. and Stepkowski, D. (2002) The effects of the interaction of myosin essential light chain isoforms with actin in skeletal muscles. *Acta Biochim Pol*, 49, 709-719.
- Nishida, Y., Shima, F., Sen, H., Tanaka, Y., Yanagihara, C., Yamawaki-Kataoka, Y., Kariya, K. and Kataoka, T. (1998) Coiled-coil interaction of N-terminal 36 residues of cyclase-associated protein with adenylyl cyclase is sufficient for its function in *Saccharomyces cerevisiae* ras pathway. *J Biol Chem*, 273, 28019-28024.
- Noegel, A.A., Rivero, F., Albrecht, R., Janssen, K.P., Kohler, J., Parent, C.A. and Schleicher, M. (1999) Assessing the role of the ASP56/CAP homologue of *Dictyostelium discoideum* and the requirements for subcellular localization. *J Cell Sci*, 112, 3195-3203.
- Noegel, A.A., Blau-Wasser, R., Sultana, H., Muller, R., Israel, L., Schleicher, M., Patel, H. and Weijer, C.J. (2004) The cyclase-associated protein CAP as regulator of cell polarity and cAMP signaling in *Dictyostelium*. *Mol Biol Cell*, 15, 934-945.
- Ohta, Y., Nishida, E., Sakai, H. and Miyamoto, E. (1989) Dephosphorylation of cofilin accompanies heat shock-induced nuclear accumulation of cofilin. *J Biol Chem*, 264, 16143-16148.
- Ono, S., Minami, N., Abe, H. and Obinata, T. (1994) Characterization of a novel cofilin isoform that is predominantly expressed in mammalian skeletal muscle. *J Biol Chem*, 269, 15280-15286.
- Onoda, K., Yu, F.X. and Yin, H.L. (1993) gCap39 is a nuclear and cytoplasmic protein. *Cell Motil Cytoskeleton*, 26, 227-238.
- Paunola, E., Mattila, P.K. and Lappalainen, P. (2002) WH2 domain: a small, versatile adapter for actin monomers. *FEBS Lett*, 513, 92-97.
- Percipalle, P., Zhao, J., Pope, B., Weeds, A., Lindberg, U. and Daneholt, B. (2001) Actin bound to the heterogeneous nuclear ribonucleoprotein hrp36 is associated with Balbiani ring mRNA from the gene to polysomes. *J Cell Biol*, 153, 229-236.
- Pizon, V., Iakovenko, A., Van Der Ven, P.F., Kelly, R., Fatu, C., Furst, D.O., Karsenti, E. and Gautel, M. (2002) Transient association of titin and myosin with microtubules in nascent myofibrils directed by the MURF2 RING-finger protein. *J Cell Sci*, 115, 4469-4482.
- Podolski JL, S.T. (1988) Association of deoxyribonuclease I with the pointed ends of actin filaments in human red blood cell membrane skeletons. *J Biol Chem*, 263, 638-645.
- Poetter, K., Jiang, H., Hassanzadeh, S., Master, S.R., Chang, A., Dalakas, M.C., Rayment, I., Sellers, J.R., Fananapazir, L. and Epstein, N.D. (1996) Mutations in either the essential or regulatory light chains of myosin are associated with a rare myopathy in human heart and skeletal muscle. *Nat Genet*, 13, 63-69.

- Rando, O.J., Zhao, K. and Crabtree, G.R. (2000) Searching for a function for nuclear actin. *Trends Cell Biol*, 10, 92-97.
- Rohatgi R, M.L., Miki H, Lopez M, Kirchhausen T, Takenawa T, Kirschner MW. (1999) The interaction between N-WASP and the Arp2/3 complex links Cdc42-dependent signals to actin assembly. *Cell*, 97, 221-231.
- Roper, K., Gregory, S.L. and Brown, N.H. (2002) The 'spectraplakins': cytoskeletal giants with characteristics of both spectrin and plakin families. *J Cell Sci*, 115, 4215-4225.
- Safer D, E.M., Nachmias VT. (1991) Thymosin b4 and Fx, an actin sequestering peptide, are indistinguishable. *J Biol Chem*, 266, 4029-4032.
- Saiki, R.K., Scharf, S., Faloona, F., Mullis, K.B., Horn, G.T., Erlich, H.A. and Arnheim, N. (1985) Enzymatic amplification of beta-globin genomic sequences and restriction site analysis for diagnosis of sickle cell anemia. *Science*, 230, 1350-1354.
- Sambrook J and Russell, D.W. (2001) *Molecular cloning A Laboratory Manual*. Cold spring Harbor Labaoratory press, New work.
- Samstag, Y., Dreizler, E.M., Ambach, A., Sczakiel, G. and Meuer, S.C. (1996) Inhibition of constitutive serine phosphatase activity in T lymphoma cells results in phosphorylation of pp19/cofilin and induces apoptosis. *J Immunol*, 156, 4167-4173.
- Schafer, D.A., Korshunova, Y.O., Schroer, T.A. and Cooper, J.A. (1994) Differential localization and sequence analysis of capping protein beta-subunit isoforms of vertebrates. *J Cell Biol*, 127, 453-465.
- Shattil SJ, H.B., Cunningham M, Lipfert L, Parsons JT, Ginsberg MH, Brugge JS. (1994) Tyrosine phosphorylation of pp125FAK in platelets requires coordinated signaling through integrin and agonist receptors. *J Biol Chem*, 269, 14738-14745.
- Shima, F., Yamawaki-Kataoka, Y., Yanagihara, C., Tamada, M., Okada, T., Kariya, K. and Kataoka, T. (1997) Effect of association with adenylyl cyclase-associated protein on the interaction of yeast adenylyl cyclase with Ras protein. *Mol Cell Biol*, 17, 1057-1064.
- Siomi, H. and Dreyfuss, G. (1995) A nuclear localization domain in the hnRNP A1 protein. *J Cell Biol*, 129, 551-560.
- Spencer, J.A., Eliazer, S., Ilaria, R.L., Jr., Richardson, J.A. and Olson, E.N. (2000) Regulation of microtubule dynamics and myogenic differentiation by MURF, a striated muscle RING-finger protein. *J Cell Biol*, 150, 771-784.
- Spencer, J.A., Eliazer, S., Ilaria, R.L., Jr., Richardson, J.A. and Olson, E.N. (2000) Regulation of microtubule dynamics and myogenic differentiation by MURF, a striated muscle RING-finger protein. *J Cell Biol*, 150, 771-784.
- Stevenson, V.A. and Theurkauf, W.E. (2000) Actin cytoskeleton: putting a CAP on actin polymerization. *Curr Biol*, 10, R695-697.

Sun, D., Leung, C.L. and Liem, R.K. (2001) Characterization of the microtubule binding domain of microtubule actin crosslinking factor (MACF): identification of a novel group of microtubule associated proteins. *J Cell Sci*, 114, 161-172.

Sun H Q, K.K., Yin H L. (1995) Actin monomer binding proteins. *Curr Opin Cell Biol*, 7, 102-110.

Svitkina, T.M., Verkhovsky, A.B. and Borisy, G.G. (1996) Plectin sidearms mediate interaction of intermediate filaments with microtubules and other components of the cytoskeleton. *J Cell Biol*, 135, 991-1007.

Swiston, J., Hubberstey, A., Yu, G. and Young, D. (1995) Differential expression of CAP and CAP2 in adult rat tissues. *Gene*, 165, 273-277.

Takenawa T, I.T. (2001) Phosphoinositides, key molecules for regulation of actin cytoskeletal organization and membrane traffic from the plasma membrane. *Biochim Biophys Acta*, 1533, 190-206.

Towbin H, S.T., Gordon J. (1979) Electrophoretic transfer of proteins from polyacrylamide gels to nitrocellulose sheets: procedure and some applications. *Proc Natl Acad Sci U S A*, 76, 4350-4354.

Vaduva G, M.N., Hopper AK. (1997) Actin-binding verprolin is a polarity development protein required for the morphogenesis and function of the yeast actin cytoskeleton. *J Cell Biol*, 139, 1821-1833.

Vartiainen, M.K., Sarkkinen, E.M., Matilainen, T., Salminen, M. and Lappalainen, P. (2003) Mammals have two twinfilin isoforms whose subcellular localizations and tissue distributions are differentially regulated. *J Biol Chem*, 278, 34347-34355.

Vojtek, A., Haarer, B., Field, J., Gerst, J., Pollard, T.D., Brown, S. and Wigler, M. (1991) Evidence for a functional link between profilin and CAP in the yeast *S. cerevisiae*. *Cell*, 66, 497-505.

Vojtek, A.B. and Cooper, J.A. (1993) Identification and characterization of a cDNA encoding mouse CAP: a homolog of the yeast adenylyl cyclase associated protein. *J Cell Sci*, 105, 777-785.

Wakatsuki, T., Schwab, B., Thompson, N.C. and Elson, E.L. (2001) Effects of cytochalasin D and latrunculin B on mechanical properties of cells. *J Cell Sci*, 114, 1025-1036.

Wallimann, T., Turner, D.C. and Eppenberger, H.M. (1977) Localization of creatine kinase isoenzymes in myofibrils. I. Chicken skeletal muscle. *J Cell Biol*, 75, 297-317.

Weber, A., Nachmias, V.T., Pennise, C.R., Pring, M. and Safer, D. (1992) Interaction of thymosin beta 4 with muscle and platelet actin: implications for actin sequestration in resting platelets. *Biochemistry*, 31, 6179-6185.

Weber, A., Pennise, C.R., Babcock, G.G. and Fowler, V.M. (1994) Tropomodulin caps the pointed ends of actin filaments. *J Cell Biol*, 127, 1627-1635.

Weeds A, M.S. (1993) F-actin capping proteins. *Curr Opin Cell Biol*, 5, 63-69.

Weighardt, F., Biamonti, G. and Riva, S. (1995) Nucleo-cytoplasmic distribution of human hnRNP proteins: a search for the targeting domains in hnRNP A1. *J Cell Sci*, 108 (Pt 2), 545-555.

Wesp, A., Hicke, L., Palecek, J., Lombardi, R., Aust, T., Munn, A.L. and Riezman, H. (1997) End4p/Sla2p interacts with actin-associated proteins for endocytosis in *Saccharomyces cerevisiae*. *Mol Biol Cell*, 8, 2291-2306.

Yang, Y., Bauer, C., Strasser, G., Wollman, R., Julien, J.P. and Fuchs, E. (1999) Integrators of the cytoskeleton that stabilize microtubules. *Cell*, 98, 229-238.

Yin HL, I.k., Janmey PA. (1988) Identification of a polyphosphoinositide-modulated domain in gelsolin which binds to the sides of actin filaments. *J Cell Biol*, 106, 805-812.

Yu, G., Swiston, J. and Young, D. (1994) Comparison of human CAP and CAP2, homologs of the yeast adenylyl cyclase-associated proteins. *J Cell Sci*, 107, 1671-1678.

Yu, J., Wang, C., Palmieri, S.J., Haarer, B.K. and Field, J. (1999) A cytoskeletal localizing domain in the cyclase-associated protein, CAP/Srv2p, regulates access to a distant SH3-binding site. *J Biol Chem*, 274, 19985-19991.

Zelicof, A., Gatica, J. and Gerst, J.E. (1993) Molecular cloning and characterization of a rat homolog of CAP, the adenylyl cyclase-associated protein from *Saccharomyces cerevisiae*. *J Biol Chem*, 268, 13448-13453.

ZigmondSH. (1996) Signal transduction and actin filament organization. *Curr Opin Cell Biol*, 8, 66-73.

Erklärung

Ich versichere, dass ich die von mir vorgelegte Dissertation selbständig angefertigt, die benutzten Quellen und Hilfsmittel vollständig angegeben und die Stellen der Arbeit- einschließlich Tabellen

und Abbildungen-, die anderen Werke im Wortlaut oder dem Sinn nach entnommen sind, in jedem Einzelfall als Entlehnung kenntlich gemacht habe; dass diese Dissertation noch keiner anderen Fakultät oder Universität zur Prüfung vorgelegen hat; dass sie- abgesehen von unten angegebenen beantragten Teilpublikationen- noch nicht veröffentlicht ist, sowie, dass ich eine Veröffentlichung vor Abschluss des Promotionsverfahrens nicht vornehmen werde. Die Bestimmungen dieser Promotionsordnung sind mir bekannt. Die von mir vorgelegte Dissertation ist von Frau Prof. Dr. Angelika A. Noegel betreut worden.

Köln den

Sunil Shekar

CURRICULUM VITAE

Name: SUNIL SHEKAR

Address: Luxemburger strasse, 124-136
Unicenter, Et-Zi: 14-04
50939, Köln, Germany.

(Permanent) # 384, 'BIMBA', 11th Cross,
Municipal Layout, Kuvempunagar,
Mandya-571401, Karnataka,
India.
Email: sunilshekar@hotmail.com

Date of birth: 18/10/1971
Nationality: Indian.

ACADEMIC QUALIFICATIONS

High School: Mysugar boys highschool, Mandya, India.
(1984-1987)

Pre-University: PUC (Physics, Chemistry, Mathematics, Biology)
(1987-1989) Government College, Mandya, India.

Bachelors
Degree: B.Sc. (Chemistry, Zoology, Sericulture)
(1989-1992) Government College, University of Mysore,
Mandya, India.

Masters
Degree: M.Sc. (Biochemistry)
(1992-1994) Manasagangothri, University of Mysore,
Mysore, India.

Post graduation
Studies: Mathematics and Natural Science faculty, University of Cologne
(2001-2005) Germany.
Doctoral work was done under the supervision of
Prof. Dr. Angelika A. Noegel in the Institute for Biochemistry I,
Medical Faculty, Cologne University, Germany.

LEBENS LAUF

Name: SUNIL SHEKAR

Adresse: Luxemburger strasse, 124-136
Unicenter, Et-Zi: 14-04
50939, Köln, Germany.

(Heimatadresse) # 384, 'BIMBA', 11th Cross,
Municipal Layout, Kuvempunagar,
Mandya-571401, Karnataka,
India.
Email: sunilshekar@hotmail.com

Geburtsdatum: 18.10.1971
Staatsangehörigkeit: Indisch

akademische Qualifikation

Schulausbildung: Mysugar boys highschool, Mandya, India.
(1984-1987)

Studium:

Bachelors

Degree: B.Sc. (Chemistry, Zoology, Sericulture)
(1989-1992) Government College, University of Mysore,
Mandya, India.

Masters

Degree: M.Sc. (Biochemistry)
(1992-1994) Manasagangothri, University of Mysore,
Mysore, India.

Promotions studium: Mathematisch-Naturwissenschaftliche Fakultät
(10.2001 -02.2005) Universität zu Köln
Betreuerin: Prof. Dr. Angelika A. Noegel
Institut für Biochemie I, Medizinische Fakultät der
Universität zu Köln.

